EXPEDITIOUS SYNTHESIS OF HYMENIALDISINE AND ITS ANALOGS AND THEIR EVALUATION AS ADJUVANTS IN CANCER THERAPY.

By

Rahman Shah Zaib Saleem

A DISSERTATION

Submitted to
Michigan State University
in partial fulfillment of the requirements
for the degree of

DOCTOR OF PHILOSOPHY

Chemistry

2011

ABSTRACT

EXPEDITIOUS SYNTHESIS OF HYMENIALDISINE AND ITS ANALOGS AND THEIR EVALUATION AS ADJUVANTS IN CANCER THERAPY.

By

Rahman Shah Zaib Saleem

The dissertation focuses primarily on three aspects of the research carried out during the PhD. These include the efforts towards synthesis of hymenialdisine and its analogs and their evaluation for improving chemotherapy; the development of the methodology to access triazolines and triazoles from oxazol-5(4H)-ones and synthesis of imidazoline for the study of the interaction of this class of compounds with the 20s proteasome using photoaffinity labeling studies.

Previous studies have shown that Checkpoint kinase 2 (ChK2) plays an important role in cell cycle regulation in response to the various DNA damaging agents including chemotherapeutics. There is evidence that the cellular role of ChK2 can be utilized to improve the existing chemotherapeutic techniques. Hymenialdisine is a natural product known to inhibit ChK2. The first part of the dissertation presents the improved synthesis of the natural product and the synthesis of the new analogs. Two classes of analogs are presented: First the 2-phenylpyrroloazepinone based analogs, prepared via single step modification of a common intermediate; and second, the benzoazepinone analogs that utilize the ring expansion strategy to achieve the synthesis of key intermediate. This part also presents the kinase profiling of these compounds.

The second part of the dissertation describes the development of the cycloaddition reaction of oxazol-5(4H)-ones and azodicarboxylates. Previously, our group has

reported the utility of oxazol-5(4H)-ones in diversity oriented synthesis enabling access to a wide range of heterocyclic scaffolds. This part presents the research work done in extending the chemistry to access triazoline and triazole compounds. The dissertation describes the initial discovery of the reaction and the exploration of the reaction substrate scope to give 1,2,4-triazoline compounds. The dissertation also describes the aromatization of these 1,2,4-triazoline compounds to respective triazole compounds.

The last part of the dissertation focuses on contributions towards the study of inhibition of 20s proteasome. The 20s proteasome is shown in the literature to decreases the efficiency of the cancer therapeutics by degrading IκB and thus allowing NF-κB to translocate into nucleus and transcribe the antiapoptotic genes in the cancer cells. Our group has prepared the imidazoline compounds as a novel class of 20s proteasome inhibitor. These compounds are non-competitive inhibitors, unlike the other clinically relevant inhibitors of the proteasome. This part of the dissertation presents the synthesis of photoaffinity labeled imidazoline to study the interaction of these compounds with the proteasome. Lastly, the evaluation of the new hymenialdisine derivatives for their ability to inhibit 20s proteasome is presented.

This dissertation is dedicated to all those who struggle to improve their lives by honest means.

ACKNOWLEDGEMENTS

Undertaking the PhD research work is an overwhelming experience and involves help and support from a number of individuals in the academic life and life outside the lab. In this regard, I was fortunate to have a group of individuals.

I am thankful to my graduate advisor Professor Dr. Jetze J. Tepe for providing me the opportunity to work in his research group. The research experience in his lab allowed me not only to improve my expertise as synthetic chemist, but also helped me become a better scientist and understand the research in the broader context. He allowed me to work relatively independently and allowed me to carry out the research in a manner which I found fulfilling. He was attentive to my thoughts and provided criticism when absolutely needed, allowing me to learn from my mistakes and not getting too upset at those.

I am also thankful to Professor Dr. William Wulff, Professor Dr. James Jackson and Professor Dr. Gary Blanchard for providing me with the helpful advice and discussions throughout my PhD. Their thinking process and their humbleness has been inspirational for me.

I am thankful to all my lab-mates including Dr. Jason Fisk, Dr. Chis Hupp, Dr. Adam Mosey, Dr. Samantha Frawly, Dr. Thu Nguyen, Brain Englud, Brandon Dutcher, Dr. Daljinder Kahlon, Brandon Meyers, Mike Kuzpit, Ke Qu, Nicole Hewlett, Benjamin Weaver, Lauren Azvedo and Sujana Pradhan for constituting to a productive research environment. I am especially thankful to Teri Lansdell for analyzing my compounds for their biological activity.

I am grateful to Dr. Richard staples for resolving single crystal X-ray structures of my samples. I am also thankful for to Dr. Dan Holmes and Dr. Kermit Johnson for help with the NMR spectroscopy. I also want to extend my thanks to Rui Huang for taking the mass spectra for my compounds in the initial days of my research and Professor Dr. Daniel Jones, Lijun Chen and Bev Chamberlin for help in the mass spectroscopy facility. I also want to extend thanks to Professor Dr. Babak Borhan, Professor Dr. Mitch Smith and Robert Maleczka for the helpful discussions.

I am also thankful to my advisor in the office of international students and scholars, Ms. Mary Gebbia and director of office of international students and scholar Mr. Peter Briggs. I am also thankful to Professor Dr. Gary VanKempen and Ms. Dorinda VanKempen. I am also thankful to Professor Dr. Alvin Spaerstein, Professor Dr. Maher Muala, Hariet Saperstein and all the members of Michigan Fulbright chapter for providing the leadership opportunity and enabling me the refreshing breathing space outside the lab environment. In the end, I want to thank my parents and sisters for their support during my PhD.

TABLE OF CONTENTS

LIST OF TABLES

LIST OF FIGURES

LIST OF SCHEMES

KEY TO SYMBOLS AND ABBREVIATIONS

53BP1--Tumor protein p53-binding protein 1

AcOH--Acetic acid

$AlCl_3$--Aluminum chloride

ATM--Ataxia telangiectasia mutated

ATP--Adenosine triphosphate

ATR--Ataxia telangiectasia and rad3-related

Bn--Benzyl

cAMP-- Cyclic adenosine monophosphate

Bax--Bcl-2-associated X protein

BRCA1--Breast cancer 1 protein

^{t}BuOH--ter-butyl alcohol

Bz--Benzoyl

CAN--Ceric ammonium nitrate

cdc25A--Cell division cycle 25A

cdc25C--Cell division cycle 25C

CD4-- Cluster of differentiation 4 protein

CD8-- Cluster of differentiation 8 protein

CDK--Cyclin-dependent kinase

cGMP-- Cyclic guanosine monophosphate

ChK1-- Check point kinase 1

ChK2--Check point kinase 2

CK1-- Casein kinase 1

CK2-- Casein kinase 2

Cy-- Cyclohexyl

d-- days

DBH-- debromohymenialdisine

DBS-- Double strand break

DCE-- Dichloroethane

DCM-- Dichloromethane

DEAD-- Diethyl azodicarboxylate

DIAD -- Diisopropyl azodicarboxylate

DMAP-- Dimethylamino pyridine

DME-- Dimethyl ether

DMF-- Dimethylforamide

DMSO-- Dimethyl sulfoxide

DNA-- Deoxyribonucleic acid

DNA-PK-- DNA-dependent protein kinase

DOS-- Diversity oriented synthesis

E2F1-- E2F transcription factor 1

EDCI-- 1-ethyl-3-(3-dimethylaminopropyl) carbodiimide

Eg2-- Eosinophil Granule mAb

Erk-- Extracellular-signal-responsive kinase

Et-- Ethyl

Et_2O-- Diethyl ether

EtOAc-- Ethyl acetate

EtOH-- Ethanol

Et_3N-- Triethyl amine

Et_3SiH-- Triethyl silane

Fas-- a member of the TNF family of receptors on the cell surface

GADD45-- Growth arrest and DNA-damage-inducible protein

GSK3β-- Glycogen synthase kinase3β

Gy-- Gray (unit of radiation)

h-- hours

H2AX-- Histone H2Ax

HCT116-- Human colon carcinoma cell line

HCV-- Hepatitis C virus

HMD-- Hymenialdisine

IC_{50}-- Half maximal inhibitory concentration

IκB-- Inhibitory protein kappa B

IKK-- IκB kinase

IR-- Ionizing radiations

KHMDS-- Potassium hexamethyldisilazane

K*i*-- Inhibition constant

KOH-- Potassium hydroxide

LiOH-- Lithium hydroxide

MAP-- Mitogen-activated protein

MAPKK-- Mitogen-activated protein kinase kinase

MCF-7-- human breast adenocarcinoma cell line

MDC1-- Mediator of DNA damage checkpoint protein 1

Mdm2-- Mouse double minute 2 protein

MdmX-- also known as Mdm4: Mouse double minute 4 protein

Me-- Methyl

MeCN-- Acetonitrile

MeI-- Methyl iodide

MEK-1-- MAP kinase/ERK kinase

MeOH-- Methanol

$MeSO_3H$-- Methanesulfonic acid

Mre11-- Meiotic recombination 11

MsCl-- Methanesulfonyl chloride

NaH-- Sodium hydride

NaOH-- Sodium hydroxide

NBS-- N-bromosuccinimide

Nbs1-- Nijmegen breakage syndrome 1 protein

NCE-- New chemical entity

NF-κB-- Nuclear factor kappa B

NH_4OH-- Ammonium hydroxide

NMR-- Nuclear magnetic resosnance

Noxa-- PMA-induced protein invovled in immediate-early apoptosis response

p21-- also known as CDKN1A (cyclin-dependent kinase inhibitor 1A)

p25-- Protein 25

P_2O_5-- Phosphorus pentoxide

p53-- Protein 53

PARP-- Poly (ADP-ribose) polymerase (PARP)

Ph-- Phenyl

PhMe-- Toluene

PPA-- Polyphosphoric acid

PKC-- Protein kinase C

PML-- Promyelocytic leukemia

PP2A-- Protein phosphatase 2A activator

nPr-- n-propyl

iPr_2EtN-- Diisopropyl ethyl amine

PTAD-- 4-phenyl-1,2,4-triazoline-3,5-dione

Puma-- p53-upregulated modulator of apoptosis

Pyr.-- Pyridine

quant.-- quantitative

RNA-- Ribonucleic acid

RT-- room temperature

SAR-- Structure activity relationship

Sat.-- Saturated

SEM-- 2-(Trimethylsilyl)ethoxymethyl group

SEM-Cl-- 2-(Trimethylsilyl)ethoxymethyl chloride

siRNA-- Small interfering RNA

soln.-- Solution

sp.-- Species

Tf_2O-- Trifluoromethanesulfonic anhydride

TFA-- Trifluoroacetic acid

TFAA-- Trifluoroacetic anhydride

THF-- Tetrahydrofuran

$TiCl_4$-- Titanium (iv) chloride

TMS-- Trimethyl silyl

Troc-Cl-- 2,2,2-Trichloroethyl chloroformate

TsOH-- p-Toluenesulfonic acid

UV-- Ultraviolet

CHAPTER 1

IMPROVED SYNTHESIS OF MARINE ALKALOID: HYMENIALDISINE AND ITS INDOLIC ANALOG

1.1. Introduction

Due to their unique structural and biological features, natural products have been used as drugs, precursors in the synthesis of drugs or templates for discovery of new drug candidates. It was about 200 years ago that the first pure, pharmacologically active compound, morphine, was isolated froveom a plant.[1] This marked the start of an era in which drugs from plants could be purified and the dose reponse became independent of the source or age of the material, leading to the isolation of a host of new natural products. Even today, natural products constitute a major portion of the new chemical entities (NCE). Over the period of last twenty five and a half years (from Jan 1981 to Jun 2006) 1010 new chemical entities were approved.[2] Out of these NCEs only 163 were biological (containing large peptide or protein, either isolated from an organism/cell or produced by biotechnologicals means using a surrogate) or vaccines. Among the remaining 847 NCEs, 310 NCEs were of synthetic origin and 537 were natural products, their derivatives or mimics (Figure 1.1).

The natural products are even more prominent in the area of the cancer treatment. During the a time period, 100 NCEs were approved for cancer. Only 19 of these NCEs were biological or vaccines, while out of remaining 81, 18 were synthetic and 63 were natural products, their derivatives or mimics (Figure 1.1).

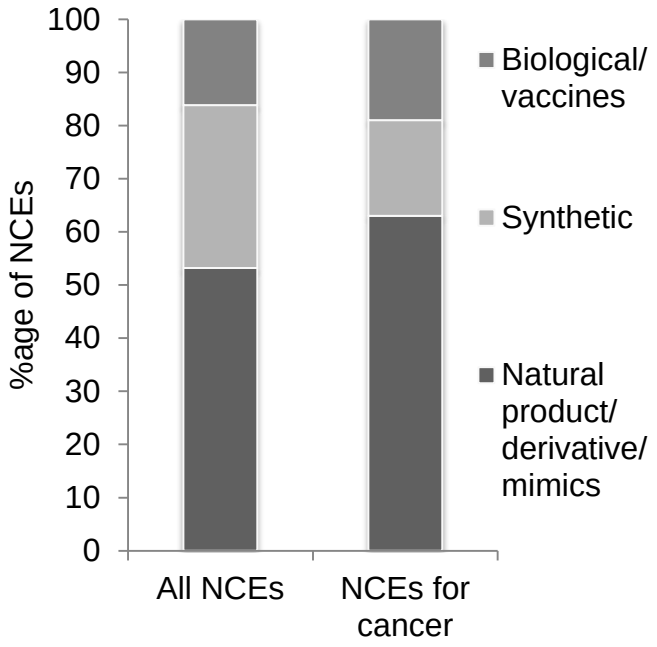

Figure 1.1. Comparison of all NCEs and NCEs for cancer

Isolation of natural products is generally a long, tedious and expensive process and often cannot be utilized for the large scale production of these compounds. Hence natural products keep inspiring synthetic chemists to develop new methodologies and develop improved routes to access the potentially useful natural products in the laboratories.

1.1.1. Hymenialsisine

Hymenialdisine (HMD (**1**)) is a natural product first reported in 1982 by Cimino and co-workers.[3] They reported the isolation and crystal structure of this yellow compound from *Axinella verrucosa* and *Acanthella aurantiaca*. It contains a fused pyrrolo[2,3-c]azepin-8-one ring system with glycocyamidine appendage as shown in figure 1.2.

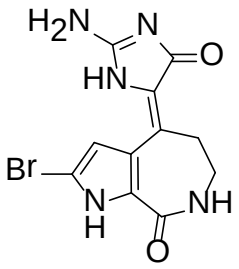

1

Figure 1.2. Structure of HMD.

Hymenialdisine is shown to inhibit a number of cellular proteins including CDKs, GSK3β, CK1, ChK2 and ChK1 at low micromolar to nanomolar range.[4] These proteins play an important role in regulating several cellular functions including gene expression, cellular proliferation, differentiation, membrane transport and apoptosis. The activity of HMD makes it an ideal lead molecule for the development of new drug candidates that can selectivity inhibit one or a selected set of the target proteins.[5]

1.1.2. Oroidin alkaloids

HMD belongs to the group of natural products broadly known as the oroidin alkaloids. This group includes oroidin, hymenidin, clathrodin, dispacamide, monobromodispacamide, debromohymenialdisine (DBH), axinohydantoins, hymenin and stevensine (Figure 1.3). Among these, DBH, Axinohydantoins, Hymenin and Stevensine share, in common, a fused bicyclic pyrrolo[2,3-c]azepin-8-one ring system with HMD.

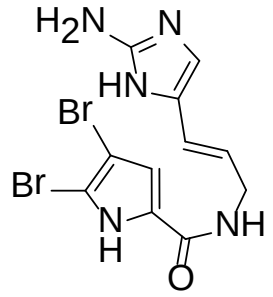

Oroidin (**2**)

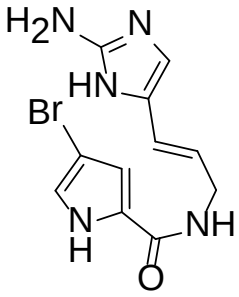

Hymenidin (**3**)

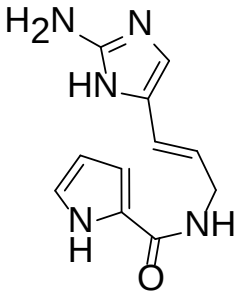

Clathrodin (**4**)

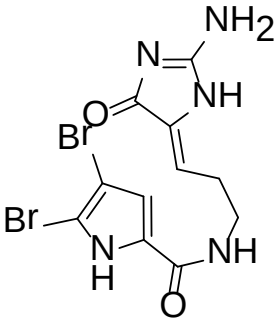

Dispacamide (**5**)

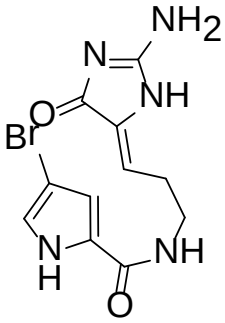

Monobromodispacamide (**6**)

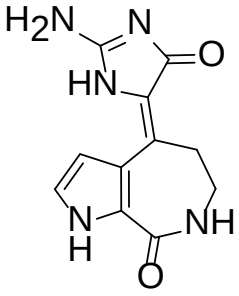

Debromohymenialdisine (**7**)

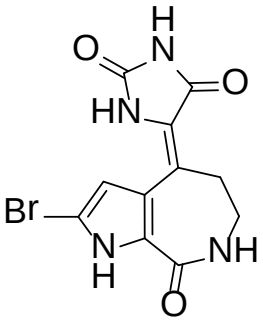

Axinohydantoin (**8**)

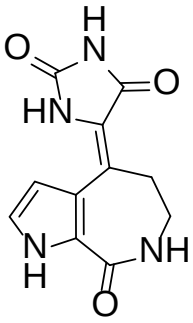

Debromoaxinohydantoin (**9**)

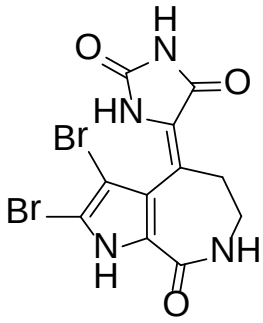

Bromoaxinohydantoin (**10**)

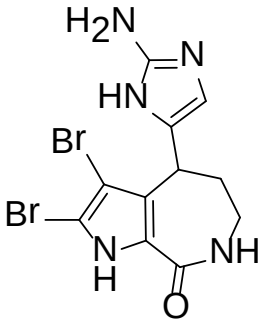

Hymenin (**11**)

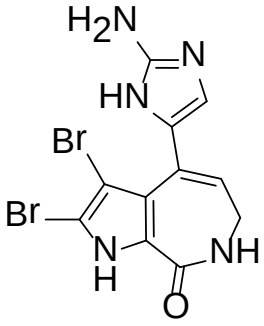

Stevensine (**12**)

Figure 1.3. Members of Oroidin alkaloids' family

Debromohymenialdisine (**7**), a debrominated analog of HMD (Figure 1.3) was first isolated from the Great Barrier Reef sponge *Phakellia* sp. in 1980 and the structure was elucidated with ^{1}H NMR, UV and chemical degradation.[6] HMD was later extracted from the Red Sea sponge *Acanthella* sp. and the Mediterranean sponge *Axinella* sp. in 1982, as well as the from *Hymeniacidon* sp. in 1983, and was characterized by X-ray crystallography.[3, 7] HMD and DBH are structurally similar compounds, differing only in the presence of bromine at C2. Axinohydantoins (**8-10**) (Figure 1.3) contain the same fused pyrroloazepine ring but instead of the glycocyamidine ring, the pyrroloazepinone ring is bonded to a hydantoin ring. Hymenin (**11**) was isolated from an Okinawan sponge *Hymeniacidon sp*. in 1984 and characterized by NMR.[8] Hymenin contains two bromine atoms on the pyrrole ring and carries a 2-aminoimidazole ring instead of a glycocyamidine ring joined to azepinone ring via a single bond. Stevensine (**12**) was isolated from *Pseudaxinyssa sp.* in 1985. It is another natural product, similar to hymenin, but contains additional unsaturation between C9 and C10 atoms.[9]

1.2. Biological role of HMD

Meijer and co-workers[4] showed that HMD is a potent inhibitor of CDKs, GSK-3β and CK1 and competes with ATP for binding to these kinases. Their results are summarized in table 1.1. Ireland and co-workers[10] reported that HMD was a very potent inhibitor of MEK-1 (IC_{50}= 6nM) and inhibited the growth of human tumor LoVo cells. Chabot-Fletcher and co-workers[11] found that it was a good inhibitor of the nuclear transcription

Table 1.1. Kinase inhibition selectivity of HMD

Enzyme	IC_{50} (nM)	Enzyme	IC_{50} (nM)
CDK1/cyclin B	22	Protein kinase C δ	1100
CDK2/cyclin A	70	Protein kinase C ϵ	6500
CDK2/cyclin E	40	Protein kinase C η	2000
CDK3/cyclin E	100	Protein kinase C ζ	60,000
CDK4/cyclin D1	600	cAMP-dependent protein kinase	8000
CDK5/p25	28	cGMP-dependent protein kinase	1700
CDK6/cyclin D2	700	GSK3-β	10
Erk1	470	ASK-γ (plant GSK-3)	80
Erk2	2000	Eg2 kinase	4000
c-raf	>10,000	CK1	35
MAPKK	1200	CK2	7000
c-Jun amino-terminal kinase	8500	Insulin receptor tyrosine kinase	75,000
Protein kinase C α	700	c-src tyrosine kinase	7000
Protein kinase C β1	1200	c-abl tyrosine kinase	4000
Protein kinase C β2	1700	Topoisomerase I	(10,000)*
Protein kinase C γ	500	Topoisomerase II α	(10,000)*

***** no effect at the highest dose tested (in parentheses).

factor NF-κB, while Tepe and co-workers[12] demonstrated that it inhibits checkpoint kinase 2 (ChK2) and checkpoint kinase 1 (ChK1) at IC_{50} values of 42nM and 1950nM, respectively.

1.3. Syntheses of HMD

Since the discovery, many research groups have attempted to synthesize this family of natural products. Althought there are reports on the practical synthesis[13] and multigram preparation of the DBH[14], HMD has been more synthetically challenging for various reasons including the poor solubility of the bromo-compounds, difficulty in separation of the regio-isomers upon monobromination, atom-scrambling in the cyclization step[15] and low yield in the steps for synthesizing glyciamidine ring. To date there are only three reports of the synthesis of HMD.[15-16]

1.3.1. First syntheses of HMD

The first total synthesis of HMD was reported by Tatsuoka and co-workers in 1995.[15] They utilized pyrrole-2-carboxylic acid **13** as the starting material. Treatment of pyrrole-2-carboxylic acid **13** with thionyl chloride in catalytic amounts of DMF in toluene at 60^{o}F, followed by condensation with β-alanine methyl ester gave compound **14**. The pyrrole derivative **14** was then brominated using NBS to give 2-bromopyrrole compound **15**. Compound **15** was hydrolyzed and subjected to cyclization. The reaction afforded 65%

yield. However, 1:1 mixture of 2- and 3-bromoaldisine was obtained. These isomers were not easily isolable and in order to facilitate the isolation, the pyrrole and amide nitrogen were protected with SEM groups. This protection and later deprotection added two extra steps to the whole scheme of the synthesis.

Subsequently, the mixture of isomers was treated with NaH and SEM-Cl in DMF followed by column chromatography affording the isolation of compound **17** in 35% yield. The Horner-Wadsworth-Emmons reaction of compound **17** with ethyl diethylphosphonoacetate gave a mixture of α,β and β,γ-unsaturated esters **18**. This mixture of esters **18** was subsequently deprotonated with KHMDS and reacted with 2-benzenesulfonyl-3-phenyloxaziridine[17] to give the α,β-unsaturated esters **19** as a single regioisomer. In order to convert the hydroxyl into a good leaving group for the subsequent reaction, compound **19** was mesylated under basic conditions to yield **20**.

In the next step, compound **20** was treated with guanidine. This reaction led to the formation of glycocyamidine ring and isomerization of the double bond to make conjugated system of compound **22**. The NMR data of the products were compared with those of the natural products and confirmed the Z-stereochemistry. In the last step, SEM-groups were removed and the product was purified over silica gel to give the natural product HMD **1**. Though the synthetic route faced some challenges, resulting in the addition of steps, Annoura and co-workers demonstrated the first successful total synthesis of the natural product.

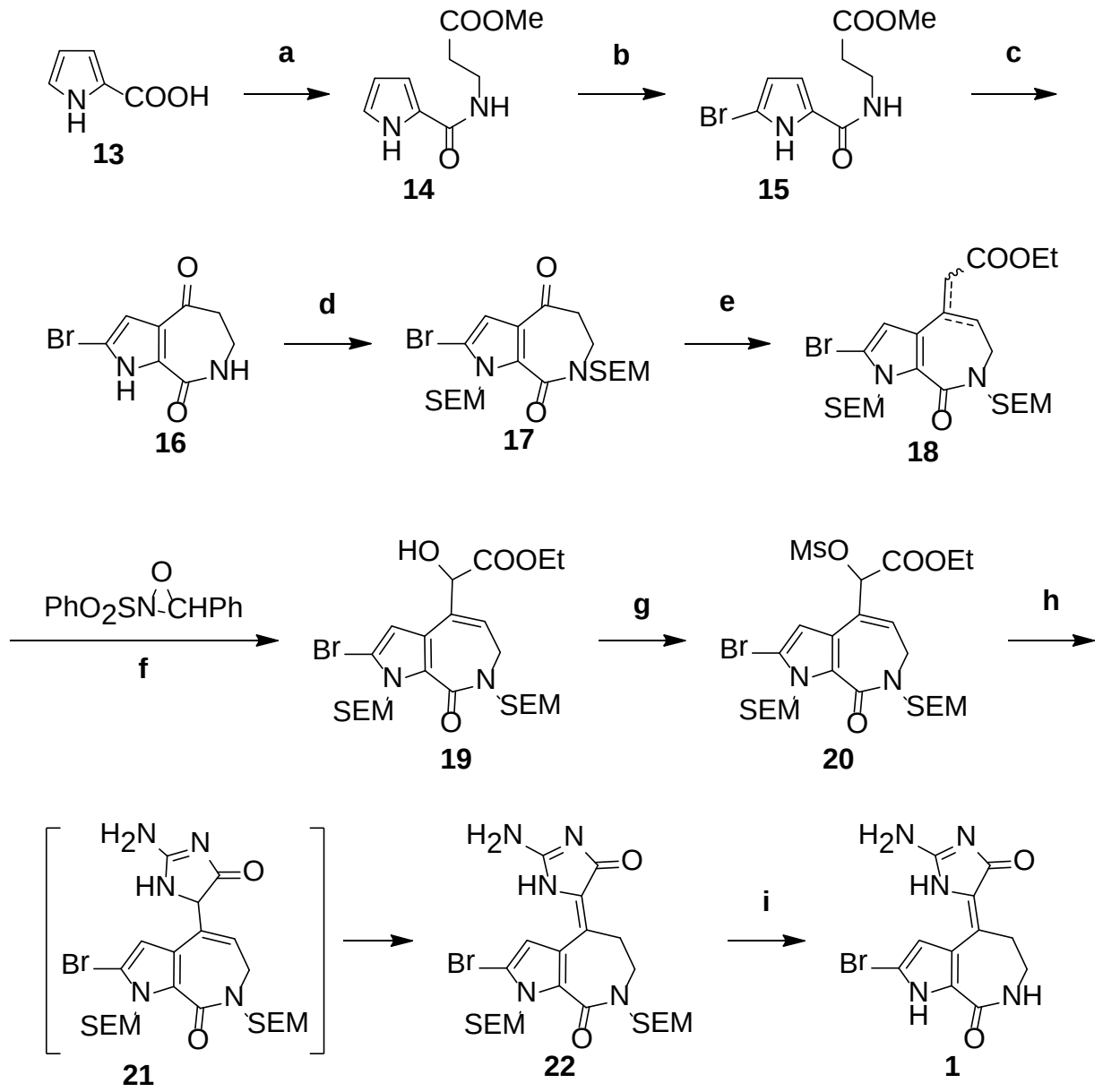

Scheme 1.1. Synthetic scheme for first synthesis of HMD

Reagents and conditions: (a) $SOCl_2$, cat. DMF, toluene, 60^oC, 1 h, then $H_2NCH_2CH_2COOMe$, Et_3N, DCM, rt, 3 h, 63%; (b) NBS, THF, rt, 2 h 56%; (c) 10% aq. NaOH-MeOH (2:1), rt, 5 h, then PPA-P_2O_5, 100^oC, 1 h 65%; (d) NaH (2 eq.), SEM-Cl

(2 eq.), DMF, rt, 2 h 35%; (e) $(EtO)_2POCH_2COOEt$, NaH, DME, 50^oC, 24 h 83%; (f) KHMDS, THF, -78^oC, 2 h 78%; (g) MsCl, Et_3N, DCM, 0^oC quant.; (h) guanidine, DMF, 50^oC, 5 h 42%; (i) 5% aq. HCl-MeOH (1:1), 80^oC, 2 h 70%.

1.3.2. Second synthesis of HMD utilizing a common bicyclic pyrrole precursor

Horne and co-worker published the syntheses of hymenin, stevensine, DBH and HMD.[16a] The authors utilized a common bicyclic pyrrole[2,3-*c*]azepine-8-one ring system. The key features of their synthesis included:

i- The coupling the azafulvene ring **23** to 2-aminoimidazole **24** (Figure 1.4) under acidic conditions to form the carbon-carbon bond between the two rings of the natural products.

ii- The utilization of protodebromination/oxidation strategy to generate the glycocyamidine ring.

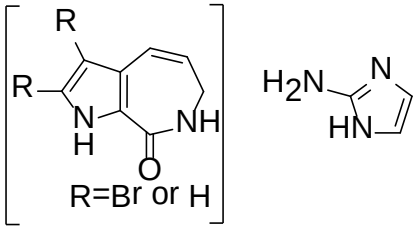

23 **24**

Figure 1.4. Azafulvene intermediate to be coupled to 2-aminoimidazole

The synthetic strategy utilized 2,3-dibromo-(trichloroacetyl)pyrrole **25** as the starting material. The treatment of 2,3-dibromo-(trichloroacetyl)pyrrole **25** with aminodioxolane gave pyrrole **26** in excellent yield.

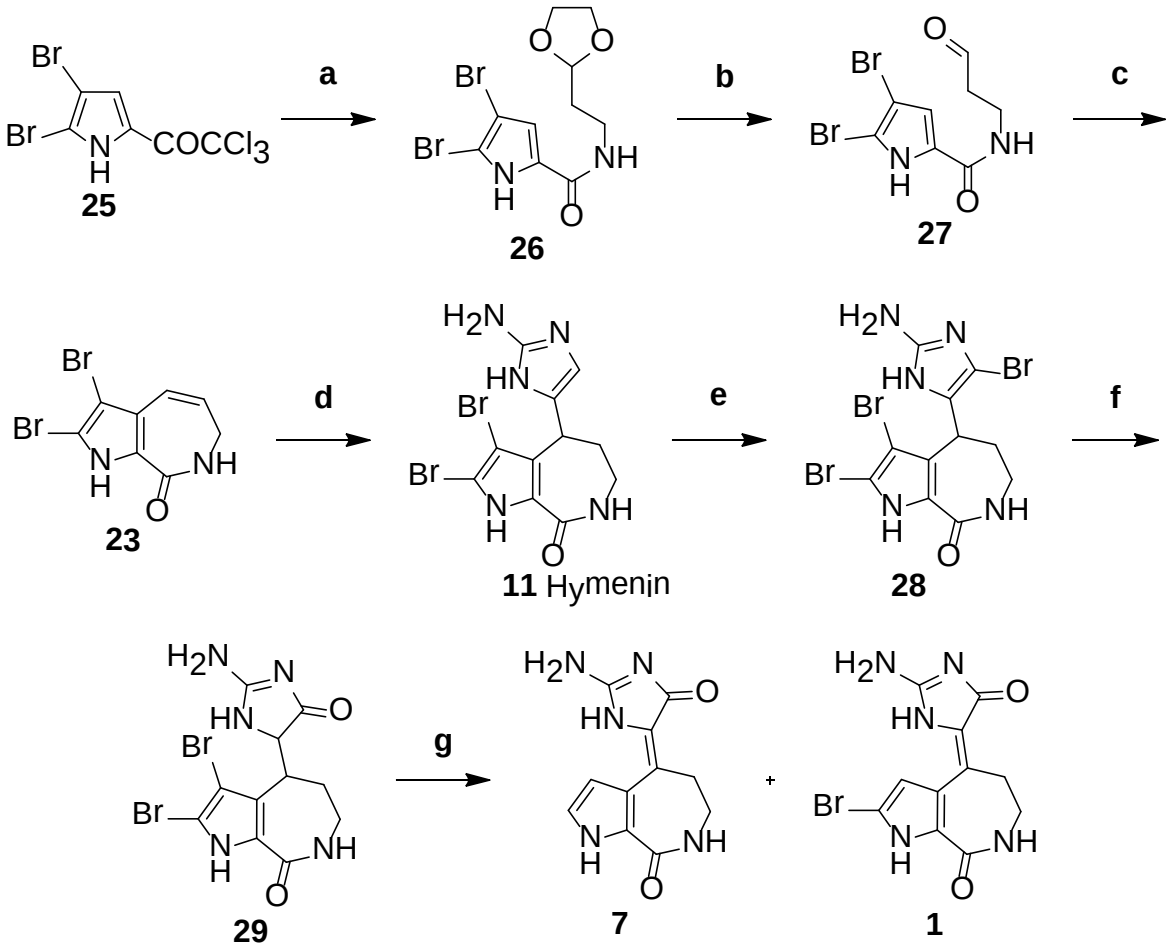

Scheme 1.2. Synthetic scheme used by Xu and co-workers

Reactions and conditions: (a) Aminodioxolane (b) TsOH, H_2O/acetone, reflux, 91%; (c) $MeSO_3H$, rt, 7d, 80%; (d) **24** $MeSO_3H$, 7d, 65% (e) Br_2, TFA, rt, 95% (f) AcOH/H_2O, reflux, 72% (g) $MeSO_3H$, HBr (cat.) 90^{O}C, sealed tube, 12h, 33% of 1 27% of 7.

Then the aldehyde was deprotected to give compound **27**, which upon treatment with methanesulfonic acid at room temperature for seven days afforded bicyclic pyrrole **23** in good yields, without the formation of homodimer (the homodimerization was an issue when this reaction was carried out without the presence of the two bromine atoms on the pyrrole ring). In the next step, compound **23** was reacted with 2-amino imidazole **24** to give the natural product hymenin **11**. Hymenin **11** was then treated with 1.2 eq of bromine in trifluoroacetic acid to afford 4'-bromohymenin **28** in 95% yields. Compound **28** was subjected to mild hydrolytic conditions to give **29** in 72% yields as a mixture of diastereoisomers. Then protodebromination and oxidation of **29** were carried out in the using methanesulfonic acid and catalytic amounts of HBr to give HMD and DBH in 33% and 27% yields respectively.

Alternatively the authors utilized the intermediate **31** to synthesize HMD. This route was the modification of the pathway utilized in the synthesis of stevensine. Compound **23** was prepared as shown above (Scheme 1.2). The addition of bromine to compound **23** in methanol afforded compound **30** in high yields. Then the reaction of compound **30** with 2-aminoimidazole **24** in methanesulfonic acid led to the formation of compound **31** in 46% yields. Under the acidic conditions compound **31** gave compound **32** in 47% yields. In the last step, compound **32** was treated with acetic acid to afford **1** in 65% yields.

The authors showed two alternate routes for the synthesis of the natural product. However the competing reactions and the reaction times of multiple days make these intricate schemes less practical.

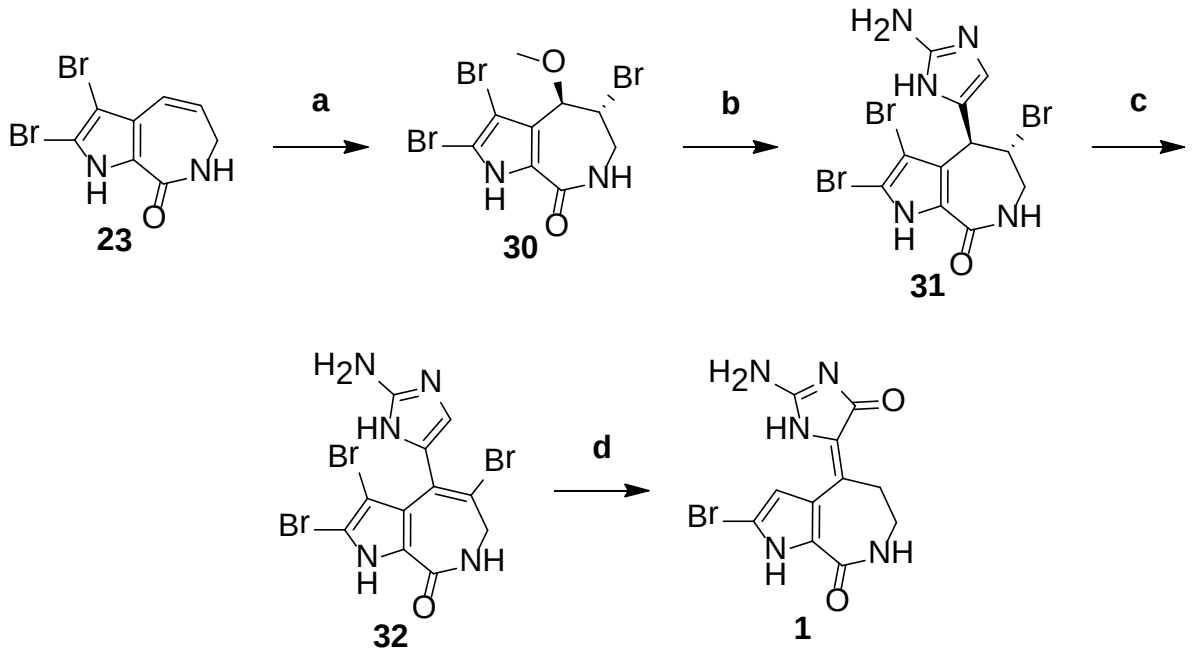

Scheme 1.3. Alternate route used by Xu and co-workers

Reactions and conditions: (a) Br_2, MeOH, 20 min, rt, 95% (b) **24**, $MeSO_3H$, rt, 46% (c) $MeSO_3H$, 90^{O}C, sealed tube, 47% (d) $AcOH/H_2O$, reflux, 3d, 65%

1.3.3. Synthesis of HMD through a coupling of bicyclic pyrrole to unprecidented imidazolone

Varasi and co-workers presented an efficient scheme for the synthesis of the HMD.[16b] They used the 2-bromoaldisine **16** as their key intermediate. The scheme started with the commercially available 2,2,2-trichloroacetyl chloride **33**. The reaction of 2,2,2-trichloroacetyl chloride **33** with ethyl 2-aminopropanoic acid hydrochloride gave compound **34**. In order to brominate compound **34**, the authors used a set of reaction conditions reported by Feldman and co-workers[18] and Domostoj and coworkers[19] to

achieve regioselective bromination to produce compound **35** in 67% yield. The brominated compound **35** was then subjected to basic hydrolysis in the subsequent step to give compound **36**.

For making the 2-bromoaldisine **16** milder Friedel-Crafts-type cyclization conditions were applied. The two step protocol involved the treatment of the compound **36** with oxalyl chloride to convert the carboxyl group into an acyl chloride in the first step. In the second step, the aluminum chloride mediated cyclization produced 2-bromoaldisine **16** without any bromine scrambling in 53% overall yield (Scheme 1.4).

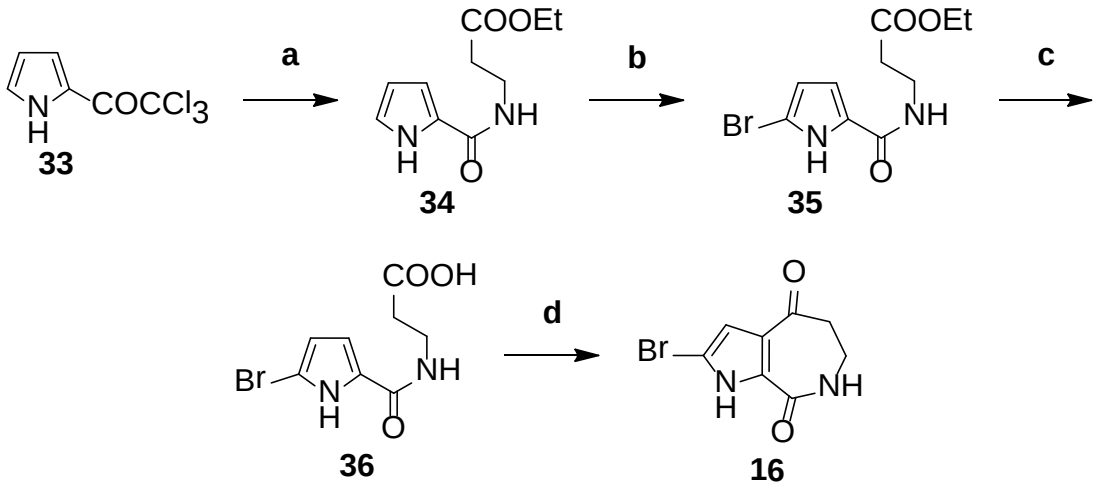

Scheme 1.4. Synthesis of aldisine 16

Reactions and conditions: (a) $H_2NCH_2CH_2COOEt.HCl$, Et_3N, MeCN, rt, 97% (b) NBS, MeOH/THF 0^oC-rt, 67% (c) 1N NaOH, rt, 18h, 92% (d) (i) $(COCl)_2$, DMF (Cat.) DCE, rt (ii) $AlCl_3$, 4^oA, rt, 53%.

At this stage, the authors decided to obtain product through intermediate **38**. Use of intermediate **38** to construct glycociamidine ring has been illustrated by Tepe and co-workers[12, 20] and was based on the report of Prager and coworkers.[21] However the reaction conditions did not bear the fruit of success and the formation of the product was not observed. The authors manipulated the reaction conditions by varying the base and solvent, in vain.

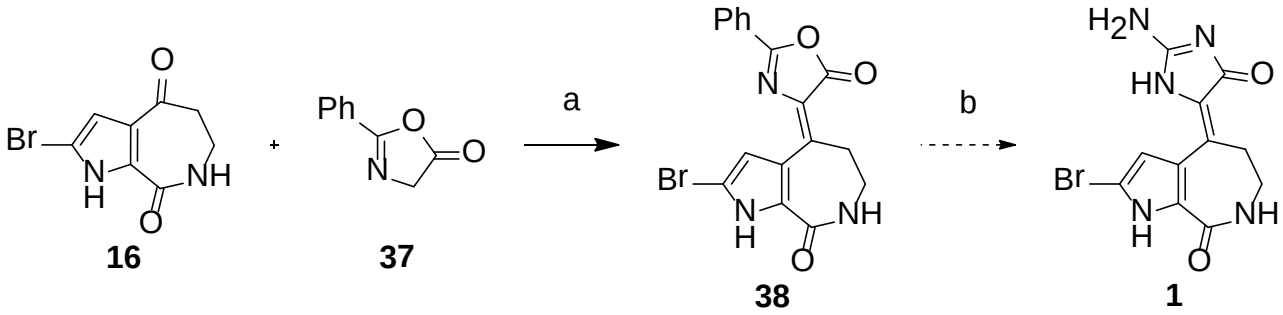

Scheme 1.5. Use of phenyl oxazolone 36 for the completion of synthesis

Reactions and conditions: (a) $TiCl_4$, py, DCM, -10^{o}C-rt 87% (b) S-Benzyl isothiouronium, Base, solvent.

This prompted the authors to design an imidazolinone-based glycociamidine ring precursor **39**. Compound **39** underwent condensation in a manner similar to phenyloxazolone **37**. However the compound **40** was sensitive to nucleophiles and chromatography and could not be purified. Therefore, compound **40** had to be immediately utilized in the next reaction. Fine tuning of the nitrogen source was required to displace methylthio-group and for deprotection of benzoyl group on compound **40**.

Compound **40** was treated with diluted (0.5 N) ammonia solution in dioxane to secure the displacement of the methylthio group, while leaving the benzoyl- group untouched. In the subsequent step, the solvent was evaporated and the crude mixture of **41** was exposed to concentrated (7 N) ammonia solution in methanol for two day. This resulted in the clean removal of the aforementioned protective group giving HMD (**1**).

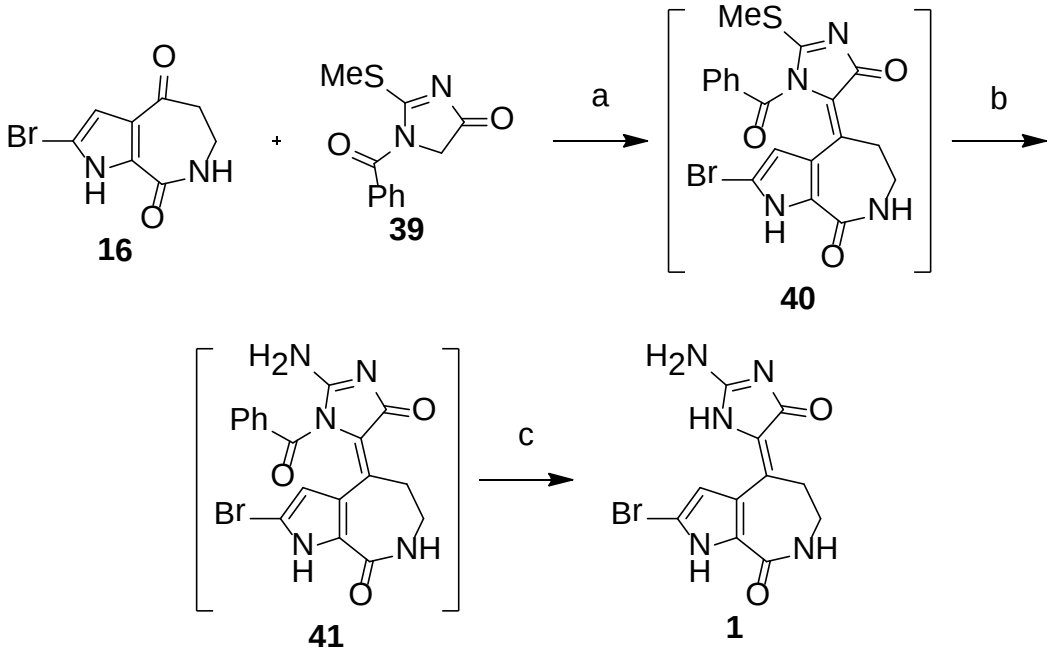

Scheme 1.6. Use of imidazolinone 38 to complete the synthesis

Reactions and conditions: (a) $TiCl_4$, py, DCM, -10^{o}C-rt (b) 0.5N NH_3, dioxane, rt, 2d (c) 7N NH_3, MeOH, rt, 2d 25% overall yield.

The above synthetic strategy provided a good route for the synthesis of HMD; however, it has some associated issues that were compromising the overall yield of the reaction.

For example the isolation of the compound **35** from its 3-bromo isomer via column chromatography is a tedious task, especially when run at 5 mmol or bigger scale. In addition, the formation of the 3-bromo isomer significantly compromises the yield of the reaction. The instability of the compound **39** was another issue and the yield in the last step was low. Therefore, this step also needed reconsideration.

We were interested in developing a route that would not only address the above issues, but also give access to diversity oriented synthesis of novel analogs via single step manipulation of a common intermediate.

1.4. Improved synthetic route for the synthesis of HMD

Due to the ability of HMD and DBH to inhibit ChK2, our group has been interested in the synthesis of these natural product and their analogs. Our interest made us to devise the modifications that address the above issues. We analysed a range of different conditions and were able to improve the selectivity of the bromination considerably. Also, in order to obtain a diverse range of analogs, the instability of the intermediate **39** and **40** was undesirable and we wanted to obtain a penultimate compound which could give new analogs via single step manipulation of the last step. We were also interested in improving the yield of the route and wanted to apply the modification to improve the synthesis of indolic derivative.

We used commercially available 2,2,2-trichloroacetyl chloride **33**, which upon reaction with β-alanine ethyl ester gave compound **34**. Unlike the previously reported procedure,[16b] we used DCM as the solvent and observed near quantitative yields of 99% of compound **34**.

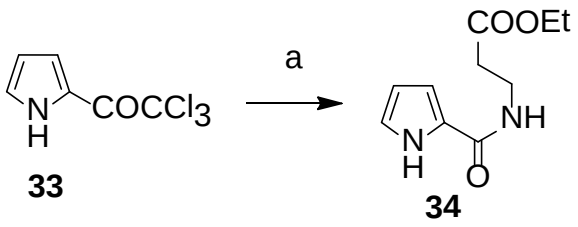

Scheme 1.7. Synthesis of compound 34

Reactions and conditions: (a) $H_2NCH_2CH_2COOEt.HCl$, Et_3N, DCM, rt, 99%

In the next step, we had to substitute the H-atom at 2-position of pyrrole ring with Br-atom. Initially, we carried out the reaction of compound **34** with NBS using the MeOH and THF as solvents and obtained decent yields. However, the process of purification was tedious as the 2-bromoisomer (the desired compound **35**), did not exhibit good difference of Rf value from the competing 3-bromoisomer **35'** and column chromatography was a tedious job and often multiple columns were required to afford purification.

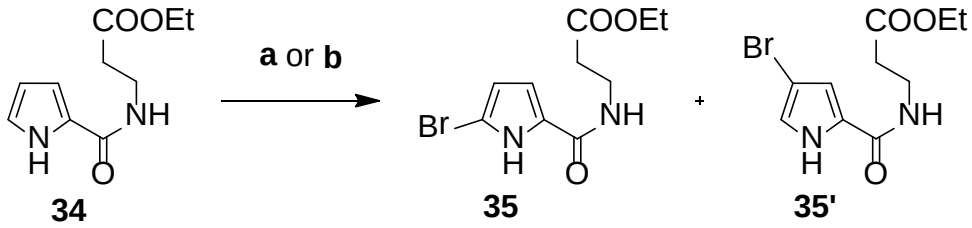

Scheme 1.8. Bromination of compound 34

Reactions and conditions: (a) NBS, MeOH/THF -78^{o}C-rt, 74% (b) NBS, MeCN -10^{o}C-rt, 57%.

Lowering of the temperature in the beginning of the reaction to -78^{o}C led to increased yield of the desired product, yet we were interested in improving the purification technique of the reaction.

As the first observation we found that the compound **35** had lower solubility in organic solvents as compared to compound **35'**. After a brief survey of solvents we found that MeCN was the solvent of choice that would completely dissolve compound **35'** but compound **35** will be partially dissolved. This provided a method of isolation of the desired product without column chromatography. The reaction was carried out in the mixture of MeOH and THF, the solvent was removed and organic residue was dissolved into MeCN. The isomer **35'**, due to better solubility would completely dissolve in the MeCN while the majority of compound **35** stayed as a precipitate, which was filtered and washed with MeCN to obtain a first crop of the pure product. The solution was concentrated allowing precipitation of second crop of product. The process was repeated one more time to get a third crop of the product. This method eliminated the need of column chromatography for purification purposes. We further investigated into the reaction and found that the reaction can be carried out in the acetonitrile, giving comparable yields.

Although this solved the problem of the isolation of the isomers, we obtained only a moderate yield. At this stage, a brief survey of the literature revealed 1,3-dibromo-5,5-dimethylhydantoin to be a useful brominating reagent.[22] We carried out the bromination using this reagent and were excited to obtain 95% yield of compound **35**.

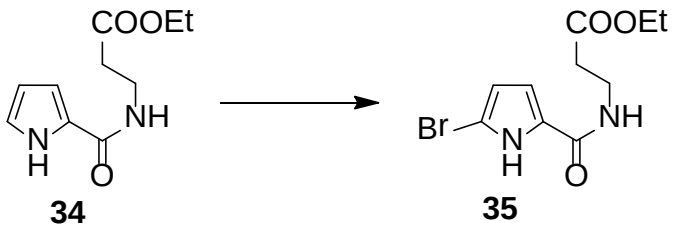

Scheme 1.9. Use of 1,3-dibromo-5,5-dimethylhydantoin for bromination

Reactions and conditions: 1,3-dibromo-5,5-dimethylhydantoin, MeOH/THF -78^{O}C-rt, 95%

Consequently compound **35** was hydrolysed (Scheme 1.10). Both LiOH and KOH worked well giving very good yields of 98%.

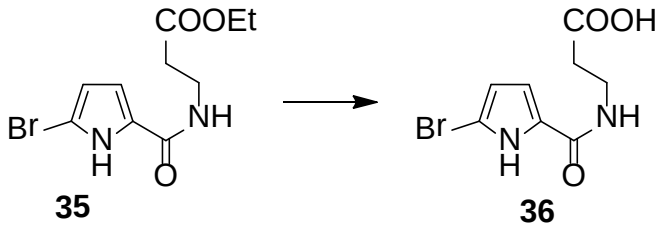

Scheme 1.10. Hydrolysis of compound 35

Reactions and conditions: LiOH or KOH, EtOH, H_2O, rt, 18h, 98%

In the next stage the ring closure of the compound **36** was carried out to provide aldisine **16**.

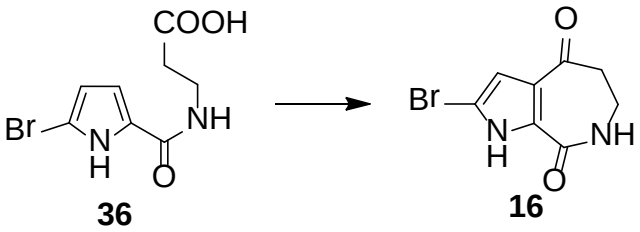

Scheme 1.11. Synthesis of aldisine 16

Reactions and conditions: (i) $(COCl)_2$, DMF (Cat.) DCM, rt, 30 min. (ii) $AlCl_3$, DCM, rt, 18h 40% or P_2O_5, $MeSO_3H$, 110^oC, 2h, 76%

In this reaction, we wanted to utilize milder conditions of aluminum chloride mediated reaction; however, the reaction results were inconsistent with low yield at times and no product formation at others. Therefore, we studied the scope of solvent and found that DCM was the solvent of choice giving 40% yield of the aldisin **16**, while other solvents did not show the formation of product. Although the conditions were milder, the yield of the reaction was not promising. At this stage we checked the reaction condition used by Tepe and co-workers,[12, 20] and utilized phosphorous pentoxide in methanesulfonic acid at elevated temperatures. Although the reaction takes place at elevated temperature, the reaction time was considerably short and the reaction yields were consistant and higher than the reaction with $AlCl_3$.

In the next step we were interested in modifying the route so that we could obtain the stable intermediate, unlike the previously reported synthesis.[16b] We envisioned that the

use of a different glycocyamidine precursor, the imidazolone **42 (**Figure 1.5**)** could eliminate the issue of the instability associated with intermediates **40** and **41**.

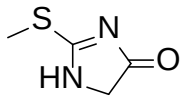

Figure 1.5. Imidazolone 42

Our plan was supported by the literature, which has cited a few examples where this molecule has been utilized to carry out Aldol condensation.[23]

We prepared compound **42** from 2-thiohydantoin as shown in scheme 1.12 using methyl iodide, Huning's base and catalytic amount of dimethylamino pyridine.

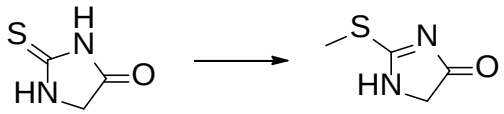

Scheme 1.12. Synthesis of imidazolone 42

Reactions and conditions: MeI, iPr_2EtN, DMAP (cat.), DCM, rt, 2.5h, 94%

Consequently we carried out the coupling of compound **42** with aldisine **16** in a titanium (IV) chloride mediated condensation[12, 20] to yield the compound **43** in very good yield. Compound **43** was stable and could be purified by column chromatography. Besides

titanium (IV) chloride, we also attempted to see the feasibility of boron trifluoride mediated reaction, however, the reaction led to the recovery of the starting material.

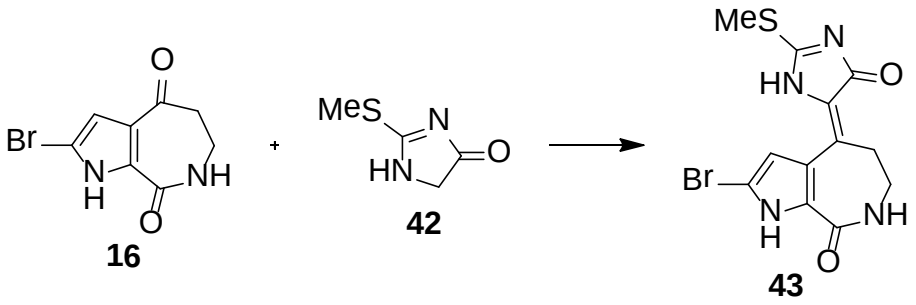

Scheme 1.13. Condensation of aldisine 16 with imidazolone 42

Reactions and conditions: $TiCl_4$, py, THF, -10^{o}C-rt, 82%

In the last step compound **43** was stirred with ammonium hydroxide in a sealed tube affording **1** in 77% yield.

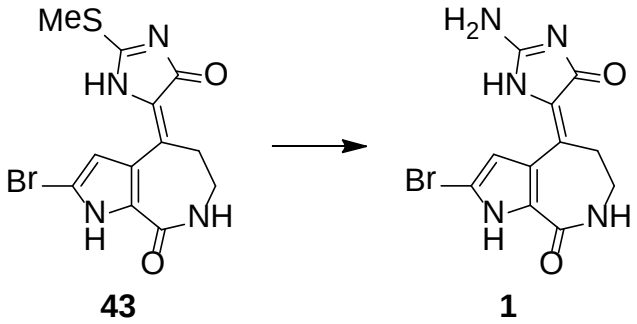

Scheme 1.14. Last step in the synthesis of HMD

Reactions and conditions: NH_4OH, THF, sealed tube, 110^{o}C, 77%

The total synthesis of the natural product was completed in six linear steps. We were able to achieve high selectivity of the bromination of the pyrrole ring and obtained the stable penultimate compound.

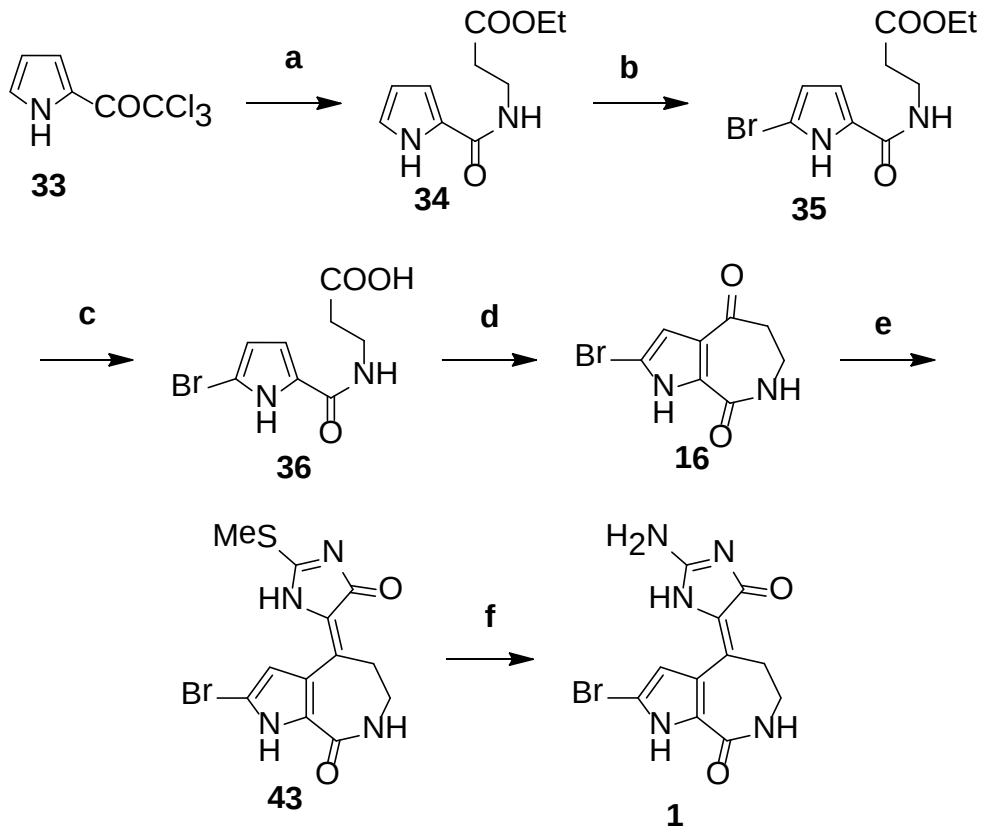

Scheme 1.15. Synthesis of HMD

Reactions and conditions: (a) $H_2NCH_2CH_2COOEt.HCl$, Et_3N, DCM, rt, 99% (b) 1,3-dibromo-5,5-dimethylhydantoin, MeOH/THF -78^{o}C-rt, 95% (c) LiOH or KOH, EtOH, H_2O, rt, 18h, 98% (d) P_2O_5, $MeSO_3H$, 110^{o}C, 2h, 76% (e) **42**, $TiCl_4$, py, THF, -10^{o}C-rt, 82% (f) NH_4OH, THF, sealed tube, 110^{o}C, 77%

As compared to previous synthesis where the last two steps yielded 25% overall yield,[16b] we were also able to increase the yield of the reaction for the last two steps to 63%. The overall synthesis is presented as in scheme 1.15. The compound **43** can be utilized for the synthesis of novel analogs of the natural product by reaction the compound with appropriate nucleophiles.

The highlights of the synthetic route include:

1- Lesser number of synthetic steps to achieve the synthesis of the natural product
2- Lack of the use of any protecting group in the synthetic approach.
3- High over all yield of the synthetic route. The comparison of the present approach to previous syntheses is presented in table 1.2

Table 1.2. Comparison of the synthetic routes use for total synthesis of HMD

Sr. No.		No. of steps	Overall yield (%)
1	Annoura and co-workers	10	0.15
2	Xu and coworkers	7	10.68*
3	Xu and coworkers-alternate route	7	9.72*
4	Papeo and coworkers	7	7.92
5	Our work	6	44.23

* Yield of first step not mentioned

1.5. Utilization of imidazolone 42 in improved synthesis of indolic derivative of HMD 49

Previously, we have reported the synthesis of indoloazepinone **49** shown in the scheme 1.16.[12, 20] The synthesis utilized commercially available indole-2-carboxylic acid. The reaction of indole-2-carboxylic acid with β-alanine ethyl ester in the presence of EDCI and DMAP afforded compound **45**.

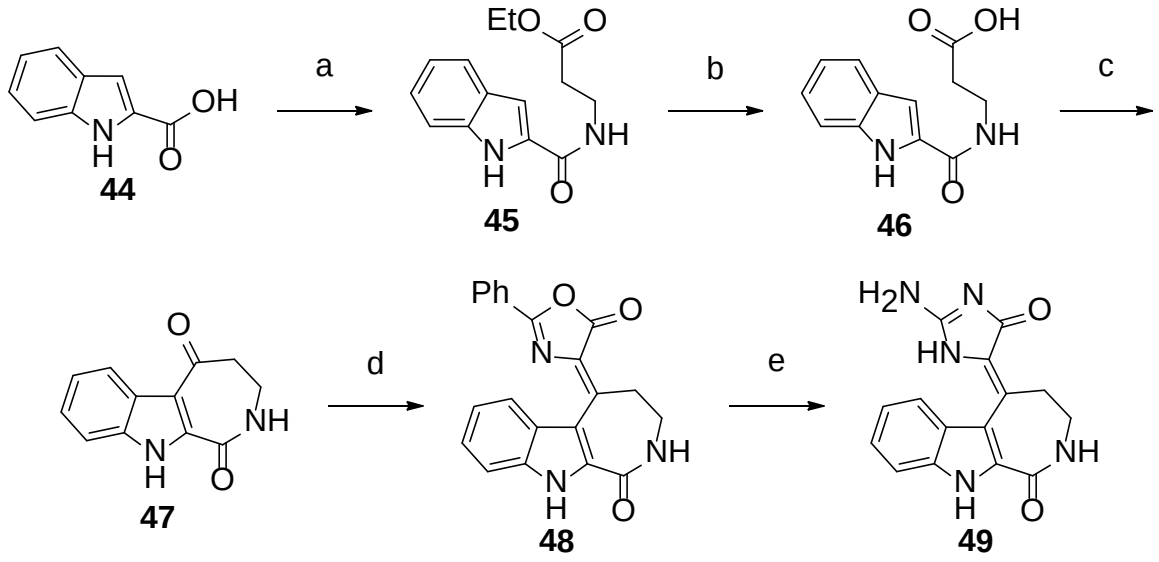

Scheme 1.16. Synthetic route to indoloazepinone derivative of HMD

Reactions and conditions: (a) $H_2NCH_2CH_2COOEt.HCl$, EDCI, DCM, rt, 98% (b) LiOH, H_2O 93% (c) P_2O_5, $MeSO_3H$ 110^oC 85% (d) **37**, $TiCl_4$, py, THF, 0^oC-rt 55% (e) S-Benzyl isothiouronium, LiH, EtOH 28%

Hydrolysis of the compound **45** followed by $P_2O_5/MeSO_3H$ mediated cyclization provided the key intermediate indoloaldisine **47**. The $TiCl_4$ mediated aldol condensation of compound **47** with **37** provided the oxazolone derivative **48**. In the last step, the oxazolone derivatives **48** was treated with S-benzylthiourea under basic conditions to give the indolic derivative of HMD in modest yields.

We were interested in improvement of the synthetic routes because the compound **48** was instable and at the same time the route suffered from low yields in the last two steps as the combined yield for these two steps was just 15%.

After utilizing compound **42** in the synthesis of HMD, we envisioned that use of this compound would lead to the stable intermediate in the penultimate step and improve the overall yield of the reaction. Therefore, indoloaldisine **47** was prepared as reported previously[12, 20] and imidazolone **42** was coupled to indoloaldisine **47** in a titanium (IV) chloride mediated condensation affording the stable compound **50** in 72% yield.

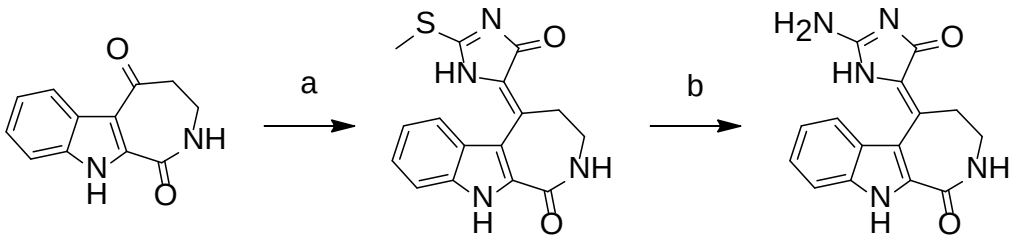

47 **50** **49**

Scheme 1.17. Improved synthesis of indoloazepinone

Reactions and conditions: (a) **42**, $TiCl_4$, py, THF, -10^{o}C-rt, 72% (b) NH_4OH, THF, sealed tube, 90^{o}C, then 10%HCl, 67%

In the next step compound **50** was heated in sealed tube with ammonium hydroxide and resulted precipitate which was collected as the HCl salt affording **49** in 67% yield.

This modification lead to the improvement of the yield as now the yield for last two reactions was 48% as compared to 15% in the previous route. This modification also gave intermediate **50,** which is stable and can be purified by column chromatography, and provides a handle to carry out SAR by modifying the reagents in the last step.

1.6. Experimental Section

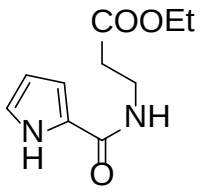

Ethyl 3-(1H-pyrrole-2-carboxamido)propanoate(34):

2,2,2-trichloro-1-(1H-pyrrol-2-yl)-ethanone **33** (1g, 4.7mmol) was dissolved in dichloromethane (20mL) and β-alanine ethyl ester hydrochloride (793mg, 5.18mmol) and triethyl amine (0.79mL, 5.64mmol) were added to the solution. The reaction mixture was stirred at room temperature for 36 hours at which time the solvent was removed on rotary evaporator. The residue, thus obtained, was dissolved in ethyl acetate (100 mL) and then transferred to a separatory funnel. The organic solution was washed with 5% HCl (100mL x 2) and then with saturated brine (100mL). The aqueous layers were discarded and the organic layer was dried over anhydrous Na_2SO_4 (1g) and filtered over charcoal. The solvent was, then, removed in vacuo yielding product **34** (980mg, 99%). m.p. 60°C; ^{1}H NMR (500 MHz, $CDCl_3$) 6.88-6.90 (1H, m), 6.57-6.59 (1H, m), 6.16-6.18 (1H, m) , 4.13 (2H, q, J = 7.0 Hz), 3.66 (2H, q, J = 6.0 Hz), 2.59 (2H, t, J = 6.0 Hz), 1.23 (3H, t, J = 7.0 Hz); ^{13}C NMR (125 MHz, $CDCl_3$) δ 172.7, 161.4, 125.7, 121.8(s), 109.5(s), 109.3(s), 60.7(d), 34.7(d), 34.1(d), 14.1(t); IR (film): 3300, 1732, 1720, 1617, 1570, 1437, 1410, 1199 cm-1; MS (ES) m/z 211.1 $[M+H]^+$; HRMS (ESI) m/z calcd for $C_{10}H_{15}N_2O_3$ $[M+H]^+$ 211.1083, found: 211.1087.

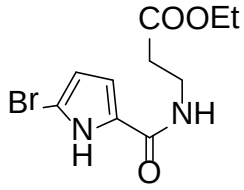

Ethyl 3-(5-bromo-1H-pyrrole-2-carboxamido)propanoate (35):

Compound **34** (6g , 28.56mmol) was dissolved in a mixture of tetrahydrofuran and methanol (2:1, 400mL) at -78°C and 1,3-dibromo-5,5-dimethylhydantoin (4g, 14.28mmol) was added to this solution. The reaction mixture was then stirred for 16 hours, during which the temperature of the mixture gradually rose to the room temperature. Then the solvent was removed using rotary evaporator and the crude material was purified by column chromatography (silica, 1:1 Ethyl acetate/Hexanes) affording **35** (7.85g, 95%). m.p. 122°C; ^{1}H NMR (500 MHz, CD_3OD) δ 6.68 (d, J = 4.0, 2.8 Hz, 1H), 6.11 (dd, J = 4.0, 2.8 Hz, 1H), 4.12 (q, J = 7.0 Hz, 2H), 3.55 (t, J = 7.0 Hz, 2H), 2.59 (t, J = 7.0 Hz, 2H), 1.23 (t, J = 7.0 Hz, 3H); ^{13}C NMR (125 MHz, CD_3OD) δ 171.3, 159.8, 126.0, 117.1, 110.9 (s), 106.9 (s), 59.9 (d), 34.8 (d), 34.0 (d), 14.1 (t); IR (film): 3340, 1715, 1643, 1559, 1529, 1394, 1374, 1325 cm^{-1}; MS (ES) m/z 289.0 $[M+H]^+$; HRMS (ESI) m/z calcd for $C_{10}H_{14}N_2O_3Br$ $[M+H]^+$ 289.0188, found: 289.0188.

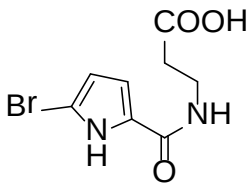

3-(5-bromo-1H-pyrrole-2-carboxamido)propanoic acid (36):

Compound **35** (13g, 4mmol) was dissolved in ethanol (100mL) in a 250mL round bottom flask. Lithium hydroxide monohydrate (3.77 g, 89.92 mmol) was dissolved in water (50mL) and added to the reaction mixture at 25°C. The reaction mixture was stirred at room temperature for 19 hours. The TLC revealed the completion of hydrolysis. At this stage the solvent was evaporated in vacuo and the resulting carboxylate salt was dissolved in H_2O (100mL). The mixture was acidified with concentrated HCl until pH=1 leading to the precipitation of the desired product. The suspension of the product was stirred for 15 minutes and then collected by filtration and dried under vacuo affording compound **36** (11.4g, 97%). m.p. 162-164°C; ^{1}H NMR (500MHz, CD_3OD) δ 6.68 (d, J=3.8Hz, 1H), 6.1 (d, J=3.8H, 1H), 3.55 (t, J=6.9, 2H), 2.58 (t, J=6.9, 2H); ^{13}C NMR (125MHz; CD_3OD) δ 175.4, 162.6, 128.5, 113.3 (s), 112.4 (s), 104.3, 36.7(d), 34.9(d); IR (film): 3433, 2533, 1704, 1686, 1653, 1595, 1560; MS (ES) m/z: 261.0$[M+H]^+$; HRMS (ES+) m/z calcd for $C_8H_{10}N_2O_3Br$ $[M+H]^+$ 260.9875, found: 260.9876.

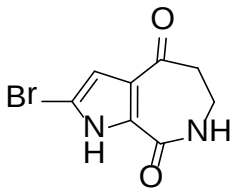

2-bromo-6,7-dihydropyrrolo[2,3-c]azepine-4,8(1H,5H)-dione (16):

Methanesulfonic acid (50mL) was warmed to 110°C in a round bottom flask and P_2O_5 (10.33 g, 72.78mmol) was added to this flask. The reaction mixture was stirred till it became a clear solution. At this stage **36** (9.5g, 36.39mmol) was added to the reaction mixture and the reaction mixture was stirred for 2 hours at 110°C. Then the contents of the flask were cooled to room temperature and neutralized with 10% aqueous $NaHCO_3$. Then the product was extracted with EtOAc (200 mL x 4). The EtOAc fractions were combined and dried over anhydrous Na_2SO_4 (2g). The solvent was removed and the crude material was purified by column chromatography (silica, ethyl acetate) affording **16** (6.7g, 76%). m.p. 144-145°C; ^{1}H NMR (500MHz, $CDCl_3$) δ 6.55 (s, 1H), 3.33-3.34 (m, 2H), 2.68-2.70 (m, 2H); ^{13}C NMR (125MHz, $CDCl_3$) δ 193.5, 161.1, 129.7, 124.6, 111.2 (s), 105.0, 43.4 (d), 36.21 (d); IR (film): 3192, 2521, 1650, 1647, 1471, 1458 cm^{-1}; MS (ES) m/z: 243.0 $[M+H]^+$; HRMS (ES+) m/z calcd for $C_8H_8N_2O_2Br$ $[M+H]^+$ 242.9769, found 242.9773.

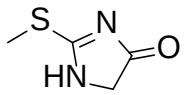

2-(methylthio)-1H-imidazol-4(5H)-one (42):

2-Thiohydantoin (3 g, 25.83 mmol) was dissolved in dichloromethane (20mL) at room temperature and iodomethane (6.4 mL, 103mmol), DIPEA (9mL, 52mmol) and DMAP (0.31g, 2.58 mmol) were added to the solution. The resulting mixture was stirred for 2.5 hours at room temperature and then the solvent was removed on rotary evaporator. The crude material was purified by column chromatography (silica, ethyl acetate) affording compound **42** (solid, 3.57 g, 94%).m.p. decomposed over 160°C. ^{1}H NMR (500 MHz, CD_3OD) δ 6.63 (broad N-H, 1H), 4.51 (s, 2H), 2.84 (s, 3H); ^{13}C NMR (125 MHz, CD_3OD) δ 178.3, 172.9, 52.6, 14.3(d); IR (KBr, pellet): 3091, 2915, 1754, 1669, 1511, 1444, 1389, 1330, 1291, 1251, 1230, 1173 cm^{-1}; MS (ES) m/z 131.0 $[M+H]^+$; HRMS (ESI): m/z calcd for $C_4H_7N_2OS$ $[M+H]^+$, 131.0279; found, 131.0284.

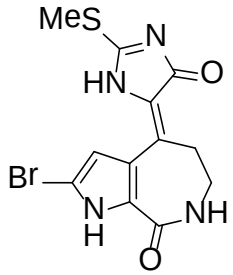

(Z)-2-bromo-4-(2-(methylthio)-4-oxo-1H-imidazol-5(4H)-ylidene)-4,5,6,7-tetrahydropyrrolo[2,3-c]azepin-8(1H)-one (43):

Compound **16** (100mg, 0.41mmol) was dissolved in THF (20mL) and compound **42** (106mg, 0.82mmol) was added to the reaction flask. The reaction mixture was cooled to $0^{\circ}C$ and 1M solution of $TiCl_4$ in DCM (1.64mL, 1.64mmol) was added to the reaction mixture in dropwise manner. The reaction mixture was stirred for 30 minutes and pyridine (0.26mL, 3.29mmol) was added to the reaction mixture dropwise. The reaction mixture was stirred for an additional 14 hours allowing it to gradually warm to room temperature. At this point saturated NH_4Cl solution (40mL) was added to the reaction mixture and contents of the flask were transferred to the separatory funnel. Then the crude product was extracted with ethyl acetate (3 x 50mL). The ethyl acetate fractions were combined and dried over anhydrous Na_2SO_4 (1g). The solvent was removed and the crude material was purified by column chromatography (silica, ethyl acetate) to afford **43** (120 mg, 82%) m.p. decomposes above $260^{o}C$; ^{1}H NMR (500MHz, DMSO-d_6) δ 7.59 (d, J=2.7Hz, 1H), 3.42-3.40 (m, 2H), 3.23-3.20 (m, 2H), 2.58 (s, 3H); ^{13}C NMR (125MHz, DMSO-d_6) δ 170.5, 161.9, 158.9, 134.2, 133.7, 128.7, 124.2, 115.4(s), 104.0, 40.0(d), 29.67(d), 12.11 (t); IR (film): 3275, 2496, 1686, 1653, 1645, 1635, 1595, 1473; MS (ES) m/z: 355.0 $[M+H]^{+}$; HRMS (ES+) m/z calcd for $C_{12}H_{12}N_4O_2S$ $[M+H]^{+}$ 354.9864, found 354.9866.

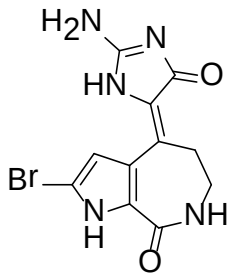

(Z)-4-(2-amino-4-oxo-1H-imidazol-5(4H)-ylidene)-2-bromo-4,5,6,7-tetrahydropyrrolo[2,3-c]azepin-8(1H)-one (1):

Compound **43** (50 mg, 0.141 mmol) was added to THF (5mL) in a sealed tube and ammonium hydroxide (5 mL) was added to the solution. The resulting mixture was heated at 90°C for 24 hours and then allowed to cool to room temperature. Then the reaction mixture was concentrated and crude material was purified by column chromatography (silica, 1:4 MeOH/DCM) to afford HMD **1** (35.1mg, 77%). m.p. decomposes above 250°C; ^{1}H NMR (500MHz, DMSO-d_6+ drop of CF_3COOH) δ 6.5 (d, J=2.5Hz, 1H), 3.24 (Br, 4H); ^{13}C NMR (125MHz, DMSO-d_6+ drop of CF_3COOH) δ 163.5, 162.7, 162.3, 129.0, 128.6, 121.9, 121.2, 111.6(s), 105.5, 39.01 (d), 32.6 (d); IR (film): 3404, 3275, 2442, 2253, 1772, 1716, 1701, 1653; MS (ES) $^{m}/_{z}$: 324.0 $[M+H]^{+}$; HRMS (ES+) m/z calcd for $C_{10}H_{15}NO_6Br$ $[M+H]^{+}$ 324.0083, found 324.0085.

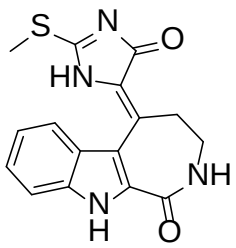

(Z)-5-(2-(methylthio)-4-oxo-1H-imidazol-5(4H)-ylidene)-2,3,4,5-tetrahydroazepino[3,4-b]indol-1(10H)-one (50):

Compound **47** (200mg, 0.5mmol) was dissolved in THF (20mL) and compound **42** (219mg, 0.93mmol) was added to the reaction flask. The resulting reaction mixture was cooled to 0^{o}C and 1M solution of $TiCl_4$ in DCM (1.9 mL, 1.9 mmol) was added to the reaction mixture in dropwise manner. The reaction mixture was stirred for 30 minutes and then pyridine (0.30mL, 3.7mmol) was added to the reaction mixture over a 15 minutes period. The reaction mixture was stirred for an additional 14 hours allowing the temperature to gradually rise to room temperature. At this point the saturated NH_4Cl solution (40mL) was added to the reaction mixture and contents of the flask were transferred to the separatory funnel. Then the crude product was extracted with ethyl acetate (4 x 40mL). The ethyl acetate fractions were combined and dried over anhydrous Na_2SO_4 (1g). The solvent was removed and the crude material was purified by column chromatography (silica, ethyl acetate) to afford **10** (110 mg, 72%). m.p. decomposes over 190^{o}C; ^{1}H NMR (500 MHz, DMSO-d_6) δ 2.33 (s, 3H), 3.34-3.40 (m, 4H), 7.06 (t, J = 7.2 Hz, 1H), 7.21 (t, J = 7.0 Hz, 1H), 7.41 (d, J = 8.2 Hz, 1H), 8.33 (t, J = 5.1 Hz, 1H), 11.59 (s, 1H), 12.19 (s, 1H); ^{13}C NMR (128.2 MHz, DMSO-d_6) δ 169.7, 164.7, 157.9, 135.9, 135.2, 134.8, 131.7, 125.9, 125.2(s), 123.8(s), 119.2(s), 115.3,

111.9(s), 38.9(d), 35.6(d), 12.0(t); IR (KBr): 3220, 1700, 1650, 1540, 1480 cm^{-1}; MS (ES) $^{m}/_{z}$: 327.1 $[M+H]^{+}$; HRMS (ES+) m/z calcd for $C_{16}H_{15}N_4O_2S$ $[M+H]^{+}$ 327.0916, found, 327.0914.

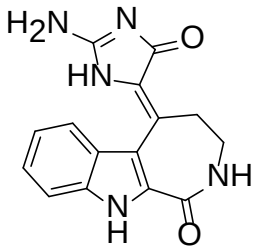

(Z)-5-(2-amino-4-oxo-1H-imidazol-5(4H)-ylidene)-2,3,4,5-tetrahydroazepino[3,4-b]indol-1(10H)-one (49): Compound **50** (1g, 3mmol) was dissolved in THF (10mL) and stirred with ammonium hydroxide (30mL) at 90°C in a sealed tube for 24 hours. The reaction mixture was allowed to cool to room temperature at which point the precipitate was filtered from the reaction mixture. The solid was collected and washed in 10% HCl and filtered a second time. The bright yellow solid was filtered and dried *in vacuo* (617 mg, 69.2%). m.p. decomposes over 260°C; ^{1}H NMR (500 MHz, DMSO-d_6) δ 12.45 (s, 1H), 10.31 (s, 1H), 9.05 (br, 1H), 8.36 (br, 2H), 7.52-7.57 (m, 2H), 7.31 (t, J = 7.9 Hz, 1H), 7.19 (t, J = 7.9 Hz, 1H), 3.32-3.39 (m, 4H); ^{13}C NMR (128.2 MHz, DMSO-d_6) δ 165.5, 163.3, 154.5, 137.0, 132.9, 128.9, 125.0, 124.6(s), 122.9, 122.4(s), 121.9(s), 113.6, 112.7(s), 39.2(d), 36.6(d); IR: (KBr) 3209, 1701, 1618, 1529, 1469, 1250 cm^{-1};

MS (ES) $^{m}/_{z}$: 296.1[M+H]$^{+}$; HRMS (ES+) m/z calcd for $C_{15}H_{13}N_5O_2$ [M+H]$^{+}$ 296.1069, found 296.1144.

References

1.7. References

1. (a) Li, J. W.; Vederas, J. C., Drug discovery and natural products: end of an era or an endless frontier? *Science* 2009, *325*, 161-5; (b) Hamilton, G. R.; Baskett, T. F., In the arms of Morpheus the development of morphine for postoperative pain relief. *Can. J. Anaesth.* 2000, *47*, 367-74; (c) Huxtable, R. J.; Schwarz, S. K., The isolation of morphine-first principles in science and ethics. *Mol. Interv.* 2001, *1*, 189-91.

2. Newman, D. J.; Cragg, G. M., Natural products as sources of new drugs over the last 25 years. *J. Nat. Prod.* 2007, *70*, 461-77.

3. Ciminoa, G.; Rosaa, S. D.; Stefanoa, S. D.; Mazzarellab, L.; Pulitia, R.; Sodano, G., Isolation and X-ray crystal structure of a novel bromo-compound from two marine sponges. *Tetrahedron Lett.* 1982, *23*, 767-8.

4. Meijer, L.; Thunnissen, A.-M.; White, A.; Garnier, M.; Nikolic, M.; Tsai, L.-H.; Walter, J.; Cleverley, K.; Salinas, P.; Wu, Y.-Z.; Biernat, J.; Mandelkow, E.-M.; Kim, S.-H.; Pettit, G., Inhibition of cyclin-dependent kinases, GSK-3β and CK1 by hymenialdisine, a marine sponge constituent. *Chem. Biol.* 2000, *7*, 51-63.

5. Wan, Y.; Hur, W.; Cho, C. Y.; Liu, Y.; Adrian, F. J.; Lozach, O.; Bach, S.; Mayer, T.; Fabbro, D.; Meijer, L.; Gray, N. S., Synthesis and target identification of hymenialdisine analogs. *Chem. Biol.* 2004, *11*, 247-59.

6. Sharma, G. M.; Buyer, J. S.; Pomerantz, M. W., Characterization of a yellow compound isolated from the marine sponge phskellia-flabellata. *J. Chem. Soc., Chem. Commun.* 1980, 435-6.

7. (a) Mattia, C. A.; Mazzarella, L.; Puliti, R., 4-(2-Amino-4-oxo-2-imidazolin-5-ylidene)-2-bromo-4,5,6,7-tetrahydropyrrolo[2,3-c]azepin-8-one methanol solvate: a new bromo compound from the sponge Acanthella Aurantiaca. *Acta Crystallogr. Sect. B: Struct. Sci.* 1982, *38*, 2513-5; (b) Kitagawa, I.; Kobayashi, M.; Kitanaka, K.; Kido, M.; Kyogoku, Y., Marine natural products. XII. On the chemical constituents of the Okinawan marine sponge Hymeniacidon aldis. *Chem. Pharm. Bull.* 1983, *31*, 2321-8.

8. Kobayashi, J.; Ohizumi, Y.; Nakamura, H.; Hirata, Y.; Wakamatsu, K.; Miyazawa, T., Hymenin, a novel alpha-adrenoreceptor blocking agent from the Okinawan marine sponge Hymeniacidon sp. *Experientia* 1986, *42*, 1064-5.

9. Denanteuil, G.; Ahond, A.; Guilhem, J.; Poupat, C.; Dau, E. T. H.; Potier, P.; Pusset, M.; Pusset, J.; Laboute, P., Marine-invertebrates from neo-caledonian lagoons .5. Isolation and identification of metabolites from a new species of sponge, Pseudaxinyssa-cantharella. *Tetrahedron* 1985, *41*, 6019-33.

10. Tasdemir, D.; Mallon, R.; Greenstein, M.; Feldberg, L. R.; Kim, S. C.; Collins, K.; Wojciechowicz, D.; Mangalindan, G. C.; Concepción, G. P.; Harper, M. K.; Ireland, C. M., Aldisine alkaloids from the Philippine Sponge Stylissa massa are potent inhibitors of mitogen-activated protein kinase kinase-1 (MEK-1). *J. Med. Chem.* 2002, *45*, 529-32.

11. Breton, J. J.; Chabot-Fletcher, M. C., The natural product hymenialdisine inhibits interleukin-8 production in U937 cells by inhibition of nuclear factor-kappaB. *J. Pharmacol. Exp. Ther.* 1997, *282*, 459-66.

12. Sharma, V.; Tepe, J. J., Potent inhibition of checkpoint kinase activity by a hymenialdisine-derived indoloazepine. *Bioorg. Med. Chem. Lett.* 2004, *14*, 4319-21.

13. Barrios Sosa, a. C.; Yakushijin, K.; Horne, D. A., A practical synthesis of (Z)-debromohymenialdisine. *J. Org. Chem.* 2000, *65*, 610-1.

14. Portevin, B.; Golsteyn, R. M.; Pierré, A.; De Nanteuil, G., An expeditious multigram preparation of the marine protein kinase inhibitor debromohymenialdisine. *Tetrahedron Lett.* 2003, *44*, 9263-5.

15. Annoura, H.; Tatsuoka, T., Total syntheses of hymenialdisine and debromohymenialdisine: Stereospecific construction of the 2-amino-4-oxo-2-imidazolin-5(Z)-disubstituted y ylidene ring system. *Tetrahedron Lett.* 1995, *36*, 413-6.

16. (a) Xu, Y.-z.; Yakushijin, K.; Horne, D. A., Synthesis of C11N5 marine sponge alkaloids: (±)-Hymenin, Stevensine, Hymenialdisine, and Debromohymenialdisine. *J. Org. Chem.* 1997, *62*, 456-4; (b) Papeo, G.; Posteri, H.; Borghi, D.; Varasi, M., A new glycociamidine ring precursor: syntheses of (Z)-hymenialdisine, (Z)-2-debromohymenialdisine, and (+/-)-endo-2-debromohymenialdisine. *Org. Lett.* 2005, *7*, 5641-4.

17. Davis, F. A.; Vishwakarma, L. C.; Billmers, J. M.; Finn, J., Synthesis of alpha-hydroxycarbonyl compounds (acyloins): Direct oxidation of enolates using 2-sulfonyloxaziridines. *J. Org. Chem.* 1984, *49*, 3241-3.

18. Feldman, K. S.; Saunders, J. C.; Wrobleski, M. L., Alkynyliodonium salts in organic synthesis. Development of a unified strategy for the syntheses of (-)-agelastatin A and (-)-agelastatin B. *J. Org. Chem.* 2002, *67*, 7096-9.

19. Domostoj, M. M.; Irving, E.; Scheinmann, F.; Hale, K. J., New total synthesis of the marine antitumor alkaloid (-)-agelastatin A. *Org. Lett.* 2004, *6*, 2615-8.

20. Sharma, V.; Lansdell, T. A.; Jin, G.; Tepe, J. J., Inhibition of cytokine production by hymenialdisine derivatives. *J. Med. Chem.* 2004, *47*, 3700-3.

21. Prager, R. H.; Tsopelas, C., Knoevenagel reactions of 6,7-dihydropyrrolo(2,3-c)azepine- 4,8(1H,5H)- dione: An approach to the synthesis of pyrrolic marine natural products. *Aust. J. Chem.* 1992, *45*, 1771-7.

22. (a) Davis, F. A.; Zhang, J. Y.; Zhang, Y. F.; Qiu, H., Improved synthesis of (-)-agelastatin A. *Synth. Commun.* 2009, *39*, 1914-9; (b) Chassaing, C.; Haudrechy, A.; Langlois, Y., 1,3-dibromo-5,5-dimethylhydantoin, a useful reagent for aromatic bromination. *Tetrahedron Lett.* 1997, *38*, 4415-6.

23. (a) Johnson, T. B.; Nicolet, B. H., Researches on hydantoins. XXXV. A new method of synthesizing glycocyamidine compounds, and the conversion of glycocyamidine into isomers of creatinine. *J. Am. Chem. Soc.* 1915, *37*, 2416-26; (b) Venuti, M. C.; Jones, G. H.; Alvarez, R.; Bruno, J. J., Inhibitors of cyclic AMP phosphodiesterase. 2. Structural variations of N-cyclohexyl-N-methyl-4-[(1,2,3,5-tetrahydro-2-oxoimidazo[2,1-b]quinazolin-7-yl)oxy]butyramide (RS-82856). *J. Med. Chem.* 1987, *30*, 303-18.

CHAPTER 2

SYNTHESIS AND KINASE PROFILING OF NOVEL 2-ARYLPYRROLOAZEPINONE BASED HMD ANALOGS

2.1. Introduction

In the past few centuries, our understanding of diseases has greatly increased. This understanding has helped us in the finding the cures of these diseases. These cures have significantly improved the human health and many diseases that were once considered incurable can now be treated. Therefore the life expectancy has increased and mortality has been reduced. In agreement, the mortality statistics of the United States of America show a continuing trend of decrease in the mortality (Table 2.1).

Table 2.1. Mortality rate in USA[a]

Year	1999	2000	2001	2002	2003	2004	2005	2006	2007	2008	2009
Total deaths	876	869	855	845	833	801	799	777	760	759	741

a. Age-adjusted death rates per 100,000 U.S. standard population, based on the year 2000 standard. source: NVSR Volume 58, Number 19. 73 pp. (PHS) 2010-1120, Deaths: Preliminary Data for 2009. NVSR Volume 59, Number 04. 69 pp. (PHS) 2011-1120, Deaths: Preliminary Data for 2008. NVSR Volume 59, Number 02. 72 pp. (PHS) 2011-1120.

Table 2.2. 15 major causes of mortality in USA

Year	1999	2001	2003	2005	2007	2009
Heart	30.4	29.0	27.9	26.4	25.1	24.3
Cancer	22.9	22.9	22.8	23.0	23.5	23.4
Cerebrovascular	7.0	6.8	6.4	5.8	5.6	5.2
Chronic lower respiratory diseases	5.2	5.1	5.2	5.4	5.4	5.7
Accidents	4.0	4.2	4.5	4.9	5.3	5.0
Alzheimer's diseases	1.9	2.2	2.6	2.9	3.0	3.2
Diabetes mellitus	2.9	3.0	3.0	3.1	3.0	2.8
Influenza and pneumonia	2.9	2.6	2.6	2.5	2.1	2.2
Nephritis, nephrotic syndrome and nephrosis	1.5	1.6	1.7	1.8	1.9	2.0
Septicemia	1.3	1.3	1.4	1.4	1.4	1.5
Intentional self-harm	1.2	1.3	1.3	1.4	1.5	1.6
Chronic liver disease and cirrhosis	1.1	1.1	1.1	1.1	1.2	1.2
Essential hypertension and hypertensive renal disease	0.7	0.8	0.9	1.0	1.0	1.0
Parkinson's disease	0.6	0.7	0.7	0.8	0.8	0.9
Assault	0.7	0.8	0.7	0.8	0.8	0.7

These statistics may seem pleasing but a look into the major causes of deaths show that today 15 causes of deaths, as shown in the Table 2.2, account for more than 80% of the mortality. Among these causes, the deaths due to two diseases, the cardiovascular disorders and the cancer account for more than 45% of all the deaths. These statistics points in the direction that cardiovascular diseases and cancer need more efforts towards the comprehending the underlying causes, the cellular processes, their mechanistic insights and search for the cure for these diseases.

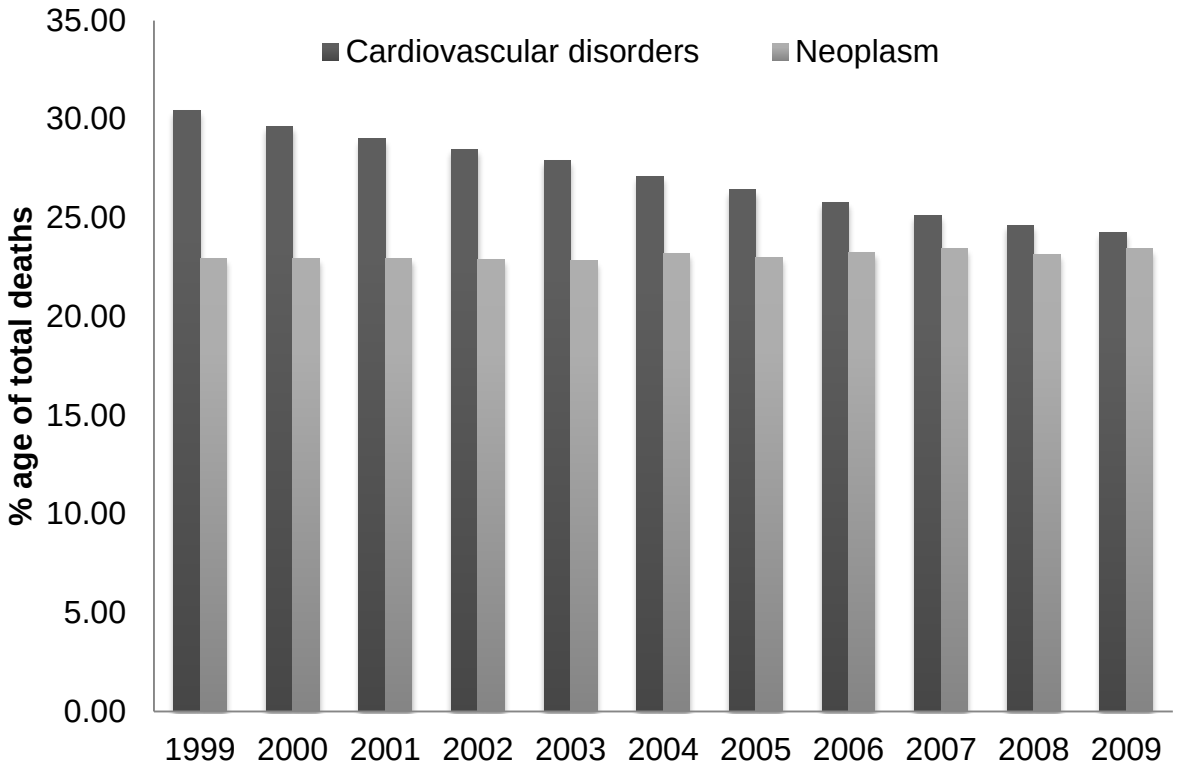

Figure 2.1. Comparison of mortality due to cardiovascular disorders vs neoplasm

Although new diseases keep showing up, owning to the alternations in the genetic material of humans and their pathogens, the major causes of death need major attention. When we compare the deaths due to the cardiovascular disorders and the cancer, we see a trend over the decade as shown in the graph in Figure 2.1. It shows that the death rate due to cardiovascular diseases is declining gradually, whereas the death rate due to cancer has been steady. This accounts for not only the discovery of new types of cancers but also for our lack of understanding of the existing types of the cancer. If the trend continues in the same directions, very soon cancer will be the major cause of deaths. This supports the need to improve our understanding of the biological processes involved in the cancer and develop superior therapies for the treatment of the cancer.

2.2. Present day treatments and their side effect

Aside from surgery, the present day cancer treatment involves chemotherapy, radiation therapy or a combination of both. However, these therapies suffer from the severe primary or secondary side effects on normal tissue. These side effects compromise the efficiency of the treatment and lead to only few months to a few years of post-treatment life expectancy.

2.3. Objective of research

Strategies that can help normal tissue withstand the severity of these therapies have the potential to improve the current therapeutic practices. In order to develop such strategies, the details of the cellular mechanisms need to be understood (mentioned in

the subsequent section). The use of DNA damaging agents has been one of the most effective therapy and has increased the survival rate of cancer patients.[1] The effectiveness of these therapies lies in their ability to induce DNA damage in the cancer cells. However, the DNA of normal cells is also damaged during these treatments and is mainly responsible for the harmful side effects. There is a need to develop the chemotherapeutic agents that can make normal tissues resistant to the DNA damaging effects. This can be achieved by understanding the differences in the cellular environment of the cancer cells and the normal cells. If we can develop the chemical compounds that can exploit these differences and block the cellular pathways of the normal cells for these side effect, we can develop adjuvant drugs for the cancer therapy. These adjuvant drugs, when used with the current treatments, will help in improving these treatments by decreasing the side effects on normal tissue.

2.4. Cellular pathway leading to damage in healthy cells

The DNA damaging agents upon damaging DNA lead to the activation of distinct responses in the cell in the form of the activation of the proteins that either attempt to repair the damaged DNA, or if the damage is beyond repair, carry out the apoptosis. One such protein which functions to selectively destroy the stressed and the abnormal cells, and is considered an “apoptotic superhero”[2] for its central role in the apoptosis, is p53.[3] More than 50% of the human tumors have mutations in the gene coding for p53.[4] As a result, the cancer cells, lack the ability to undergo p53 mediated apoptosis and continue to grow and divide. However, in normal cells that have normal p53 coding

gene, p53 triggers the apoptosis while performing its role as the “Guardian of genome”.[5] This apoptosis in the normal cells leads to the reduced effectiveness of the in-practice cancer treatments. Blocking the apoptosis in the normal cells will allow the cells more time to undergo repair and reduce the side effects of the therapies. Inhibiting p53 can inhibit the apoptosis in these cells. The preliminary work performed on cells that were derived from p53 knock-out mice[6] showed that p53 was required for the radiation induced cell death, but not necessary for all forms of apoptosis, supporting the importance of p53 in mediating the DNA-damage induced apoptosis. In the cancer therapies where DNA damage is induced by the DNA damaging agents or ionizing radiations, p53 plays an important role in apoptosis. However, direct inhibition of p53 is not a desired strategy to avoid the apoptosis in the normal cells as the studies have shown inconsistent results. In one report, it was shown that thermocytes isolated from p53 knockout mice showed complete resistance to γ-radiation induced lethality.[7] However the concurrent paper[8] showed that γ-radiation was capable of killing the proliferating T lymphocytes derived from the same p53 knockout mice.

2.5. Deeper look at the pathway

Among others, DNA damage leads to the activation of two major cellular pathways as shown in Figure 2.2.[9] Double strand breaks activate the ATM-ChK2 pathway while the replication lesions activate the ATR-ChK1 pathway. There is crosstalk between the two pathways and certain lesions activate both. In these cases ATM-ChK2 pathway is

activated transiently while ATR-ChK1 pathway is activated later in a more sustained way.[10] The expression of ChK1 upon replication damage is consistent with the cell cycle dependent expression of ChK1 which increases during S-phase and peaks in G_2, while ChK2 is expressed throughout the cell cycle and consistent with the broader role of its response to double strand breaks both during S-phase and independent of replication.[11]

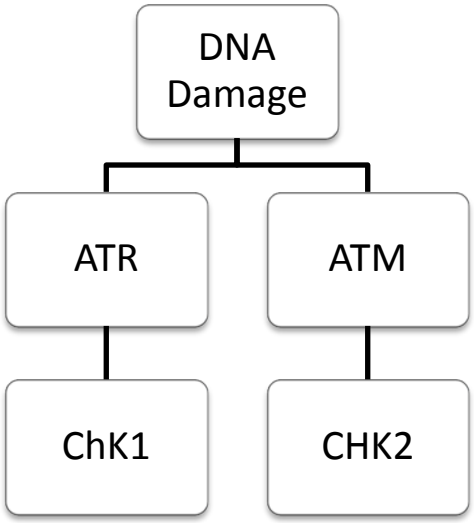

Figure 2.2. DNA damage responses

Upon activation, both the ChK1 and ChK2 activate a host of downstream proteins.[12] The ionizing radiations, used in chemotherapy, cause the double strand breaks and hence activate the ATM-ChK2 pathway. This pathway plays important role in p53 mediated apoptosis. The sequence of events that leads to apoptosis by this pathway can be divided into following series of events:

1. Group of chromatin events at site of DBS
2. Activation of damage sensors
3. Events of activation of ATM (kinase)
4. Events of ChK2 activation (Effector)
5. Events of cell cycle arrest
6. Events of p53 activation
7. Events leading to apoptosis

2.5.1. Group of chromatin events at DBS site

The DNA double strand break causes the phosphorylation of histone H2AX on serine 139 by DNA-PK and ATM.[13] The phosphorylated H2AX (known as γ-H2AX) is required for binding the sensor proteins to the altered chromatin and to keep the ends of the broken strands in proximity.[14] γ-H2AX provides the platform for the sensor proteins to attach at the damage site.

2.5.2. Activation of damage sensors

Once H2AX has been phosphorylated; the next step is the attachment of the sensor proteins. The BRCT protein complex, which include 53BP1, MDC1, Nbs1 and BRCA1, get attached to the damage site and contribute towards full activation of ATM in part by providing the scaffold for recruitment of the ATM.[15]

2.5.3. Activation of ATM

ATM normally exists as inactive dimer in the cellular environment. Binding of the dimer, to the altered DNA site, results in a conformational change that leads to autophosphorylation at serine 1981.[16] This autophosphorylation dissociates the dimer yielding an ATM monomer. The ATM monomer is the active form of the kinase. Once activated, ATM phosphorylates many proteins,[17] starting with BRCT domain sensor proteins, probably giving a positive feedback of attachment and activation. Downstream, it activates a number of proteins, including MdmX, p53, E2F1 and ChK2. Many proteins activated by ATM are also activated by ChK2 as well, probably providing multiple handles to control the pathway in response to different stimuli.

2.5.4. Activation of ChK2

ATM activates ChK2 by phosphorylating ChK2 at threonine 68.[18] ChK2 exists as monomer in the cellular environment and phosphorylation by ATM results in the dimerization of ChK2. The ChK2 then undergoes further autophosphorylation of threonine 383, 387 and serine 516 activating the kinase.[19] Once activated, ChK2 signals the activation of a number of proteins involved in the cell cycle control and the apoptosis. The ChK2 substrates, besides itself, include cdc25A, cdc25C, p53, MdmX, p53, PML, E2F1 and PP2A.

2.5.5. Events of cell cycle arrest

Cdc25 phosphatases, upon activation by ChK2, activate cyclin dependent kinases and lead to the cell cycle arrest. Cell cycle arrest is important, as it gives the damaged cells the time to repair before completing the cell cycle and passing the defect to the next cell generation. The Cdc25A controls the progression of cell cycle through G1-S phase and Cdc25C controls the progression through G2 phase.[20]

2.5.6. Events of p53 activation and apoptosis

The p53 is a major target of ChK2. Under the normal cellular conditions, the p53 levels in the cell are kept low with the assistance of Mdm2. Mdm2 binds to p53. This binding leads to polyubiquitination and then degradation of the p53. Thus Mdm2-p53 interaction keeps the transportation of p53 across nuclear membrane and transcriptional activity under check.[21] The cellular concentration of Mdm2 is regulated by MdmX. MdmX actives Mdm2, which in turn leads to the decrease in the p53 levels. ChK2 boosts the expression of p53 in two ways, directly as well as indirectly. In the direct mode of activation, the p53 is activated by ChK2 by phosphoraylation at serine 20.[22] This phosphorylation inhibits binding of p53 with Mdm2. This inhibition of their interaction avoids the polyubiquitination and degradation of p53, thus increasing the cellular concentration and transcriptional activity of p53. Indirectly ChK2 activates p53 by phosphorylating MdmX. Phosphorylated MdmX lack the ability to activate Mdm2, which in turn cannot keep p53 in check.

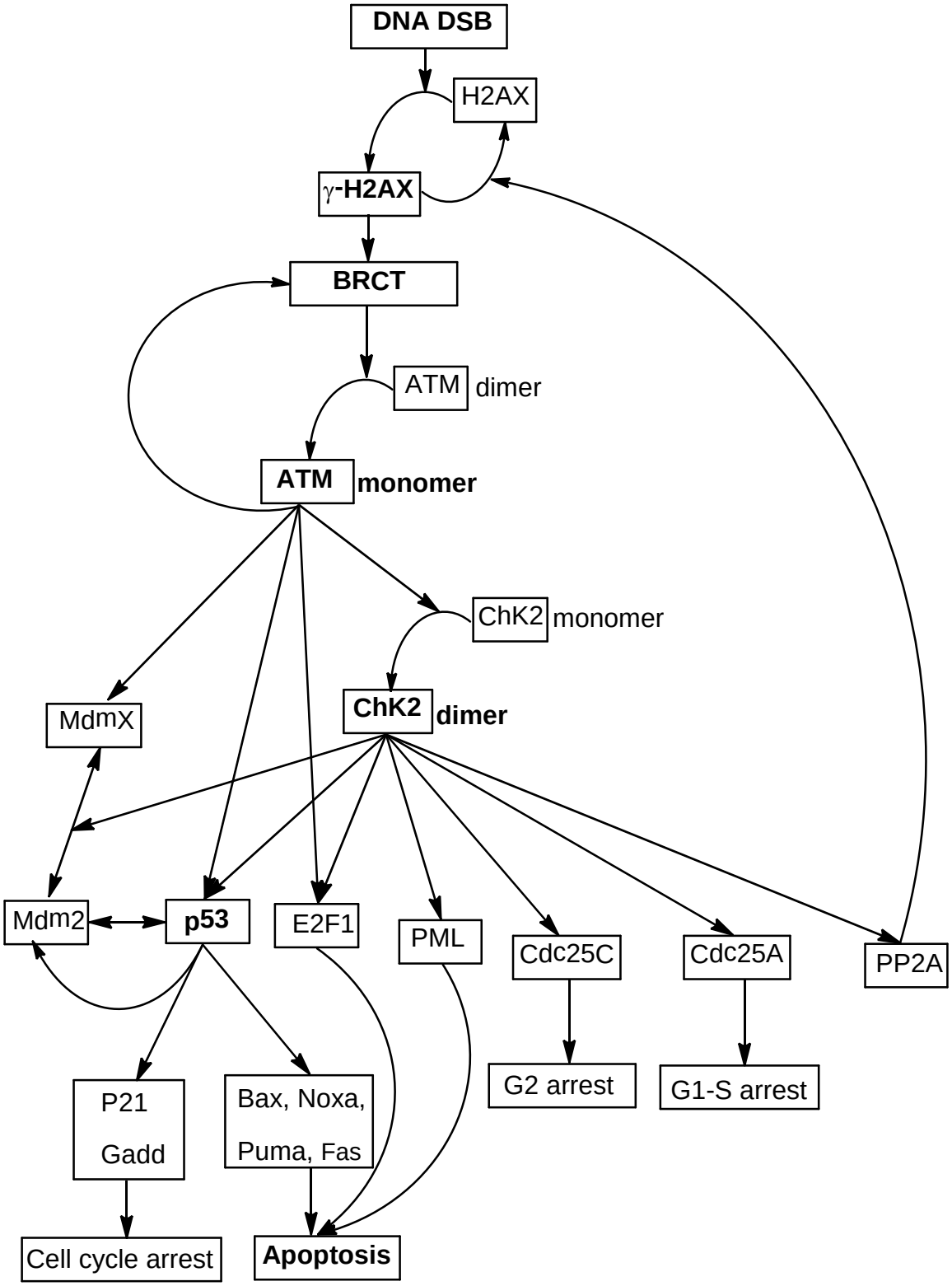

Figure 2.3. DNA damage response upon IR

2.5.7. Events leading to apoptosis

Once activated, the p53 protein transcriptionally activates a host of proteins that lead to cell cycle arrest or apoptosis. The cell cycle arrest is carried out by transcriptional activation of p21, and Gadd45, while the activation of the genes like *Bax*, *Noxa*, *Puma* and *Fas* means the cell is directed towards apoptosis. After activating these genes, p53 also has the ability to inactivate itself by activating Mdm2. ChK2 also activates PML and E2F1 proteins that are involved in apoptosis either via p53 dependent pathways or independent pathways.

Besides ChK2 also plays role in cell recovery from DSB by activation of PP2A which leads to its binding with γ-H2AX foci. This binding causes the dephosphorylation of γ-H2AX, which is signal for removal of sensor proteins from the damage site.

2.6. Aim of the research

p53 plays central role in apoptosis, however, it has proven to be the one most often mutated in human cancers, the frequency of these mutations varies from one cancer type to another (Figure 2.4), however, overall ~50% of the cancer cells have p53 mutations.[23] Even in the cancer types in which p53 mutations are rare, p53 functions are indirectly abolished, whereas it is fully functional in normal cell types.[24] This makes the normal cells more susceptible to apoptosis than most of the tumor cells.[5] Bartek and co-workers and Halazonetis and coworkers showed in their studies that a significant fraction of cancer types have overexpressed activated ChK2,[25] these tumors may have

dependency on the activated ChK2 and this activated ChK2 might be required for the survival and aberrant replication of the cancer cells. Inhibiting ChK2 could potentially improve the cancer therapies in two ways. In the cancer cells, ChK2 inhibition will check the higher levels of ChK2 and stop the DNA repair and aberrant replication. In the normal cells, inhibiting ChK2 will block the p53 mediated apoptosis, giving cells more time to undergo repair. Therefore ChK2 inhibitors are a good target for the drug development.

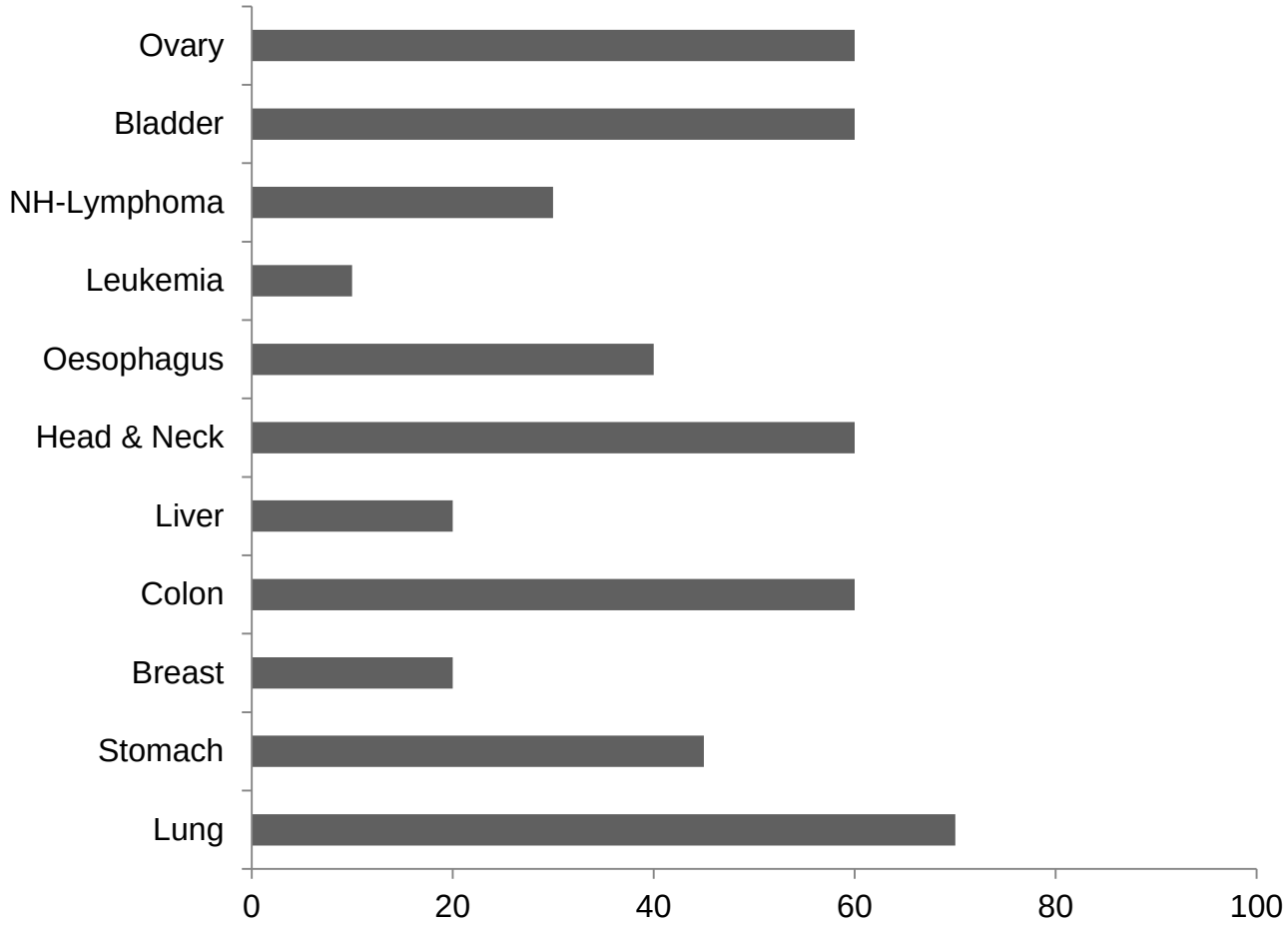

Figure 2.4. Frequency of p53 mutation rate in different cancer types.

ChK2 inhibitors will sensitize the cancer cells by interfering with the dependency of the cancer cells on over-expressed ChK2 and resistance to the apoptosis in the normal cells by inhibiting p53 mediated apoptosis and allowing the cell time to undergo repairs.

2.7. Proof of the principle

Motoyama and co-workers showed in their studies that the ChK2$^{-/-}$ mice appear to be normal, fertile and more resistant to IR induced apoptosis than the wild type mice (Figure 2.5)[26] suggesting that the inhibition of the ChK2 may not affect the somatic growth or fertility but can facilitate in blocking the apoptosis upon IR treatment.

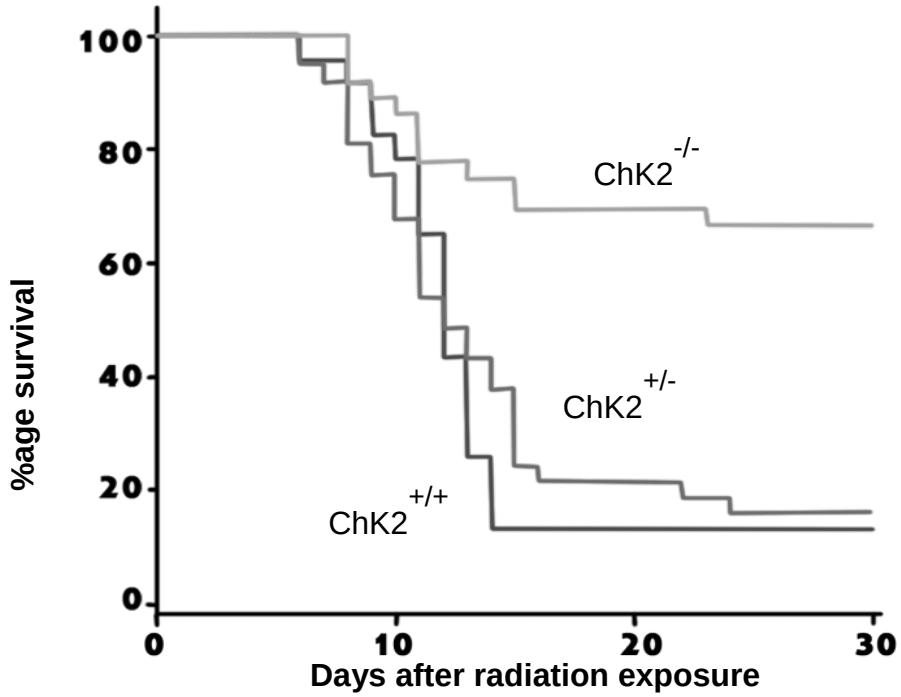

Figure 2.5. Kaplan–Meier survival curve of age-matched 8-16-week-old ChK2$^{+/+}$ (n = 23), ChK2$^{+/-}$ (n = 37) and ChK2$^{-/-}$ (n = 36) mice after exposure to 8 Gy of X-rays

The use of the ChK2 inhibiting agents in conjugation with the current cancer therapies has the potential to enhance the efficiency of these therapies by reducing their deleterious effect on the normal tissues of the body. $ChK2^{-/-}$ thermocytes were resistant to DNA-damage induced apoptosis.[26a] These $ChK2^{-/-}$ cells were defective for p53 stabilization and for transcriptive role of p53 in response to γ-irradiation. The introduction of ChK2 gene in these cells led to the restoration of p53 dependent transcription in response to γ-irradiation. Although partial stabilization of p53 was shown in the $ChK2^{-/-}$ cells in response to IR; however, these cells were deficient in the transcriptional activity of p53. This showed that ChK2 plays a pivotal role in the activity of p53 by regulating its transcriptional activation as well as its stabilization after IR-induced damage. Inhibition of ChK2 in mouse thymocytes[27] and isolated $CD4^{+}$ and $CD8^{+}$ human lymphocytes[28] also showed a decrease in the apoptosis in response to IR. These and other studies[27-29] indicate that inhibition of ChK2 in normal cells could increase survival following the IR by selectively reducing p53-mediated cell death.

In addition to the protective affects in normal cells, ChK2 inhibitors have been shown to potentiate the effects of the cytotoxic drugs.[30] Pommier and co-workers[30a] demonstrated that in the human embryonic kidney cells with inactive p53, the inhibition of ChK2 promotes apoptosis, suggesting that the ChK2 inhibition would make the p53-defective cancer cells more prone to the apoptosis. In other studies, it was shown that transfection of MCF-7 cells with ChK2 siRNA[31] enhances the effect of paclitaxel.[32]

ChK2 inhibition augmented the levels of mitotic catastrophe when used together with doxorubicin[33] or cisplatin[34] by releasing mitochondrial pro-apoptotic proteins. Recent studies also demonstrate that inhibition of the ChK2 without any additional genotoxic agent may also be advantageous for therapeutic development for tumors possessing increased levels of activated ChK2.[35] Tumor cells in which ChK2 is constitutively activated have plausibly adapted to ChK2 dependence in order to survive. A recent study by Pommier and co-workers[35b] showed the antiproliferative activity of ChK2 inhibitor PV1019 and ChK2 siRNA in cancer cell lines that were over-expressed in ChK2. These findings in the literature solidify the hypothesis that inhibition of ChK2 could be a very useful strategy in cancer therapy as it has potential to enhance apoptosis in cancer cells and at the same time it is protective of the normal cells.

2.8. Other potential applications of ChK2 inhibitors

The ChK2 pathway is activated in response to genotoxic stresses. Suppression of this pathway can also be a useful strategy for treating various viral infections.[36] The studies have shown that various viruses, including Epstein-Barr Virus,[37] herpes simplex virus 1,2,[38] Human cytomegalovirus,[39] Murine gammaherpesvirus 68,[40] Polyomavirus,[36c] Adeno-associated virus,[41] simian virus 40,[42] retro human immunodeficiency virus type 1 (HIV-1)[36d, 43]and Hepatitis C virus (HCV), have the ability to activate the DNA damage response (ATM) pathway and then use the damage responses to promote the

survival of the infected cells and facilitate their own viral reproduction.[44] The replication of HCV RNA was shown to be suppressed in ATM or ChK2 knockdown mice that.[36b]

Most common strategy in the treatment of the viral infections has been to target the virus (protein or nucleic acid). However rapid division of the virus leading to the fast rate of mutations leads to evolution of the stains that develop resistance to the drug molecules. It would be very novel approach to use the drugs that would inhibit the target pathways, in the host cell that viruses exploit, as the treatment for viral infections.

2.9. ChK2 inhibitors in literature

In the recent years inhibition of ChK2 has attracted some attention and few ChK2 inhibitors have been reported in the literature. The characterized inhibitors of ChK2 include the indolocarbazole UCN-01 **(51)**[45] Gö6976**(52)**[46], EXEL-9844**(53)**[47], NSC109555**(54)**[29c], PV1019**(55)**[35b] VRX0466617**(56)**[27], 2-(quinazolin-2-yl) phenol (2QP) based inhibitors[35c] like CCT241533**(57)**[48], 2-aminopyridine based inhibitors (2AP) **(58)**[29d], the aryl benzimidazole bases inhibitors **(59)** and the natural products HMD **(1)** and DBH **(7)**.[49]

UCN-01(7-hydroxystaurosporine) **(51)** was reported to be a potent inhibitor of ChK2 (~10nM)[45] in human colon carcinoma HCT116 cells, however it has severe draw backs including its strong binding with human plasma protein α1-acid glycoprotein and low bioavailability.[50]

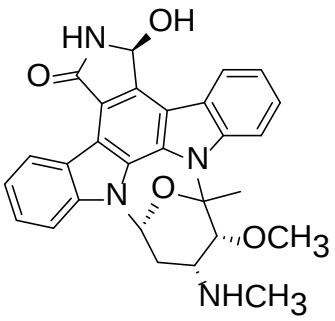

UCN-01 (**51**)

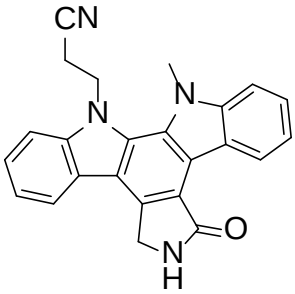

Go6976 (**52**)

EXEL-9844 (**53**)

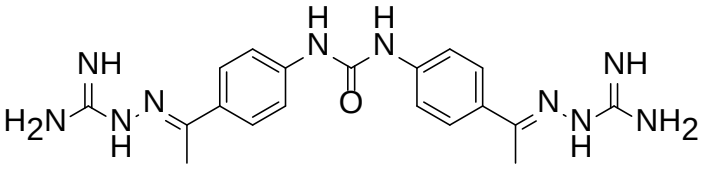

NSC 109555 (**54**)

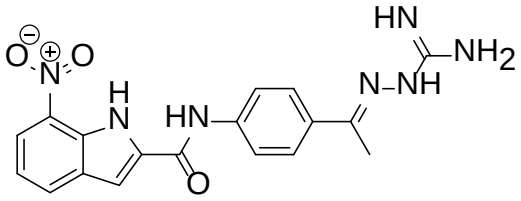

PV11019 (**55**)

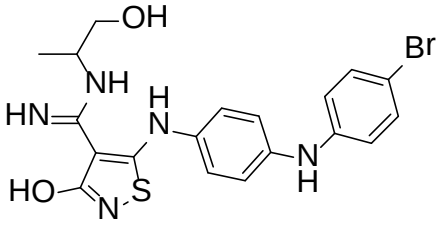

VRX0466617 (**56**)

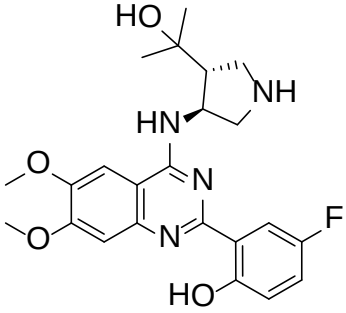

CCT241533; A 2QP based inhibitor (**57**)

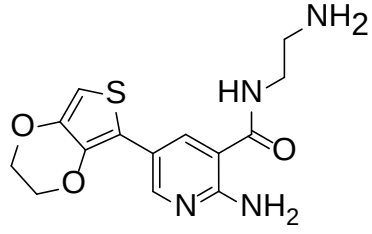

2-AP based inhibitor (**58**)

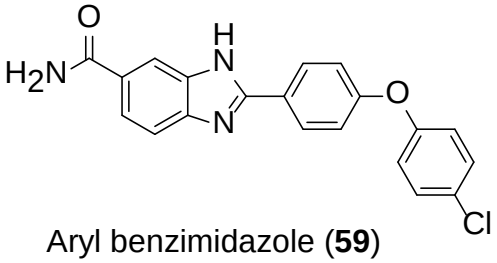

Aryl benzimidazole (**59**)

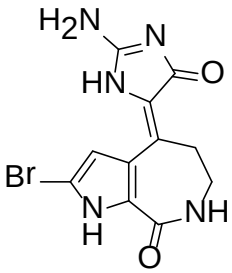

HMD (**1**)

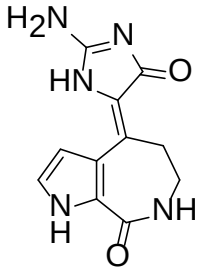

DBH (**7**)

Figure 2.6. Known ChK2 inhibitors

Gö6976 **(52)** unlike UCN-01 did avoid the issue of binding with blood plasma, it was equally potent in human serum studies in abrogating S- and G_2 phase arrest and by cell viability studies it was shown to be non-toxic as single agent, however it suffers from being equipotent for ChK2 and ChK1.[46]

EXEL-9844 **(53)** is a potent, ATP-competitive inhibitor of ChK1 and ChK2. Its *Ki* value for ChK2 is 0.07 nM, while for ChK1 *Ki* is 2.2 nM. It was shown to potentiate the anti-tumor activity of gemcitabine in vivo without unacceptable increase in the toxicity. As the single agent it had very limited activity. The compound is orally available and showed effects in cellular assays that are also seen with loss of ChK1 alone. The potential problem of using a ChK1 inhibitor in anti-cancer therapy is that it can sensitize the normal cells to genotoxins.[47, 51] Inhibiting ChK1 in normal cells would be undesirable as it is known that $ChK1^{-/-}$ mice are not viable.[52]

NSC109555 **(54)** was a compound from the family of bis(guanylhydrazones). It was found through screening of library to be another ATP-competitive inhibitor of ChK2. It inhibited ChK2 with IC_{50} value of 240nM while for ChK1, its IC_{50} was greater than >10000nM. However it failed to show the activity in the cells for some reasons that may include off-target activities or poor cell permeability.[29c]

PV1019 **(55)** is successor of NSC 109555.[35b] It was shown to be a selective submicromolar inhibitor of ChK2 in vitro with IC_{50} of 24-260nM for ChK2 and 15.73µM

for ChK1. It was also found active in inhibiting ChK2 in cellular assays by inhibiting autophosphorylation and Cdc25c phosphorylation. It also protected normal mouse thermocytes against ionizing radiation induced apoptosis and showed synergistic antiproliferative activity with topotecan, camptothecin, and radiation in human tumor cell lines. It is 655 times more selective for ChK2 over ChK1, however, the IC_{50} values showed 100-fold difference in vitro kinase assay and cellular kinase assay.

VRX0466617 **(56)** is a more potent ATP competitive inhibitor of ChK2 among the library of compounds analyzed by Larson and co-workers.[27, 29b] It acts by blocking the autophosphorylation of ChK2. Its K*i* for ChK2 is 11nM, while its IC_{50} for ChK2 is 120nM and for ChK1 IC_{50} >10000nM. It blocks the ChK2 activity but did not significantly change the cell cycle distribution or prevents the G2/M arrest in short-term cultures. Also, it did not show the synergy with a number of cancer agents.

Caldwell and co-workers published a study of the 2-(quinazolin-2-yl)phenol based inhibitors of ChK2[35c] and showed that CCT241533 **(57)** was the better inhibitor among the library of inhibitors that they tested with IC_{50} value for ChK2 3nM while for ChK1 it was 190nM. CCT241533 could not potentiate the cytotoxicity of a selection of genotoxic agents in several cell lines. However, it was shown to potentiate the cytotoxicity of PARP inhibitors in p53 deficient cell lines by inhibition of ChK2, suggesting that combination of ChK2 inhibitor and PARP inhibitors could be an avenue for the cancer therapy.[48]

2-Amino pyridine based (2AP)[29d] compounds were identified through high throughput screening as inhibitors of ChK2. These compounds also bind in ATP-competitive manner. Compounds of this library showed activity in cell-based assays by inhibiting ChK2. The most potent compound **(58)** as shown in Figure 2.6 has IC_{50} value of 28nM for ChK2 and 2.5μM for ChK1.

Arienti and co-workers reported a SAR study carried out at Johnson & Johnson Pharmaceutical Research and Development Division for ChK2 inhibitors.[28] They identified a series of 2-arylbenzimidazole inhibiters of the kinase. The optimization process lead to compound that was selective and potent inhibitor **(59)** of ChK2 shown in Figure 2.6. IC_{50} for this compound was 15nM for ChK2 and it demonstrated a dose-dependent, radioprotective effect on human CD4+ and CD8+ primary cells.

Along with synthetic compounds UCN-01 and 2-arylbenzimidazole, DBH and HMD were the only natural products at the start of the present work that were known to inhibit ChK2. These are sponge derived natural products isolated and purified in early 1980s.[49a, 53] HMD and DBH are structurally similar compounds, differing only by the presence of bromine at C2-atom of HMD. These natural products comprise of a pyrroloazepine ring that is connected to a glycocyamidine ring through a double bond. DBH is a mild inhibitor of the checkpoint kinases with IC_{50} of 725nM for ChK1 183nM for ChK2.[54] On the other hand HMD is more potent inhibitor and has IC_{50} value of 42nM for ChK2 and 1950nM for ChK1.[54] However it suffers from its low selectivity[49a, 55] and exhibits nano-molar inhibition of GSK-3β (IC_{50} 10nM), CDK5 (IC_{50} 28nM) and MEK-

1 (IC_{50} 9nM)[56]. This lack of the selectivity of the natural product prompted the interest of our group to synthesize an indolic-derivative **(49)** of the natural product as shown in Figure 2.7.[54]

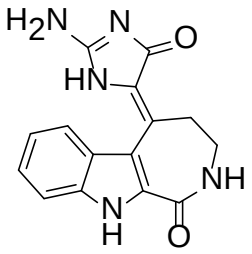

Figure 2.7. Indolic derivative of HMD (49)

2.10. Synthesis and profiling of indoloazepinone analog 49

The synthesis is presented in the figure 1.16.[54, 57] The compound **49** was then evaluated for its ability to inhibit ChK1, ChK2 and a selected set of kinases. The comparison of the compound **49** for its inhibitory ability as compared to HMD and DBH is given in Table 2.3. The indolic derivative exhibited a very potent inhibition of ChK2 activity at the low nanomolar range (IC_{50}=8 nM) and unlike the natural product DBH it exhibited an increased selectivity for the checkpoint kinases. Compared to HMD, it had a significant increase in potency for ChK1 and ChK2 inhibition. While for the other kinases tested, it showed a significant drop in activity.

Table 2.3. IC_{50} values for kinase inhibition by Indolic derivative, HMD and DBH

Kinase	IC_{50} (nM)		
	49	HMD	DBH
CK1δ(h)	1352	35[49b, 58]	NA
CK2(h)	>10,000	7000[49b, 58]	NA
MEK1(h)	89	6[59]	824[59]
PKCα(h)	2539	700[49b, 58]	NA
PKCβII(h)	3381	1200[49b, 58]	NA
ChK1	220	1950	725
ChK2	14	42	183

2.11. Efforts towards synthesis of compound 60

We were especially interested in synthesizing molecule **60** and compare the effect of substituting the bromine atom of the natural product with a phenyl ring. At the same time we wanted to compare the reactivity of compound **60** with compound **49,** which differ in that the compound **60** has the phenyl ring attached at the 2-position of the pyrrole ring and can rotate to orient itself better in the binding pocket whereas in compound **49**, the phenyl ring is fused to the pyrrole forming an indole ring and making it a rigid structure and not allowing the rotation of the phenyl ring.

In order to prepare compound **60**, we envisioned that we can utilize the Br-atom of HMD and use phenyl boronic acid to carry out the Suzuki reaction. However, upon reaction of HMD with phenyl boronic acid using Pd-catalyst under Suzuki reaction conditions with did not observed the desired product (Scheme 2.1). Instead, we observed the dehalogenation-protonation or the reactant leading to the formation of DBH as the product.

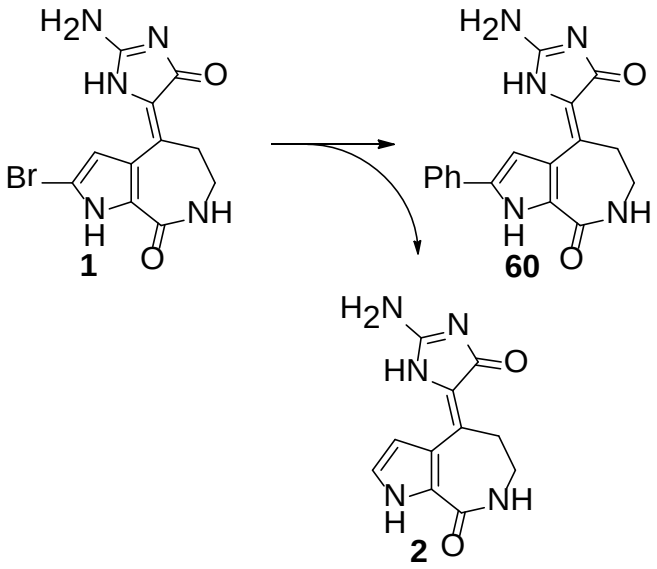

Scheme 2.1. Suzuki reaction of HMD

Reactions and conditions: $PhB(OH)_2$, $Pd(PPh_3)_4$, aq. Na_2CO_3, EtOH, PhMe, 95^oC, 18h, 98%

Change of solvent to DMF or EtOH did not change the course of the reaction to desired product. At this stage, we considered making compound **61** and synthesize the desired product in two steps from compound **61**.

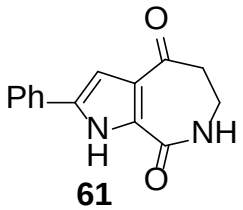

61

Figure 2.8: Key intermediate in the synthesis of 60

We anticipated carrying out the Suzuki reaction on compound **16** or compound **35** which were intermediates in the synthesis of HMD. The reaction worked well with the compound **16** giving decent yields of the product. However, a more efficient route involved the Suzuki coupling of the compound **35**. The reaction conditions enabled two reactions in one pot with excellent yield. Upon subjecting compound **35** to Suzuki reaction conditions, it not only underwent the substitution of the Br-atom with phenyl ring, it also underwent the hydrolysis of the ethyl ester giving compound **62** as shown in the Scheme 2.2.

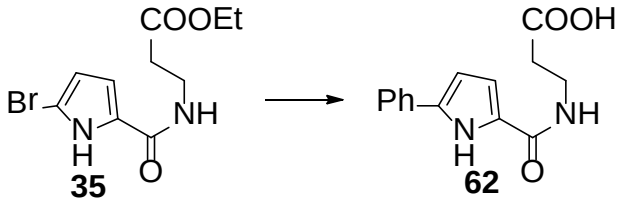

35 **62**

Scheme 2.2. Suzuki reaction of compound 35

Reactions and conditions: $PhB(OH)_2$, $Pd(PPh_3)_4$, aq. Na_2CO_3, EtOH, PhMe, 95^{o}C, 18h, 98%

In the next step compound **62** was subjected to intramolecular Friedel-Craft cyclization, affording the key intermediate **61** in very good yield as shown in Scheme 2.3.

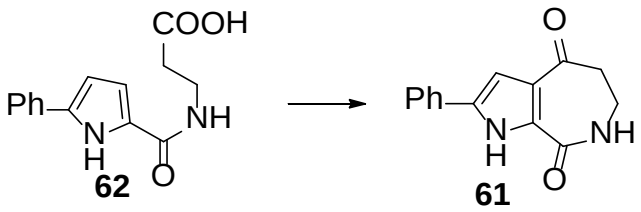

Scheme 2.3. Friedel-Craft reaction of compound 62

Reactions and conditions: P_2O_5, PPA, 130^{o}C, 2h, 75%

In the next reaction, compound **61** was condensed with compound **42** in the titanium tetrachloride mediated aldol reaction producing compound **63** in very good yield as shown in the Scheme 2.4.

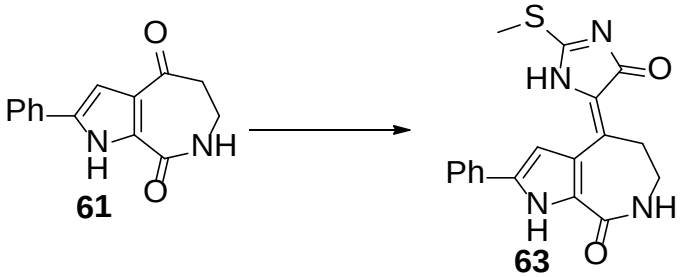

Scheme 2.4. Synthesis of compound 63

Reactions and conditions: 42, $TiCl_4$, py, THF, 0^{o}C-rt, 73%

Compound **63** was then heated with ammonium hydroxide in sealed tube producing the desired natural product analog, compound **60** as shown in the Scheme 2.5.

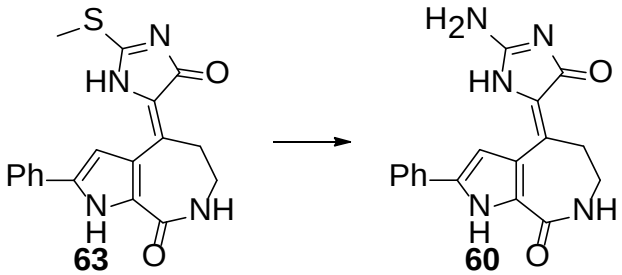

Scheme 2.5. Completion of the synthesis of compound 60

Reactions and conditions: NH_4OH, THF, sealed tube, 110^oC, 24h, 69%

2.12. Kinase profiling of compound 60

Compound **60** was profiled for its kinase activity by Theresa A. Lansdell. It was subjected to Cisbio HTRF serine/threonine KinEASE assay and showed IC_{50} value of 27nM for ChK2 and 490nM. The comparison of the ability of the analog **60** to inhibit ChK1 and ChK2 as compared to the natural products HMD and DBH and the indolo-analog **49** is presented in Table 2.4. The compound **60,** is a very potent inhibitor of ChK2. for ChK1. The IC_{50} for this compound for inhibiting ChK2 lies in the statistical range of compound **49** and HMD and it is better inhibitor than DBH.

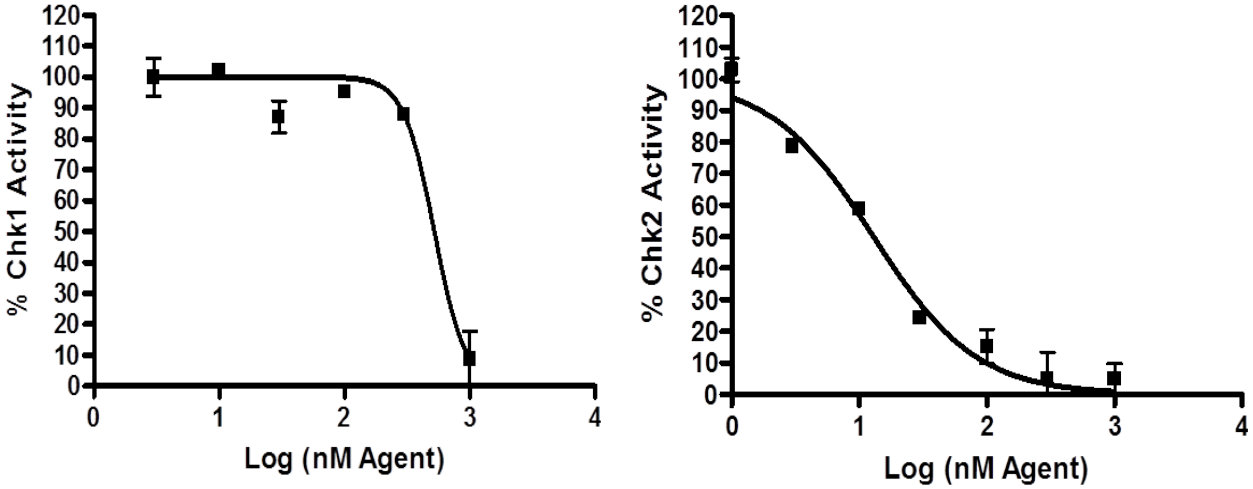

Figure 2.9. Kinase activity of compound 60 (ChK1 on the left, ChK2 in the right)

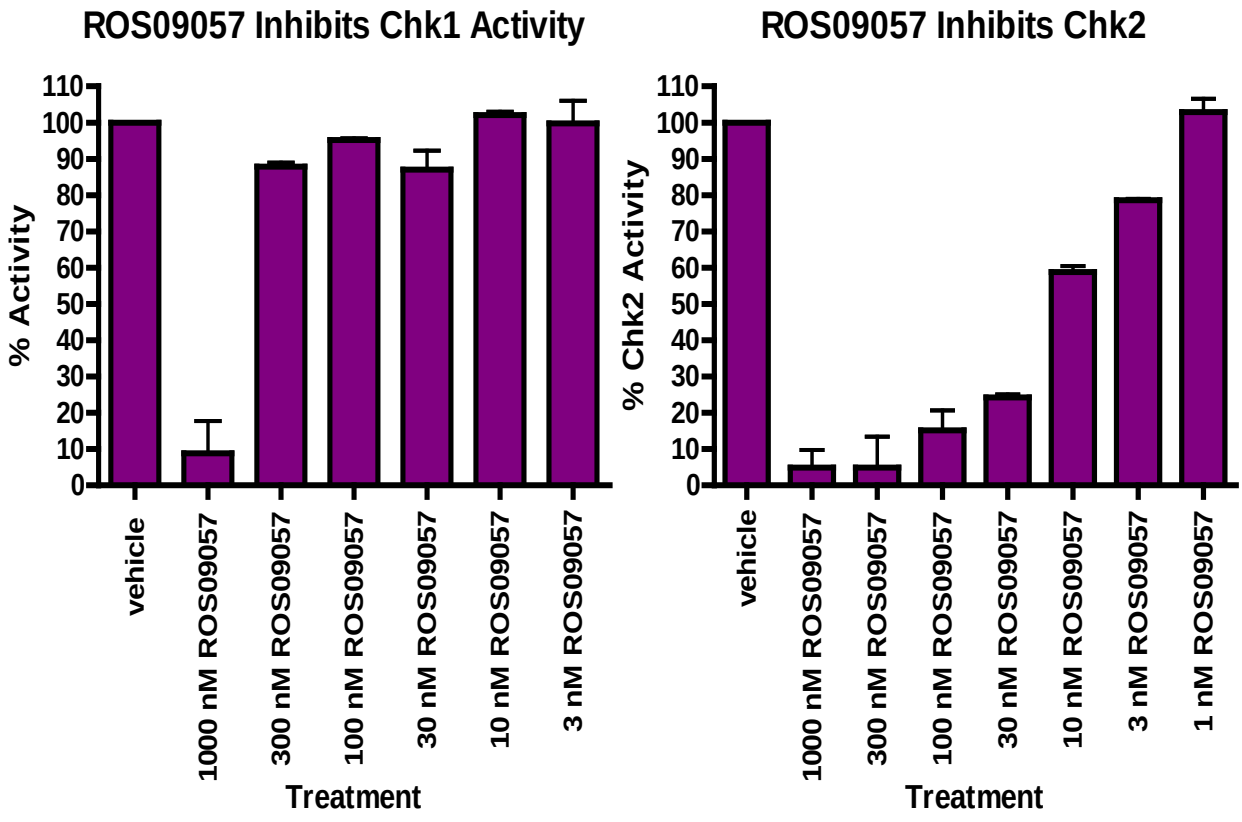

Figure 2.10. Kinase activity of compound 60 (ChK1 on the left, ChK2 in the right)

In terms of its selectivity for ChK2 over ChK1, compound **60** is slightly better than compound **49** and it has marked improvement over DBH. However, its selectivity for ChK2 over ChK1 is still lower than HMD. The compound **60** provides a good lead for the study of SAR to obtain the candidate with excellent potency and selectivity for inhibiting ChK2 to radio-protect the healthy cells.

Table 2.4: Comparison of kinase profile of Compound 60 with HMD, DBH and compound 49

Compound	IC_{50}		Selectivity (ChK1/ChK2)
	ChK1	ChK2	
Compound **60**	490	27	18.1
Compound **49**	220	14	15.7
DBH	725	183	4.0
HMD	1950	42	46.4

2.13. Synthesis of the derivative of compound 60

We were encouraged with the kinase profiling results of the compound **60**. In order to improve selectivity and potency, we were interested in modifying the structure of compound **60**. We wanted to prepare a representative library of the new derivative of HMD, related to compound **60.** A closer look at the crystal structure of DBH in the ATP binding pocket revealed two potential sites of modifications.

i)

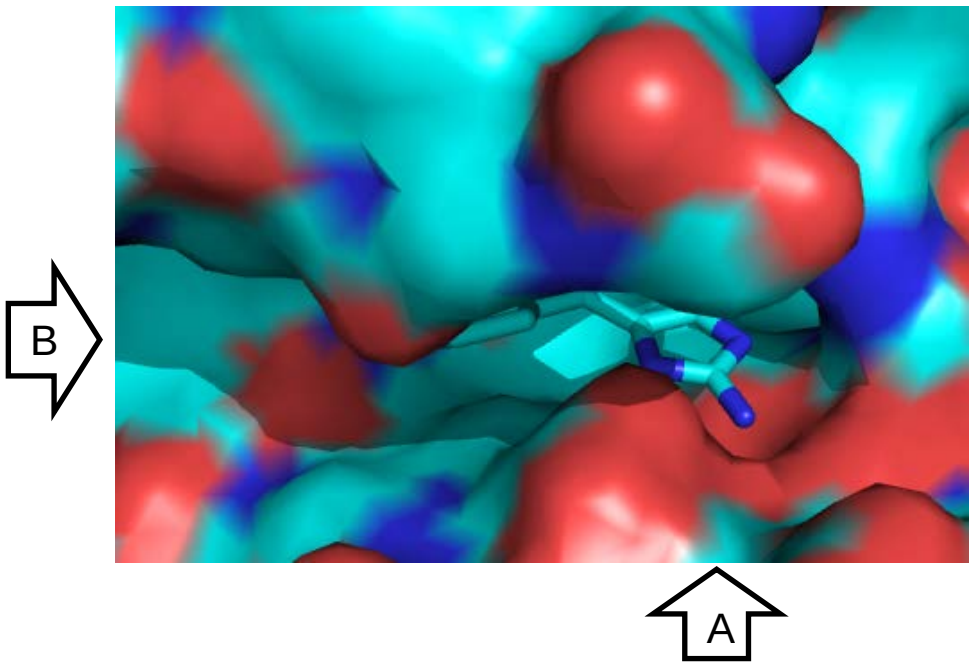

ii)

Figure 2.11. i) Crystal structure of DBH in ATP binding pocket of ChK2 ii) Overlap of DBH and ADP in the binding pocket of ChK2 ("For interpretation of the references to color in this and all other figures, the reader is referred to the electronic version of this dissertation").

a- Modification at site A: Figure 2.11i shows that the NH_2-group on glycocyamidine ring was projecting from its cavity into another un-occupied large hydrophilic area which is involved in the binding interactions with phosphate chain of ATP (Figure 2.11ii) but DBH does not extend into this region. We envisioned that putting substitution at this amine will lead to extra drug-protein interaction leading to the increase in the potency and gain in selectivity.

b- Modification at site B: In compound **60**, the phenyl ring was un-substituted. We planned to prepare new derivatives of the natural product with functionalized aromatic ring. We envisioned that the presence of hetero-atoms attached to the phenyl ring could potentially lead to new interactions, hence improving the potency of the molecule.

2.13.1. Modification at site A

With the aim to synthesize representative library of new HMD analogs by modification at the free amine of the glycocyamidine ring, we planned the synthesis of compound **64-69** shown in Figure 2.12.

We envisioned that we can utilize compound **63,** which was used in the synthesis of the compound **60**, as common precursor. The design of the reaction involved the reaction of the compound **63** with appropriate amine, thus making available the new analogs via a single step modification of a common intermediate **63** as shown in Scheme 2.6.

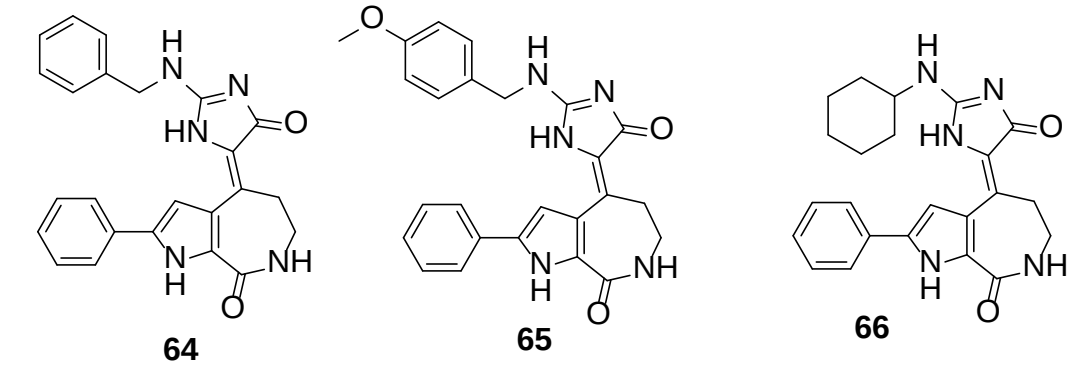

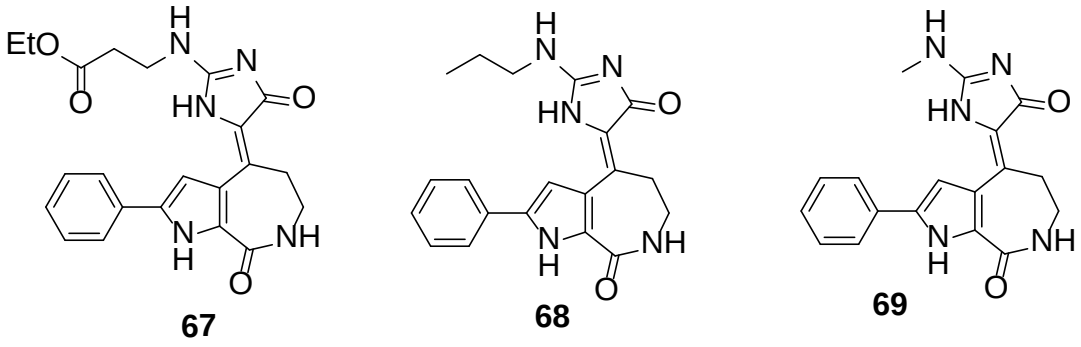

Figure 2.12. Novel analogs of HMD

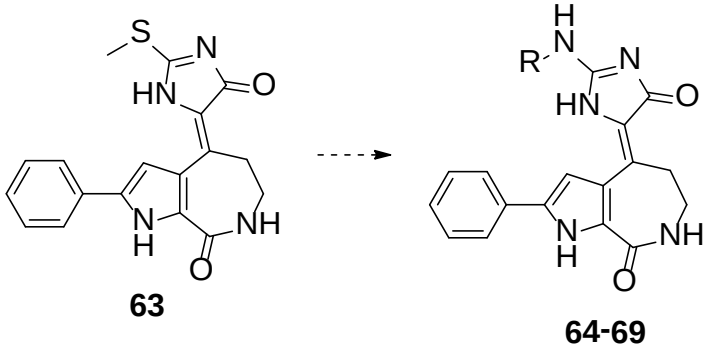

Scheme 2.6. Design for the synthesis of new analogs

Reactions and conditions: RNH_2, THF, heat

The compound **63** was dissolved in THF and heated in sealed tube with benzyl amine for compound **64**, 4-methoxybenzyl amine for compound **65**, cyclohexyl amine for compound **66**, β-alanine ethyl ester hydrochloride for compound **67**, n-propyl amine for

Table 2.5: Synthesis of new analogs of HMD

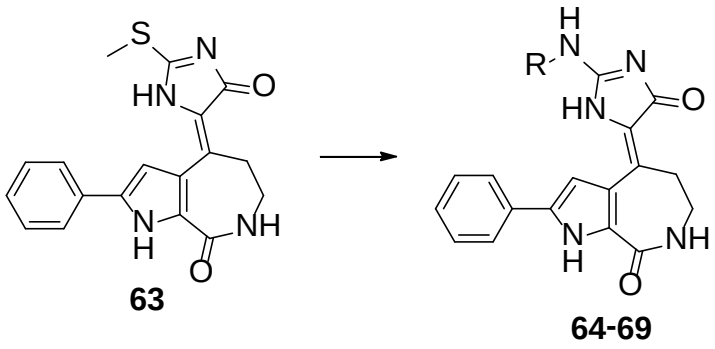

Reactions and conditions: RNH_2, THF, 90^oC, sealed tube 67-80%

	R-	Product	Yield(%)
1	Bn-	**64**	78
2	$4\text{-}MeOC_6H_4CH_2$-	**65**	62
3	Cy-	**66**	80
4	$EtOOCCH_2CH_2$-	**67**	67
5	nPr-	**68**	77
6	Me-	**69**	74

compound **68** and methyl amine hydrochloride for compound **69.**

Pyridine was added to the reaction mixture for the reactions where the amine was only available as hydrochloride salt. The reactions took place smoothly affording good to very good yields of the natural product derivative as shown in Table 2.5.

2.13.2. Modification at site B: Attaching different aryl groups at position 5 of the pyrrole ring

In second category of derivatives, we embarked on the journey of synthesizing new analogs by replacing the phenyl group with two aromatic rings. The first aromatic ring was 3,4-dimethoxy phenyl ring to make compound **70** and the other aromatic ring was 4-methoxy phenyl ring to give compound **71**.

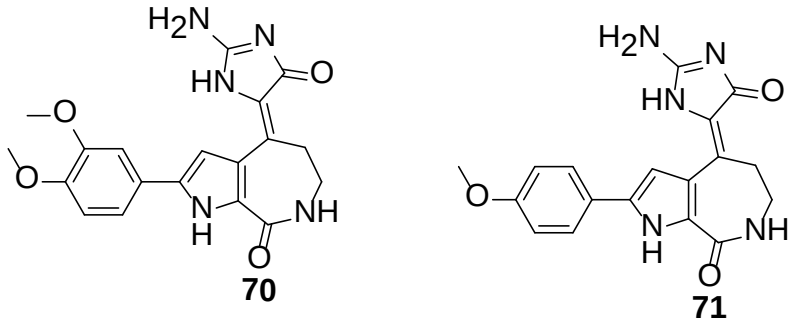

Figure 2.13. New analogs of HMD

Previously, we were not able to achieve the Suzuki coupling of HMD, rather the debromination-protonation lead to the formation of DBH. So we planned to prepare the 2-aryl derivative **72** from aryl aldisine **73** in two steps. We considered that the synthesis

of aryl aldisine **73** can be achieved by Suzuki reaction of compound **16** as shown in Scheme 2.7.

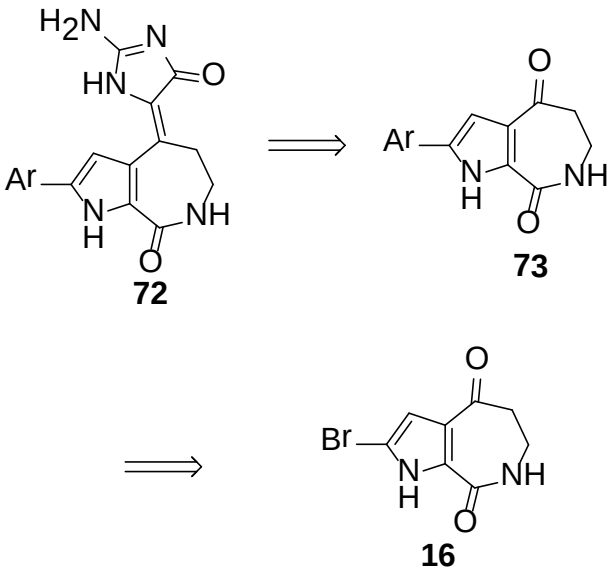

Scheme 2.7. Retrosynthetic analysis for the synthesis of new analogs

2.13.2.1. Synthesis of compound 70

The compound **70** was synthesized as shown in the Scheme 2.8. Compound **16** underwent Suzuki coupling with 3,4-dimethoxyphenyl boronic acid **74** using tetrakis(triphenylphosphine)palladium(0) as catalyst to give azepindione **75**. Compound **75** was then subjected to aldol condensation with compound **42** to yield compound **76**. In the last step compound **126** was heated in a sealed tube with ammonium hydroxide to yield the desired compound **120**.

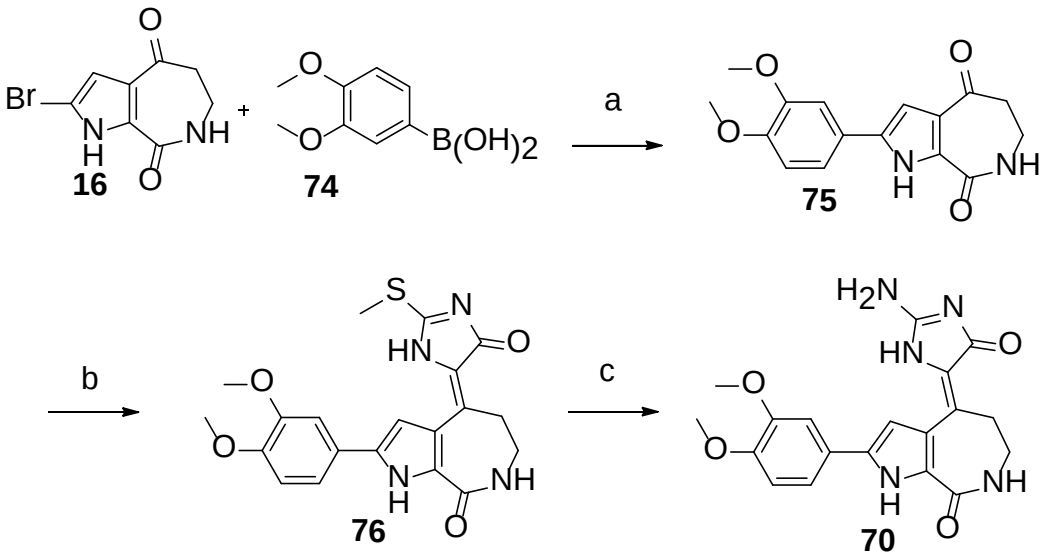

Scheme 2.8. Synthesis of compound 70

Reactions and conditions: (a) $Pd(PPh_3)_4$, Na_2CO_3, EtOH, PhMe, H_2O, , 95^{o}C, 18h, 82% (b) **42**, $TiCl_4$, py, THF, 0^{o}C-rt, 60% (c) NH_4OH, THF, sealed tube, 110^{o}C, 24h, 52%

2.13.2.2. Synthesis of compound 71

The compound **71** was also synthesized using similar strategy as the one applied for the synthesis of compound **70**. The synthetic strategy is presented in the Scheme 2.9. The compound **16** was reacted with 4-methoxyphenyl boronic acid **77** using Tetrakis(triphenylphosphine)palladium(0) as catalyst for Suzuki coupling to yield compound **78**. Compound **78** was then subjected to aldol condensation with compound **42** to yield compound **79**. Heating compound **79** with ammonium hydroxide in a sealed tube afforded the desired compound **71**.

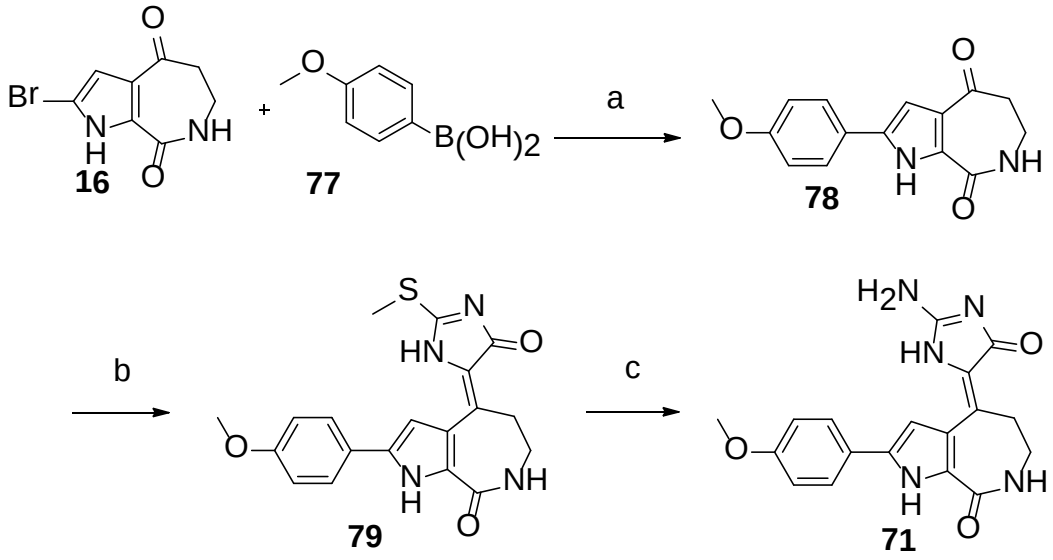

Scheme 2.9. Synthesis of compound 71

Reactions and conditions: (a) $Pd(PPh_3)_4$, Na_2CO_3, EtOH, PhMe, H_2O, , 95^{o}C, 18h, 82% (b) **42**, $TiCl_4$, py, THF, 0^{o}C-rt, 49% (c) NH_4OH, THF, sealed tube, 110^{o}C, 24h, 65%

2.14. Kinase profiling of the derivatives

After synthesizing compound **64-71**, these compounds were subjected to kinase profiling by Theresa A. Lansdell. Cisbio HTRF serine/threonine KinEASE assay was used to access the inhibitory activity of these compounds for ChK2 and ChK1 and the results are tabulated in Table 2.6. These results are exciting because previously our group synthesized (unpublished work) a derivative of indoloazepinone **80** (Figure 2.14) with dimethylamino-group on the glycocyamidine ring and it was found to be inactive in inhibiting ChK2.

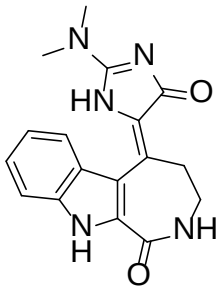

80

Figure 2.14: Dimethyl amino analog of indoloazepinone 80

When we compared compound **60** to compounds **64** and **65** containing benzyl and 4-methoxybenzyl, the placement of the benzyl group did not altered the IC_{50} value for ChK2, however the selectivity for ChK2 was increased in comparison to ChK1, this compound had IC_{50} values comparable to HMD. 4-Methoxybenzyl group in compound **65,** on the other hand eroded the ability of the analog to inhibit both ChK2 and ChK1. This compound was unable to inhibit ChK1 and its IC_{50} value for ChK2 was too high to consider it a good candidate. When comparing compound **60** with compounds **66-69,** all of which contained aliphatic substituents, the profiling results were also interesting.

The results showed that the presence of the substituent on the N-atom, leads to the erosion of the ability to inhibit the ChK2 and ChK1. However, this effect was more pronounced for ChK1 as compared to ChK2 and shows the correlation with the size of the substituent. In general, smaller substituents exhibited better IC_{50} values and as the size of the substituent increases, the IC_{50} value deteriorated.

Table 2.6: Kinase profiling of compounds 60, 64-71

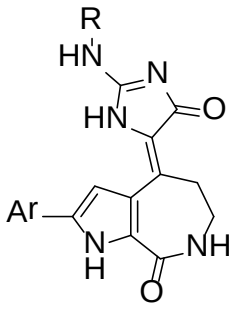

Compound			IC_{50}	
No.	Ar	R	ChK2 (nM)	ChK1 (nM)
60	Ph	H	27	491
64	Ph	Bn	38	1843
65	Ph	4-$MeOC_6H_4CH_2$	589	>10000
66	Ph	Cy	1526	>10000
67	Ph	$EtOOCCH_2CH_2$	320	>10000
68	Ph	$CH_3CH_2CH_2$	128	NA*
69	Ph	CH_3	111	>10000
70	3,4-dimethoxyphenyl	H	123	1637
71	4-methoxyphenyl	H	23.7	NT*

* NA= Not Active, NT= Not Tested

The order of activity of these substituents was: Me> CH_2CH_2COOEt> Cy. The compound **69** with methyl substituent was most active in inhibiting ChK2, whereas compound **66** with cyclohexyl group inhibited ChK2 only in high concentrations. Compound **66** was unable to inhibit ChK1, whereas compound **67** and **69** exhibit very high IC_{50}**.** These results lead to the conclusion that selectivity of HMD analogs for inhibiting ChK2 can be increased by placing a substituent at the N-atom on glycocyamidine ring. However, as compound **80** where both the H-atoms were replaced by the methyl groups, was inactive, so these results also show that this N-atom is involved in key donaptor interactions and need at least one H-atom to establish these interactions. As the bulkier groups led to the erosion of the potency of these analogs and compound **69** gave the best selectivity and good IC_{50} value for ChK2, it is the best analog for the future analysis and further profiling.

In the second series of compounds, where the phenyl group was replaced with the 3,4-dimethoxy phenyl and 4-methoxyphenyl rings, the results were interesting. The compound **70** was potent inhibitor, however the presence of two methoxy-groups lead to the decrease in the potency to inhibit ChK2. The presence of these methoxy groups also lead to the decrease in ability to inhibit ChK1 as compared to compound **60**. On the other hand, presence of p-methoxy group on compound **71** did not change to IC_{50} value as compared to compound **60**. It will be interesting to see the effect of this substation in inhibiting ChK1.

2.15. Experimental Section

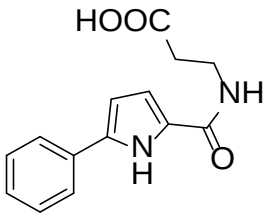

3-(5-phenyl-1H-pyrrole-2-carboxamido)propanoic acid (62): Compound **35** (213mg, 0.74mmol) was added in a mixture of toluene and ethanol (3:1, 40mL) and phenyl boronic acid (109mg, 0.89mmol) and tetrakis (triphenylphosphine) palladium (43mg, 5mol%) were added to the reaction mixture. The a solution of sodium carbonate (235mg, 2.22mmol) in water (3mL) was added to the reaction mixture and the mixture was heated to 95°C for 18 hours. Then the reaction mixture was cooled down to room temperature and partitioned between 10% aqueous sodium bicarbonate solution (50mL) and ethyl acetate (50mL). The organic layer was discarded while the aqueous sodium bicarbonate layer was acidified with 5% HCl solution and the product was extracted into ethyl acetate (4 x 40mL). The ethyl acetate fractions were combined and dried over anhydrous Na_2SO_4 (500 mg). The solvent was removed and the crude material was purified by column chromatography (silica, EtOAc) to afford **62** (188mg, 98%). m.p. 172°C; ^{1}H NMR (500 MHz, CD_3OD) δ 7.64 (2H, d, J = 7.5Hz), 7.36 (2H, t, J = 7.5Hz), 7.22 (1H, t, J = 7.5Hz), 6.82 (1H, d, J = 4.0Hz), 6.51 (1H, d, J = 4.0 Hz), 3.59 (2H, t, J = 7.0 Hz), 2.61 (2H, t, J = 7.0 Hz); ^{13}C NMR (125 MHz, CD_3OD) δ 175.5, 163.7, 137.2,

133.4, 130.3, 129.9, 128.1, 125.7, 113.9, 108.1, 36.5, 35.0; IR (film): 3418, 3266, 2923, 1712, 1604, 1567, 1539, 1457, 1435, 1282, 1218, 1198 cm^{-1}; MS (ES+) m/z 259.1$[M+H]^+$; HRMS (ES+) m/z calcd for $C_{14}H_{15}N_2O_3$ $[M+H]^+$ 259.1083, found 259.1089.

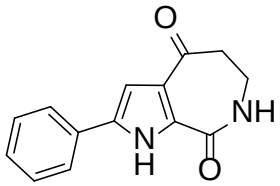

2-phenyl-6,7-dihydropyrrolo[2,3-c]azepine-4,8(1H,5H)-dione (61):

Polyphosphoric acid (10g) was warmed to 130°C in a round bottom flask and P_2O_5 (764mg, 5.38mmol) was added to this flask. The reaction mixture was stirred till it became a clear solution. At this stage **62** (695mg, 2.69mmol) was added to the reaction mixture and the reaction mixture was stirred for 2 hours at 110°C. Then the reaction mixture was cooled to room temperature and neutralized with 10% aqueous $NaHCO_3$ and the product was extracted with Ethyl acetate (100mL x 4). The ethyl acetate fractions were combined and dried over anhydrous Na_2SO_4 (1g). The solvent was removed and the crude material was purified by column chromatography (silica, ethyl acetate) affording **61** (484mg, 75%). m.p. 222°C; ^{1}H NMR (500 MHz, DMSO-d_6) δ 7.90 (2H, d, J = 7.5 Hz), 7.38 (2H, t, J = 7.5 Hz), 7.28 (1H, t, J = 7.5 Hz), 6.98 (1H, s), 3.48-

3.50 (2H, m), 2.78-2.80 (2H, m); ^{13}C NMR (125 MHz, DMSO-d_6) δ 194.5, 162.1, 135.3, 130.6, 128.9, 128.7, 127.6, 125.4, 124.6, 107.0, 43.7, 36.5; IR (film): 3204, 1644, 1510, 1513, 1467, 1437, 1399, 1363; MS (ES+) m/z: 241.1$[M+H]^+$; HRMS (ES+): m/z calcd for $C_{14}H_{13}N_2O_2$ $[M+H]^+$ 241.0977, found, 241.0982.

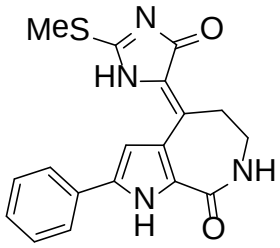

(Z)-4-(2-(methylthio)-4-oxo-1H-imidazol-5(4H)-ylidene)-2-phenyl-4,5,6,7-tetrahydropyrrolo[2,3-c]azepin-8(1H)-one (63): Compound **61** (449mg, 1.87mmol) was dissolved in THF (25mL) and compound **42** (487mg, 3.74mmol) was added to the reaction flask. The reaction mixture was cooled to 0°C and 1M solution of $TiCl_4$ in DCM (7.48mL, 7.48mmol) was added to the reaction mixture in drop-wise manner. The reaction mixture was stirred for 30 minutes and pyridine (1.19 mL, 14.95 mmol) was added to the reaction mixture dropwise over 15 min. The reaction mixture was stirred for an additional 14 hours allowing it to gradually warm to room temperature. At this point saturated NH_4Cl solution (40mL) was added to the reaction mixture and contents of the flask were transferred to the separatory funnel. Then the crude product was extracted with ethyl acetate (50mL x 3). The ethyl acetate fractions were combined and dried over

anhydrous Na_2SO_4(500mg). The solvent was removed and the crude material was purified by column chromatography (silica, EtOAc) to afford **63** (480mg, 73%). m.p. decomposed over 250°C; ^{1}H NMR (500 MHz, DMSO-d_6) δ 8.01 (1H, s), 7.82 (2H, d, J = 7.5 Hz), 7.26 (1H, t, J = 7.5 Hz), 3.44-3.46 (2H, m), 3.27-3.28 (2H, m), 2.65 (3H, s); ^{13}C NMR (125 MHz, DMSO-d_6) δ 170.6, 162.8, 158.3, 135.4, 134.3, 133.6, 131.3, 128.7, 128.4, 127.1, 125.0, 124.0, 111.8, 39.1, 30.3, 12.1; IR (film): 3184, 3046, 2929, 1691, 1658, 1623, 1605, 1508, 1470, 1436, 1411 cm^{-1}; MS (ES+) m/z: 353.1 $[M+H]^+$; HRMS (ES+) m/z calcd. for $C_{18}H_{17}N_4O_2S$ $[M+H]^+$ 353.1072, found, 353.1082.

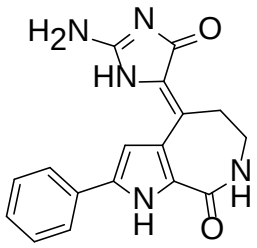

(Z)-4-(2-amino-4-oxo-1H-imidazol-5(4H)-ylidene)-2-phenyl-4,5,6,7-tetrahydropyrrolo[2,3-c]azepin-8(1H)-one (60): Compound **63** (115 mg, 0.32 mmol) was added to THF in a sealed tube and ammonium hydroxide (5mL) was added to the solution. The resulting mixture was heated at 90°C for 24 hours and then allowed to cool to room temperature. Then the reaction mixture was concentrated crude material was purified by column chromatography (silica, MeOH/DCM 1:4) to obtain **60** (321mg, 69%). m.p. decomposed above 250°C; ^{1}H NMR (500 MHz, DMSO-d_6 +CF_3COOH) δ

7.89 (2H, d, J = 74 Hz), 7.38 (2H, t, J = 7.4 Hz), 7.27 (1H, t, J = 7.4 Hz), 6.86 (1H, s), 3.29 (4H, br); ^{13}C NMR (125 MHz, DMSO-d_6 +CF_3COOH) δ 163.7, 163.5, 163.5, 154.6, 135.9, 131.1, 130.2, 128.9, 128.2, 127.8, 125.8, 121.6, 121.0, 107.6, 39.2, 33.2; IR (film): 2915, 2857, 2444, 1697, 1683, 1650, 1634, 1621, 1607, 1578, 1560, 1542, 1509, 1470, 1456 cm^{-1}; MS (ES+) m/z: 322.1 $[M+H]^+$; HRMS (ES+) m/z calcd for $C_{17}H_{16}N_5O_2$ $[M+H]^+$ 322.1310, found 322.1304.

General procedure for preparing compounds 64-69:

Compound **63** (0.5-1mmol) was dissolved in THF (5mL) in a sealed tube. Appropriate amine (4eq) was added to the solution. In case when amine was available as HCl-salt (for preparation of compound **67** and **69**), pyridine (4eq) was added to the reaction mixture. The resulting mixture was heated at 90°C for 18 hours and then allowed to cool to room temperature. Then the reaction mixture was concentrated and crude material was purified by column chromatography (silica, MeOH/DCM 1:4) to afford the respective natural product analogs **64-69** (67-80%).

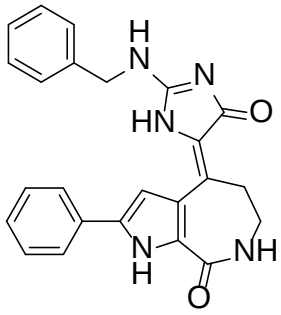

(Z)-4-(2-(benzylamino)-4-oxo-1H-imidazol-5(4H)-ylidene)-2-phenyl-4,5,6,7-tetrahydropyrrolo[2,3-c]azepin-8(1H)-one (64):

^{1}H NMR (600MHz, DMSO-d_6+drop of CF_3COOH) δ 7.86 (2H, d, J=7.8Hz), 7.35-7.39 (5H, m), 7.25-7.30 (2H, m), 6.87 (1H, s), 4.59 (2H, br), 3.31 (4H, br); ^{13}C NMR (150MHz, DMSO-d_6+drop of CF_3COOH) δ 163.8, 163.7, 154.0, 136.5, 136.0, 131.1, 130.6, 128.9 (s) , 128.4, 128.1 (s), 127.9 (s), 127.7 (s), 127.6, 125.8 (s), 121.0, 107.7 (s), 46.3 (d), 39.2 (d), 33.2 (d); IR (film): 3077, 2924, 2800, 1690, 1680, 1640, 1489, 1427, 1200, 1136cm^{-1}; MS (ES+) m/z: 412.2 $[M+H]^+$; m.p. decomposes above 220-222^{o}C HRMS (ES+) calcd for $C_{24}H_{22}N_5O_2$ $[M+H]^+$ 412.1774, found 412.1778.

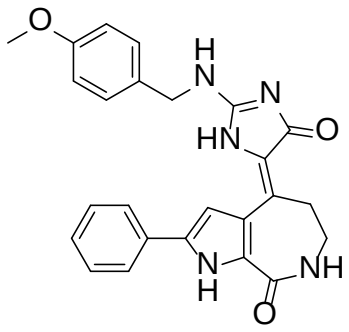

(Z)-4-(2-((4-methoxybenzyl)amino)-4-oxo-1H-imidazol-5(4H)-ylidene)-2-phenyl-4,5,6,7-tetrahydropyrrolo[2,3-c]azepin -8(1H)-one (65):

^{1}H NMR (600MHz, DMSO-d_6+drop of CF_3COOH) δ 7.88 (2H, d, J=7.6), 7.36-7.40 (2H, m), 7.26-7.32 (3H, m), 6.92-6.96 (2H, m), 6.87 (1H, s), 4.52 (2H, d, J=5.4), 6.87 (1H, s), 3.73 (3H, s), 3.31 (4H, br); ^{13}C NMR (150MHz, DMSO-d_6+drop of CF_3COOH) δ 163.7, 163.4, 159.2, 153.6, 135.7, 130.9, 130.2, 129.1 (s), 128.6 (s), 128.1, 127.7 (s), 125.6 (s), 121.4, 120.7, 114.4 (s), 107.5 (s), 55.2 (t), 45.6 (d), 39.3 (d), 32.9 (d); IR (film): 2922, 2849, 1696, 1680, 1634, 1516, 1476, 1433, 1203, 1180, 1132 cm^{-1}; MS (ES+) m/z: 442.2 $[M+H]^+$; m.p. decomposes above 250^{o}C; HRMS (ES+) calcd for $C_{25}H_{24}N_5O_3$ $[M+H]^+$ 442.1879, found 442.1880.

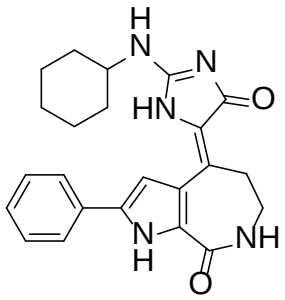

(Z)-4-(2-(cyclohexylamino)-4-oxo-1H-imidazol-5(4H)-ylidene)-2-phenyl-4,5,6,7-tetrahydropyrrolo[2,3-c]azepin-8(1H)-one (66):

^{1}H NMR (500MHz, CD_3OD+drop of CF_3COOH at 50^{o}C) δ 7.75(2H, d, J=7.6Hz), 7.42(2H, t, J=7.6Hz), 7.33(1H, t, J=7.6Hz), 6.89 (1H, s), 3.46 (4H, br), 1.98 (2H, br), 1.80 (2H, br), 1.66 (1H, d, J=12.9), 1.41-1. 47 (4H, m), 1.28(1H, Br); ^{13}C NMR (125MHz, CD_3OD +drop of CF_3COOH at 50^{o}C) δ 166.0 , 164.1, 160.3, 154.0, 138.5, 132.4, 132.1, 130.0, 129.2, 128.3 (s), 126.5 (s), 124.0 (s), 54.4, 40.9 (s), 33.5 (s), 32.0 (s), 26.0 (s), 25.3 (d); IR (film): 2930, 2855, 2800, 1727, 1700, 1676, 1615, 1663, 1516, 1466, 1450, 1205, 1181, 1136 cm^{-1}; MS (ES+) m/z: 404.2 $[M+H]^{+}$; m.p. decomposes above 250^{o}C; HRMS (ES+) calcd for $C_{23}H_{26}N_5O_2$ $[M+H]^{+}$ 404.20887, found 404.2088.

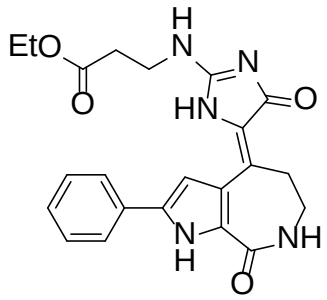

(Z)-ethyl 3-((4-oxo-5-(8-oxo-2-phenyl-5,6,7,8-tetrahydropyrrolo[2,3-c]azepin-4(1H)-ylidene)-4,5-dihydro-1H-imidazol-2-yl)amino)propanoate (67):

^{1}H NMR (500MHz, DMSO-d_6+drop of CF_3COOH) δ 7.88 (2H, d, J=7.6Hz), 7.39 (2H, t, J=7.6Hz), 7.29 (1H, t, J=7.6Hz), 6.84 (1H, br), 4.08 (2H, q, J=7.1Hz), 3.59 (2H, br), 3.31 (4H, br), 2.67 (2H, m), 1.18 (3H, t, J=7.1Hz); ^{13}C NMR (125MHz, DMSO-d_6+drop of CF_3COOH) δ 171.0, 163.6, 163.5, 153.9, 135.8, 131.0, 130.2, 128.8 (s), 128.2, 127.8 (s), 125.7 (s), 121.4, 120.7, 107.3 (s), 60.5 (d), 39.9 (d), 39.8 (d), 33.3 (d), 33.1 (d), 14.1 (t); IR (film): 3222, 2921, 2993, 1728, 1717, 1696, 1686, 1653, 1636, 1617, 1203, 1138 cm^{-1}; MS (ES+) m/z: 422.2 $[M+H]^+$; m.p. 227-229^{o}C; HRMS (ES+) calcd for $C_{22}H_{24}N_5O_4$ $[M+H]^+$ 422.1828, found 422.1831.

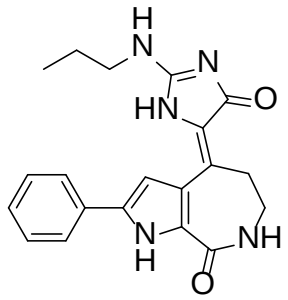

(Z)-4-(4-oxo-2-(propylamino)-1H-imidazol-5(4H)-ylidene)-2-phenyl-4,5,6,7-tetrahydropyrrolo[2,3-c]azepin-8(1H)-one (68):

^{1}H NMR (600MHz, DMSO-d_6+drop of CF_3COOH) δ 7.88 (2H, d, J=7.57Hz), 7.39 (2H, t, J=7.69 Hz), 7.25 - 7.31 (1H, t, J=7.69 Hz), 6.86 (1H, d, J=2.20Hz), 3.22 - 3.36 (m, 6H), 1.49 - 1.58 (2H, m), 0.88 (3H, t, J=7.32); ^{13}C NMR (150MHz, DMSO-d_6+drop of CF_3COOH) δ 163.7, 163.4, 153.6, 135.7, 135.7, 130.9, 129.7, 128.7 (s), 128.0, 127.6 (s), 125.6 (s), 121.4, 120.7, 107.4 (s), 44.5 (d), 39.2 (d), 32.9 (d), 22.3 (d), 10.7 (t); IR (film): 2920, 1700, 1684, 1635, 1472, 1435, 1385, 1264, 1206, 1132 cm^{-1}; MS (ES+) m/z: 364.2 $[M+H]^+$; m.p. decomposes above 270^{o}C; HRMS (ES+) calcd for $C_{20}H_{22}N_5O_2$ $[M+H]^+$ 364.1774, found 364.1777.

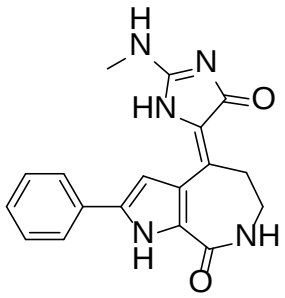

(Z)-4-(2-(methylamino)-4-oxo-1H-imidazol-5(4H)-ylidene)-2-phenyl-4,5,6,7-tetrahydropyrrolo[2,3-c]azepin-8(1H)-one (69):

^{1}H NMR (500MHz, DMSO-d_6+drop of CF_3COOH) δ 7.89 (2H, d, J=7.78 Hz), 7.37 - 7.41 (2H, 7, J=7.76), 7.22 (1H, 7, J=7.76), 6.85 (1H,s), 3.31 (4H, br), 2.97 (3H, d, J=4.58); ^{13}C NMR (125MHz, DMSO-d_6+drop of CF_3COOH) δ 163.6, 163.3, 154.3, 135.6, 130.9, 129.7, 128.7 (s), 128.1, 127.6 (s), 125.6 (s), 121.4, 120.8, 107.5 (s), 39.1 (d), 32.8 (d), 29.6 (t); IR (film): 2975, 2920, 1701, 1684, 1635, 1617, 1676, 1559, 1437, 1385, 1265, 1198, 1191, 1128 cm^{-1}; MS (ES+) m/z: 336.1 $[M+H]^+$; m.p. 240-242^{o}C; HRMS (ES+) calcd for $C_{18}H_{18}N_5O_2$ $[M+H]^+$ 336.1461, found 336.1464.

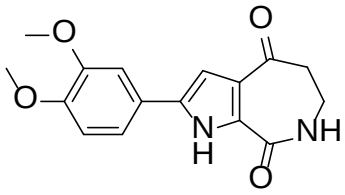

2-(3,4-dimethoxyphenyl)-6,7-dihydropyrrolo[2,3-c]azepine-4,8(1H,5H)-dione (75):

Compound **16** (185mg, 0.76mmol) was added in a mixture of toluene and ethanol (3:1, 40 mL) and 3,4-dimethoxyphenyl boronic acid **74** (166mg, 0.91mmol) and tetrakis

(triphenylphosphine) palladium (44mg, 5mmol%) were added to the reaction mixture. The a solution of sodium carbonate (242mg, 2.28mmol) in water (3 mL) was added to the reaction mixture and the mixture was heated to 95°C for 18 hours. Then the reaction mixture was allowed to cool to room temperature and partitioned between 10% aqueous sodium bicarbonate solution (50 mL) and ethyl acetate (50 mL). The organic layer was discarded while the aqueous sodium bicarbonate layer was acidified with 5% HCl solution and the product was extracted into ethyl acetate (4 x 40 mL). The dichloromethane fractions were combined and dried over anhydrous sodium sulfate (500 mg). The solvent was removed and the crude material was purified by column chromatography (silica, ethyl acetate) to afford **75** (229mg, 82%). ^{1}H NMR (500MHz, DMSO-d_6) δ 7.57 (1H, d, J=1.95 Hz), 7.41 (1H, dd, J=8.42, 2.08 Hz), 6.94 (2H, dd, J=5.62, 2.69 Hz), 3.84 (3H, s), 3.76 (3H, s), 3.38 - 3.40 (2H, m), 2.72 - 2.74 (2H, m); ^{13}C NMR (125MHz, DMSO-d_6) δ 194.36, 162.3, 148.8, 148.4, 135.7, 128.3, 124.7, 123.5, 117.9 (s), 112.0 (s), 109.2 (s), 106.2 (s), 55.7 (t), 55.5 (t), 43.7 (d), 36.6 (d); IR (film): 2923, 2849, 1653, 1644, 1636, 1491, 1468, 1256 cm^{-1}; MS (ES+) m/z: 301.1 $[M+H]^+$; m.p. decomposes above 180°C; HRMS (ES+) calcd for $C_{16}H_{17}N_2O_4$ $[M+H]^+$ 301.1188, found 301.1192.

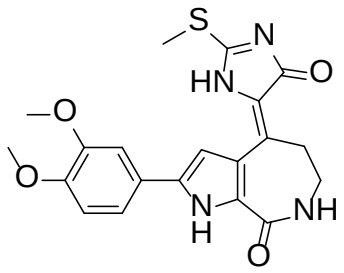

(Z)-2-(3,4-dimethoxyphenyl)-4-(2-(methylthio)-4-oxo-1H-imidazol-5(4H)-ylidene)-4,5,6,7-tetrahydropyrrolo[2,3-c]azepin-8(1H)-one (76):

Compound **75** (185mg, 0.62mmol) was dissolved in THF (20 mL) and compound **42** (160mg, 1.23mmol) was added to the reaction flask. The reaction mixture was cooled to 0°C and 1M solution of $TiCl_4$ in DCM (2.46mL, 2.46mmol) was added to the reaction mixture in drop-wise manner. The reaction mixture was stirred for 30 minutes and then pyridine (0.39mL, 4.92mmol) was added to the reaction mixture in drop-wise manner over 15 minutes. The reaction mixture was stirred for an additional 14 hours allowing it to gradually warm to room temperature. At this point saturated NH_4Cl solution (40mL) was added to the reaction mixture and contents of the flask were transferred to the separatory funnel. Then the crude product was extracted with ethyl acetate (50mL x 3). The ethyl acetate fractions were combined and dried over anhydrous Na_2SO_4 (1g). The solvent was removed and the crude material was purified by column chromatography (silica, ethyl acetate) to afford **76** (152mg, 60%). ^{1}H NMR (500MHz, DMSO-d_6) δ 7.99 (1H, d, J=2.93 Hz), 7.51 (1H, d, J=1.95 Hz), 7.33 (1H, dd, J=8.30, 1.95 Hz), 6.98 (1H, d, J=8.55 Hz), 3.77 (3H, s), 3.83 (3H, s), 3.43 - 3.45 (2H, m), 3.26 - 3.28 (2H, m), 2.66 (3H,

s); ^{13}C NMR (125MHz, DMSO-d_6) δ 170.6, 162.9, 158.1, 148.8, 148.1, 135.5, 134.6, 133.4, 127.8, 124.1, 124.0, 117.2 (s), 112.0 (s), 111.0 (s), 108.8 (s), 55.5 (t), 55.4 (t), 39.2 (d), 30.2 (d), 12.3 (t); IR (film): 2921, 2860, 1686, 1678, 1653, 1636, 1507, 1487, 1456, 1437, 1385, 1248, 1184, 1136 cm^{-1}; MS (ES+) m/z: 413.2 $[M+H]^+$; m.p. decomposes above 250^{o}C; HRMS (ES+) calcd for $C_{20}H_{21}N_4O_4S$ $[M+H]^+$ 413.1284, found 413.1293.

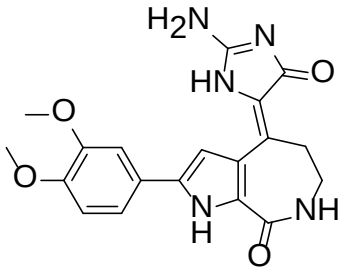

(Z)-4-(2-amino-4-oxo-1H-imidazol-5(4H)-ylidene)-2-(3,4-dimethoxyphenyl)-4,5,6,7-tetrahydropyrrolo[2,3-c]azepin-8(1H)-one (70):

Compound **76** (105mg, 0.25mmol) was added to THF (5mL) in a sealed tube and ammonium hydroxide (5mL) was added to the solution. The resulting mixture was heated at 90^{o}C for 18 hours and then allowed to cool down to room temperature. Then the reaction mixture was concentrated and crude material was purified by column chromatography (silica, MeOH/DCM 1:4) affording **70** (50mg, 52%). ^{1}H NMR (600MHz, DMSO-d_6+drop of CF_3COOH) δ 7.57 (1H, d, J=2.20 Hz), 7.41 (1H, dd, J=8.30, 1.95

Hz), 6.96 (1H, d, J=8.55 Hz), 6.77 (1H, d, J=2.44 Hz), 3.84 (3H, s), 3.77 (3H, s), 3.31 (4H, br); ^{13}C NMR (150MHz, DMSO-d_6+drop of CF_3COOH) δ 163.5, 163.2, 154.4, 149.1, 148.7, 136.0, 130.4, 127.4, 123.9, 121.4, 120.6, 118.2 (s), 112.4 (s), 109.7 (s), 106.4 (s), 55.8 (t), 55.7 (t), 39.2 (d), 32.9 (d); IR (film): 2921, 2851, 1701, 1684, 1653, 1558, 1489, 1473, 1456, 1258, 1204, 1181 cm^{-1}; MS (ES+) m/z: 382.2 $[M+H]^+$; m.p. decomposes above 250^{0}C; HRMS (ES+) calcd for $C_{19}H_{20}N_5O_4$ $[M+H]^+$ 382.1515, found 382.1526.

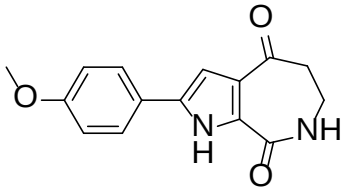

2-(4-methoxyphenyl)-6,7-dihydropyrrolo[2,3-c]azepine-4,8(1H,5H)-dione (78):

Compound **16** (243mg, 1mmol) was added in a mixture of toluene and ethanol (3:1, 40 mL) and 4-methoxyphenyl boronic acid **77** (182mg, 1.2mmol) and tetrakis (triphenylphosphine) palladium (58mg, 5mmol%) were added to the reaction mixture. Then a solution of sodium carbonate (318mg, 3mmol) in water (3mL) was added to the reaction mixture and the mixture was heated to 95°C for 18 hours. Then the reaction mixture was allowed to cool to room temperature and partitioned between 10% aqueous sodium bicarbonate solution (50 mL) and ethyl acetate (50mL). The organic layer was discarded while the aqueous sodium bicarbonate layer was acidified with 5% HCl solution and the product was extracted into ethyl acetate (40mL x 4). The ethyl acetate

fractions were combined and dried over anhydrous sodium sulfate (500mg). The solvent was removed and the crude material was purified by column chromatography (silica, ethyl acetate) to afford **78** (189mg, 82%). ^{1}H NMR (500MHz, DMSO-d_6) δ 7.83 (2H, d, J=8.55 Hz), 6.94 (2H, d, J=8.79 Hz), 6.86 (1H, d, J=2.44 Hz), 3.77 (3H, s), 3.35 - 3.38 (2H, m), 2.70 - 2.72 (2H, m); ^{13}C NMR (125MHz) (DMSO-d_6) δ 194.5, 162.1, 158.9, 135.4, 128.3, 126.8 (s), 124.6, 123.3, 114.1 (s), 105.9 (s), 55.2 (t), 43.7 (d), 36.5 (d); IR (film): 3212, 3135, 2897, 1653, 1636, 1456, 1256 cm^{-1}; MS (ES+) m/z: 271.1 $[M+H]^+$, m.p. decomposes above 255-256^{o}C; HRMS (ES+) calcd for $C_{15}H_{15}N_2O_3$ $[M+H]^+$ 271.1083, found 271.1085.

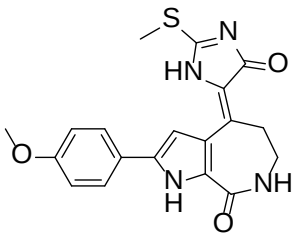

(Z)-2-(4-methoxyphenyl)-4-(2-(methylthio)-4-oxo-1H-imidazol-5(4H)-ylidene)-4,5,6,7-tetrahydropyrrolo[2,3-c]azepin-8(1H)-one (79):

Compound **78** (410mg, 1.52mmol) was dissolved in THF (20mL) and compound **42** (783mg, 3.03mmol) was added to the reaction flask. The reaction mixture was cooled to 0^{o}C and 1M solution of $TiCl_4$ in DCM (6mL, 6mmol) was added to the reaction mixture in drop-wise manner. The reaction mixture was stirred for 30 minutes and pyridine (0.97mL, 12.1mmol) was added to the reaction mixture drop-wise manner over 15

minutes. The reaction mixture was stirred for an additional 14 hours allowing it to gradually warm to room temperature. At this point saturated NH_4Cl solution (40mL) was added to the reaction mixture and contents of the flask were transferred to the separatory funnel. Then the crude product was extracted with ethyl acetate (50mL x 3). The ethyl acetate fractions were combined and dried over anhydrous Na_2SO_4 (500mg). The solvent was removed and the crude material was purified by column chromatography (silica, ethyl acetate) to afford **79** (285mg, 49%). ^{1}H NMR (500MHz, DMSO-d_6) δ 7.90 (1H, s), 7.76 (2H, d, J=8.30 Hz,), 6.95 (2H, d, J=8.30 Hz), 3.77 (3H, s), 3.42 - 3.45 (2H, m), 3.25-3.27 (2H, m), 2.4 (3H, s); ^{13}C NMR (125MHz; DMSO-d_6) δ 170.6, 162.8, 158.6, 135.5, 134.4, 133.5, 131.5, 127.8, 126.4 (s), 124.0, 123.9, 114.2 (s), 110.7 (s), 55.1 (t), 39.2 (d), 30.3 (d), 12.2 (t); IR (film): 2980, 2910, 1676, 1632, 1588, 1478, 1456, 1435, 1252, 1179 cm^{-1}; MS (ES+) m/z: 383.1$[M+H]^+$; m.p. decomposes above 240^{O}C; HRMS (ES+) calcd for $C_{19}H_{19}N_4O_3S$ $[M+H]^+$ 383.1178; found 383.1185

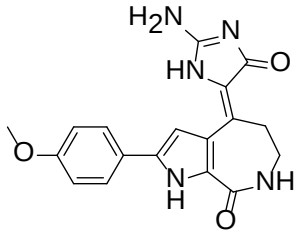

(Z)-4-(2-amino-4-oxo-1H-imidazol-5(4H)-ylidene)-2-(4-methoxyphenyl)-4,5,6,7-tetrahydropyrrolo[2,3-c]azepin-8(1H)-one (71):

Compound **79** (75mg, 0.2mmol) was added to THF (5mL) in a sealed tube and ammonium hydroxide (5mL) was added to the solution. The resulting mixture was heated at 90^{o}C for 18 hours and then allowed to cool to room temperature. Then the reaction mixture was concentrated and crude material was purified by column chromatography (silica, MeOH/DCM 1:4) affording **71** (69mg, 65%). ^{1}H NMR (500MHz, DMSO-d_6+drop of CF_3COOH) δ 7.84 (2H, d, J=8.54 Hz), 6.96 (2H, d, J=8.54 Hz), 6.76 (1H, s), 3.77 (3H, s), 3.29 (4H, br); ^{13}C NMR (125MHz, DMSO-d_6+drop of CF_3COOH) δ 163.7, 163.6s, 154.7, 136.1, 130.6, 127.8, 127.4 (s), 126.9, 123.9, 121.7, 120.9, 114.5 (s), 106.6 (s), 55.6 (t), 39.6 (d), 33.2 (d); IR (film): 2995, 2935, 1696, 1684, 1653, 1636, 1617, 1559, 1539, 1491, 1456, 1437, 1385, 1260, 1206, 1138 cm^{-1}; MS (ES+) m/z: 352.1 $[M+H]^{+}$; m.p. decomposes above 250^{o}C; HRMS (ES+) calcd for $C_{18}H_{18}N_5O_3$ $[M+H]^{+}$ 352.1410, found 352.1412.

The structure of compound **64** was also verified by taking x-ray single crystal analysis by Dr. Richard Staples

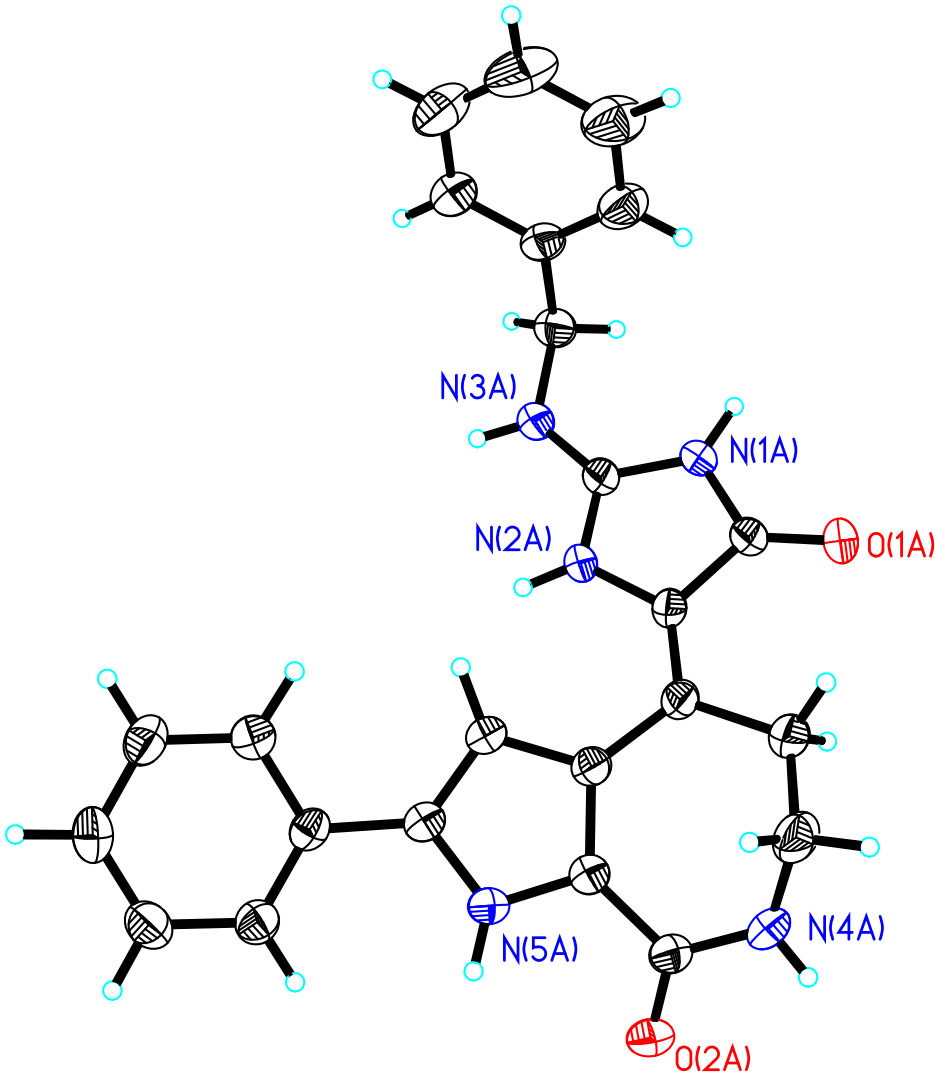

Figure 2.15. Single crystal stucture of compound 64

References

2.16. References

1. Hurley, L. H., DNA and its associated processes as targets for cancer therapy. *Nat. Rev. Cancer* **2002,** *2*, 188-200.

2. Vousden, K. H., p53: Death star. *Cell* **2000,** *103*, 691-4.

3. Giaccia, A. J.; Kastan, M. B., The complexity of p53 modulation: emerging patterns from divergent signals. *Gene. Dev.* **1998,** *12*, 2973-83.

4. (a) Levine, A. J.; Momand, J.; Finlay, C. A., The p53 tumour suppressor gene. *Nature* **1991,** *351*, 453-6; (b) Hollstein, M.; Sidransky, D.; Vogelstein, B.; Harris, C. C., p53 mutations in human cancers. *Science* **1991,** *253*, 49-53; (c) LEVINE, A., p53, the cellular gatekeeper for growth and division. *Cell* **1997,** *88*, 323-31; (d) Hollstein, M.; Rice, K.; Greenblatt, M. S.; Soussi, T.; Fuchs, R.; Sorlie, T.; Hovig, E.; Smith-Sorensen, B.; Montesano, R.; Harris, C. C., Database of p53 gene somatic mutations in human tumors and cell lines. *Nucleic Acids Res.* **1994,** *22*, 3551-5.

5. Levesque, A. a.; Eastman, A., p53-based cancer therapies: Is defective p53 the Achilles heel of the tumor? *Carcinogenesis* **2007,** *28*, 13-20.

6. Lowe, S. W.; Schmitt, E. M.; Smith, S. W.; Osborne, B. A.; Jacks, T., p53 is required for radiation-induced apoptosis in mouse thymocytes. *Nature* **1993,** *362*, 847-9.

7. Lowe, S. W.; Bodis, S.; Mcclatchey, A.; Remington, L.; Ruley, H. E.; Fisher, D. E.; Housman, D. E.; Jacks, T., p53 status and the efficacy of cancer-therapy in-vivo. *Science* **1994,** *266*, 807-10.

8. Strassera, A.; Harrisa, A. W.; Jacksb, T.; Cory, S., DNA damage can induce apoptosis in proliferating lymphoid cells via p53-independent mechanisms inhibitable by Bcl-2. *Cell* **1994,** *79*, 329-39.

9. Bartek, J.; Lukas, J., Chk1 and Chk2 kinases in checkpoint control and cancer. *Cancer cell* **2003,** *3*, 421-9.

10. Jazayeri, A.; Falck, J.; Lukas, C.; Bartek, J.; Smith, G. C. M.; Lukas, J.; Jackson, S. P., ATM- and cell cycle-dependent regulation of ATR in response to DNA double-strand breaks. *Nat. Cell Biol.* **2006,** *8*, 37-45.

11. Lukas, C.; Bartkova, J.; Latella, L.; Falck, J.; Mailand, N.; Schroeder, T.; Sehested, M.; Lukas, J.; Bartek, J., DNA damage-activated kinase Chk2 is independent of proliferation or differentiation yet correlates with tissue biology. *Cancer Res.* **2001,** *61*, 4990.

12. Pommier, Y.; Sordet, O.; Rao, A.; Zhang, H.; Kohn, K. W., Targeting Chk2 kinase: Molecular interaction maps and therapeutic rationale. *Curr. Pharm. Design* **2005,** *11*, 2855-572.

13. (a) Rogakou, E. P.; Pilch, D. R.; Orr, A. H.; Ivanova, V. S.; Bonner, W. M., DNA double-stranded breaks induce histone H2AX phosphorylation on serine 139. *J. Biol. Chem.* **1998,** *273*, 5858-68; (b) Rogakou, E. P.; Nieves-Neira, W.; Boon, C.; Pommier, Y.; Bonner, W. M., Initiation of DNA fragmentation during apoptosis induces phosphorylation of H2AX histone at serine 139. *J. Biol. Chem.* **2000,** *275*, 9390-5.

14. Bassing, C. H.; Alt, F. W., H2AX may function as an anchor to hold broken chromosomal DNA ends in close proximity. *Cell cycle* **2004,** *3*, 149-53.

15. (a) Glover, J. N. M.; Williams, R. S.; Lee, M. S., Interactions between BRCT repeats and phosphoproteins: tangled up in two. *Trends Biochem. Sci* **2004,** *29*, 579-85; (b) Stucki, M.; Jackson, S. P., GammaH2AX and MDC1: anchoring the DNA-damage-response machinery to broken chromosomes. *DNA repair* **2006,** *5*, 534-43.

16. Bakkenist, C. J.; Kastan, M. B., DNA damage activates ATM through intermolecular autophosphorylation and dimer dissociation. *Nature* **2003,** *421*, 499-506.

17. Kurz, E. U.; Lees-Miller, S. P., DNA damage-induced activation of ATM and ATM-dependent signaling pathways. *DNA repair* **2004,** *3*, 889-900.

18. Ahn, J. Y.; Schwarz, J. K.; Piwnica-Worms, H.; Canman, C. E., Threonine 68 phosphorylation by ataxia telangiectasia mutated is required for efficient activation of Chk2 in response to ionizing radiation. *Cancer Res.* **2000,** *60*, 5934-6.

19. Schwarz, J. K.; Lovly, C. M.; Piwnica-Worms, H., Regulation of the Chk2 protein kinase by oligomerization-mediated cis- and trans-phosphorylation. *Mol. Cancer Res.* **2003,** *1*, 598-609.

20. (a) Nilsson, I.; Hoffmann, I., Cell cycle regulation by the Cdc25 phosphatase family. *Prog. Cell Cycle Res.* **2000,** *4*, 107-14; (b) Bartek, J.; Lukas, J., Mammalian G1- and S-phase checkpoints in response to DNA damage. *Curr. Opin. Cell Biol.* **2001,** *13*, 738-47; (c) Bartek, J.; Lukas, J., Pathways governing G1/S transition and their response to DNA damage. *FEBS Lett.* **2001,** *490*, 117-22; (d) Goh, W. C.; Manel, N.; Emerman, M., The human immunodeficiency virus Vpr protein binds Cdc25C: implications for G2 arrest. *Virology* **2004,** *318*, 337-49; (e) Oconnor, P. M.; Ferris, D. K.; Hoffmann, I.; Jackman, J.; Draetta, G.; Kohn, K. W., Role of the Cdc25c phosphatase in G(2) arrest induced by nitrogen-mustard. *P. Natl. Acad. Sci. USA* **1994,** *91*, 9480-4.

21. Moll, U. M.; Petrenko, O., The MDM2-p53 interaction. *Mol. Cancer Res.* **2003,** *1*, 1001-8.

22. Meulmeester, E.; Pereg, Y.; Shiloh, Y.; Jochemsen, A. G., ATM-mediated phosphorylations inhibit Mdmx/Mdm2 stabilization by HAUSP in favor of p53 activation. *Cell cycle* **2005,** *4*, 1166-70.

23. (a) Greenblatt, M. S.; Bennett, W. P.; Hollstein, M.; Harris, C. C., Mutations in the p53 tumor suppressor gene: clues to cancer etiology and molecular pathogenesis. *Cancer Res.* **1994,** *54*, 4855-78; (b) Soussi, T.; Dehouche, K.; Béroud, C., P53 Website and Analysis of P53 Gene Mutations in Human Cancer: Forging a Link Between Epidemiology and Carcinogenesis. *Hum. Mutat.* **2000,** *15*, 105-13.

24. (a) Moll, U. M.; LaQuaglia, M.; Benard, J.; Riou, G., Wild-type p53 protein undergoes cytoplasmic sequestration in undifferentiated neuroblastomas but not in differentiated tumors. *P. Natl. Acad. Sci. USA* **1995,** *92*, 4407-11; (b) Oliner, J. D.; Kinzler, K. W.; Meltzer, P. S.; George, D. L.; Vogelstein, B., Amplification of a gene encoding a p53-associated protein in human sarcomas. *Nature* **1992,** *358*, 80-3; (c) Crook, T.; Wrede, D.; Tidy, J. A.; Mason, W. P.; Evans, D. J.; Vousden, K. H., Clonal p53 mutation in primary cervical cancer: association with human-papillomavirus-negative tumours. *Lancet* **1992,** *339*, 1070-3.

25. (a) Bartkova, J.; Horejsí, Z.; Koed, K.; Krämer, A.; Tort, F.; Zieger, K.; Guldberg, P.; Sehested, M.; Nesland, J. M.; Lukas, C.; Ørntoft, T.; Lukas, J.; Bartek, J., DNA damage response as a candidate anti-cancer barrier in early human tumorigenesis. *Nature* **2005,** *434*, 864-70; (b) Gorgoulis, V. G.; Vassiliou, L.-V. F.; Karakaidos, P.; Zacharatos, P.; Kotsinas, A.; Liloglou, T.; Venere, M.; Ditullio, R. A.; Kastrinakis, N. G.; Levy, B.; Kletsas, D.; Yoneta, A.; Herlyn, M.; Kittas, C.; Halazonetis, T. D., Activation of the DNA damage checkpoint and genomic instability in human precancerous lesions. *Nature* **2005,** *434*, 907-13.

26. (a) Takai, H.; Naka, K.; Okada, Y.; Watanabe, M.; Harada, N.; Saito, S. i.; Anderson, C. W.; Appella, E.; Nakanishi, M.; Suzuki, H.; Nagashima, K.; Sawa, H.; Ikeda, K.; Motoyama, N., Chk2-deficient mice exhibit radioresistance and defective p53-mediated transcription. *EMBO J.* **2002,** *21*, 5195-205; (b) Hirao, A.; Cheung, A.; Duncan, G.; Girard, P.-M.; Elia, A. J.; Wakeham, A.; Okada, H.; Sarkissian, T.; Wong, J. A.; Sakai, T.; de Stanchina, E.; Bristow, R. G.; Suda, T.; Lowe, S. W.; Jeggo, P. A.; Elledge, S. J.; Mak, T. W., Chk2 is a tumor suppressor that regulates apoptosis in both an ataxia telangiectasia mutated (ATM)-dependent and an ATM-independent manner. *Mol. Cell. Biol.* **2002,** *22*, 6521-32; (c) Hirao, A.; Kong, Y.-Y.; Matsuoka, S.; Wakeham, A.; Ruland, J.; Yoshida, H.; Liu, D.; Elledge, S. J.; Mak, T. W., DNA damage-induced activation of p53 by the checkpoint kinase Chk2. *Science* **2000,** *287*, 1824-7; (d) Ahn, J.; Urist, M.; Prives, C., The Chk2 protein kinase. *DNA repair* **2004,** *3*, 1039-47.

27. Carlessi, L.; Buscemi, G.; Larson, G.; Hong, Z.; Wu, J. Z.; Delia, D., Biochemical and cellular characterization of VRX0466617, a novel and selective inhibitor for the checkpoint kinase Chk2. *Mol. Cancer Ther.* **2007,** *6*, 935-44.

28. Arienti, K. L.; Brunmark, A.; Axe, F. U.; McClure, K.; Lee, A.; Blevitt, J.; Neff, D. K.; Huang, L.; Crawford, S.; Pandit, C. R.; Karlsson, L.; Breitenbucher, J. G., Checkpoint kinase inhibitors: SAR and radioprotective properties of a series of 2-arylbenzimidazoles. *J. Med. Chem.* **2005,** *48*, 1873-85.

29. (a) McClure, K. J.; Huang, L.; Arienti, K. L.; Axe, F. U.; Brunmark, A.; Blevitt, J.; Guy Breitenbucher, J., Novel non-benzimidazole chk2 kinase inhibitors. *Bioorg. Med. Chem. Lett.* **2006,** *16*, 1924-8; (b) Larson, G.; Yan, S.; Chen, H.; Rong, F.; Hong, Z.; Wu, J. Z., Identification of novel, selective and potent Chk2 inhibitors. *Bioorg. Med. Chem. Lett.* **2007,** *17*, 172-5; (c) Jobson, A. G.; Cardellina, J. H.; Scudiero, D.; Kondapaka, S.; Zhang, H.; Kim, H.; Shoemaker, R.; Pommier, Y., Identification of a bis-guanylhydrazone [4,4'-Diacetyldiphenylurea-bis(guanylhydrazone); NSC 109555] as a novel chemotype for inhibition of Chk2 kinase. *Mol. Pharmacol.* **2007,** *72*, 876-84; (d) Hilton, S.; Naud, S.; Caldwell, J. J.; Boxall, K.; Burns, S.; Anderson, V. E.; Antoni, L.; Allen, C. E.; Pearl, L. H.; Oliver, A. W.; Wynne Aherne, G.; Garrett, M. D.; Collins, I., Identification and characterisation of 2-aminopyridine inhibitors of checkpoint kinase 2. *Biorg. Med. Chem.* **2010,** *18*, 707-18.

30. (a) Yu, Q.; Rose, J. H.; Zhang, H.; Pommier, Y., Antisense inhibition of Chk2/hCds1 expression attenuates DNA damage-induced S and G2 checkpoints and enhances apoptotic activity in HEK-293 cells. *FEBS Lett.* **2001,** *505*, 7-12; (b) Ghosh, J. C.; Dohi, T.; Raskett, C. M.; Kowalik, T. F.; Altieri, D. C., Activated checkpoint kinase 2 provides a survival signal for tumor cells. *Cancer Res.* **2006,** *66*, 11576-9.

31. Ahn, J. W.; Urist, M.; Prives, C., Questioning the role of checkpoint kinase 2 in the p53 DNA damage response. *J. Biol. Chem.* **2003,** *278*, 20480-9.

32. Chabalier-Taste, C.; Racca, C.; Dozier, C.; Larminat, F., BRCA1 is regulated by Chk2 in response to spindle damage. *BBA-Mol. Cell Res.* **2008,** *1783*, 2223-33.

33. Castedo, M.; Perfettini, J. L.; Roumier, T.; Valent, A.; Raslova, H.; Yakushijin, K.; Horne, D.; Feunteun, J.; Lenoir, G.; Medema, R.; Vainchenker, W.; Kroemer, G., Mitotic catastrophe constitutes a special case of apoptosis whose suppression entails aneuploidy. *Oncogene* **2004,** *23*, 4362-70.

34. Vaklfahmetoglu, H.; Olsson, M.; Tamm, C.; Heidari, N.; Orrenius, S.; Zhivotovsky, B., DNA damage induces two distinct modes of cell death in ovarian carcinomas. *Cell Death Differ.* **2008,** *15*, 555-66.

35. (a) Antoni, L.; Sodha, N.; Collins, I.; Garrett, M. D., CHK2 kinase: cancer susceptibility and cancer therapy - two sides of the same coin? *Nat. Rev. Cancer* **2007,** *7*, 925-36; (b) Jobson, A. G.; Lountos, G. T.; Lorenzi, P. L.; Llamas, J.; Connelly, J.; Cerna, D.; Tropea, J. E.; Onda, A.; Zoppoli, G.; Kondapaka, S.; Zhang, G.; Caplen, N. J.; Cardellina, J. H.; Yoo, S. S.; Monks, A.; Self, C.; Waugh, D. S.; Shoemaker, R. H.; Pommier, Y., Cellular inhibition of checkpoint kinase 2 (Chk2) and potentiation of

camptothecins and radiation by the novel Chk2 inhibitor PV1019 [7-nitro-1H-indole-2-carboxylic acid {4-[1-(guanidinohydrazone)-ethyl]-phenyl}-amide]. *J. Pharmacol. Exp. Ther.* **2009,** *331*, 816-26; (c) Caldwell, J. J.; Welsh, E. J.; Matijssen, C.; Anderson, V. E.; Antoni, L.; Boxall, K.; Urban, F.; Hayes, A.; Raynaud, F. I.; Rigoreau, L. J. M.; Raynham, T.; Aherne, G. W.; Pearl, L. H.; Oliver, A. W.; Garrett, M. D.; Collins, I., Structure-based design of potent and selective 2-(quinazolin-2-yl)phenol inhibitors of checkpoint kinase 2. *J. Med. Chem.* **2011,** *54*, 580-90.

36. (a) Ariumi, Y.; Trono, D., Ataxia-telangiectasia-mutated (ATM) protein can enhance human immunodeficiency virus type 1 replication by stimulating Rev function. *J. Virol.* **2006,** *80*, 2445-52; (b) Ariumi, Y.; Kuroki, M.; Dansako, H.; Abe, K.-I.; Ikeda, M.; Wakita, T.; Kato, N., The DNA damage sensors ataxia-telangiectasia mutated kinase and checkpoint kinase 2 are required for hepatitis C virus RNA replication. *J. Virol.* **2008,** *82*, 9639-46; (c) Lilley, C. E.; Schwartz, R. A.; Weitzman, M. D., Using or abusing: viruses and the cellular DNA damage response. *Trends Microbiol.* **2007,** *15*, 119-26; (d) Lau, A.; Swinbank, K. M.; Ahmed, P. S.; Taylor, D. L.; Jackson, S. P.; Smith, G. C. M.; O'Connor, M. J., Suppression of HIV-1 infection by a small molecule inhibitor of the ATM kinase. *Nat. Cell Biol.* **2005,** *7*, 493-500.

37. Kudoh, A.; Fujita, M.; Zhang, L.; Shirata, N.; Daikoku, T.; Sugaya, Y.; Isomura, H.; Nishiyama, Y.; Tsurumi, T., Epstein-Barr virus lytic replication elicits ATM checkpoint signal transduction while providing an S-phase-like cellular environment. *J. Biol. Chem.* **2005,** *280*, 8156-63.

38. (a) Shirata, N.; Kudoh, A.; Daikoku, T.; Tatsumi, Y.; Fujita, M.; Kiyono, T.; Sugaya, Y.; Isomura, H.; Ishizaki, K.; Tsurumi, T., Activation of ataxia telangiectasia-mutated DNA damage checkpoint signal transduction elicited by herpes simplex virus infection. *J. Biol. Chem.* **2005,** *280*, 30336-41; (b) Lilley, C. E.; Carson, C. T.; Muotri, A. R.; Gage, F. H.; Weitzman, M. D., DNA repair proteins affect the lifecycle of herpes simplex virus 1. *P. Natl. Acad. Sci. USA* **2005,** *102*, 5844-9; (c) Wilkinson, D. E.; Weller, S. K., Recruitment of cellular recombination and repair proteins to sites of herpes simplex virus Type 1 DNA replication is dependent on the composition of viral proteins within prereplicative sites and correlates with the induction of the DNA damage response. *J. Virol.* **2004,** *78*, 4783-96.

39. Gaspar, M.; Shenk, T., Human cytomegalovirus inhibits a DNA damage response by mislocalizing checkpoint proteins. *P. Natl. Acad. Sci. USA* **2006,** *103*, 2821-6.

40. Liang, X.; Pickering, M. T.; Cho, N.-H.; Chang, H.; Volkert, M. R.; Kowalik, T. F.; Jung, J. U., Deregulation of DNA damage signal transduction by herpesvirus latency-associated M2. *J. Virol.* **2006,** *80*, 5862-74.

41. Berthet, C.; Raj, K.; Saudan, P.; Beard, P., How adeno-associated virus Rep78 protein arrests cells completely in S phase. *P. Natl. Acad. Sci. USA* **2005,** *102*, 13634-9.

42. Shi, Y.; Dodson, G. E.; Shaikh, S.; Rundell, K.; Tibbetts, R. S., Ataxia-telangiectasia-mutated (ATM) is a T-antigen kinase that controls SV40 viral replication in vivo. *J. Biol. Chem.* **2005,** *280*, 40195-200.

43. Skalka, a. M.; Katz, R. A., Retroviral DNA integration and the DNA damage response. *Cell Death Differ.* **2005,** *12 Suppl 1*, 971-8.

44. (a) Ariumi, Y.; Kuroki, M.; Dansako, H.; Abe, K. I.; Ikeda, M.; Wakita, T.; Kato, N., The DNA damage sensors ataxia-telangiectasia mutated kinase and checkpoint kinase 2 are required for hepatitis C virus RNA replication. *J. Virol.* **2008,** *82*, 9639-46; (b) Shirata, N.; Kudoh, A.; Daikoku, T.; Tatsumi, Y.; Fujita, M.; Kiyono, T.; Sugaya, Y.; Isomura, H.; Ishizaki, K.; Tsurumi, T., Activation of ataxia telangiectasia-mutated DNA damage checkpoint signal transduction elicited by herpes simplex virus infection. *J. Biol. Chem.* **2005,** *280*, 30336-41; (c) Haoudi, A.; Daniels, R. C.; Wong, E.; Kupfer, G.; Semmes, O. J., Human T-cell leukemia virus-I tax oncoprotein functionally targets a subnuclear complex involved in cellular DNA damage-response. *J. Biol. Chem.* **2003,** *278*, 37736-44; (d) Choudhuri, T.; Verma, S. C.; Lan, K.; Murakami, M.; Robertson, E. S., The ATM/ATR signaling effector Chk2 is targeted by Epstein-Barr virus nuclear antigen 3C to release the G(2)/M cell cycle block. *J. Virol.* **2007,** *81*, 6718-30.

45. Yu, Q.; Rose, J. L.; Zhang, H.; Takemura, H.; Kohn, K. W.; Pommier, Y., UCN-01 inhibits p53 up-regulation and abrogates gamma-radiation-induced G2-M checkpoint independently of p53 by targeting both of the checkpoint kinases, Chk2 and Chk1. *Cancer Res.* **2002,** *62*, 5743-8.

46. Kohn, E. A.; Yoo, C. J.; Eastman, A., The protein kinase C inhibitor Go6976 is a potent inhibitor of DNA damage-induced S and G2 cell cycle checkpoints. *Cancer Res.* **2003,** *63*, 31.

47. Matthews, D. J.; Yakes, F. M.; Chen, J.; Tadano, M.; Bornheim, L.; Clary, D. O.; Tai, A.; Wagner, J. M.; Miller, N.; Kim, Y. D.; Robertson, S.; Murray, L.; Karnitz, L. M., Pharmacological abrogation of S-phase checkpoint enhances the anti-tumor activity of gemcitabine in vivo. *Cell cycle* **2007,** *6*, 104-10.

48. Anderson, V. E.; Walton, M. I.; Eve, P. D.; Boxall, K. J.; Antoni, L.; Caldwell, J. J.; Aherne, W.; Pearl, L. H.; Oliver, A. W.; Collins, I.; Garrett, M. D., CCT241533 is a potent and selective inhibitor of CHK2 that potentiates the cytotoxicity of PARP inhibitors. *Cancer Res.* **2011,** *71*, 463-72.

49. (a) Curman, D.; Cinel, B.; Williams, D. E.; Rundle, N.; Block, W. D.; Goodarzi, A. A.; Hutchins, J. R.; Clarke, P. R.; Zhou, B. B.; Lees-Miller, S. P.; Andersen, R. J.; Roberge, M., Inhibition of the G2 DNA damage checkpoint and of protein kinases Chk1 and Chk2 by the marine sponge alkaloid debromohymenialdisine. *J. Biol. Chem.* **2001,** *276*, 17914-9; (b) Wan, Y.; Hur, W.; Cho, C. Y.; Liu, Y.; Adrian, F. J.; Lozach, O.; Bach,

S.; Mayer, T.; Fabbro, D.; Meijer, L.; Gray, N. S., Synthesis and target identification of hymenialdisine analogs. *Chem. Biol.* **2004,** *11*, 247-59.

50. (a) Shao, R. G.; Cao, C. X.; Shimizu, T.; O'Connor, P. M.; Kohn, K. W.; Pommier, Y., Abrogation of an S-phase checkpoint and potentiation of camptothecin cytotoxicity by 7-hydroxystaurosporine (UCN-01) in human cancer cell lines, possibly influenced by p53 function. *Cancer Res.* **1997,** *57*, 4029; (b) Akinaga, S.; Nomura, K.; Gomi, K.; Okabe, M., Enhancement of antitumor activity of mitomycin C in vitro and in vivo by UCN-01, a selective inhibitor of protein kinase C. *Cancer Chemo.Th. Pharm.* **1993,** *32*, 183-9; (c) Fuse, E.; Kuwabara, T.; Sparreboom, A.; Sausville, E. a.; Figg, W. D., Review of UCN-01 development: a lesson in the importance of clinical pharmacology. *J. Clin. Pharmacol.* **2005,** *45*, 394-403.

51. (a) Riesterer, O.; Matsumoto, F.; Wang, L.; Pickett, J.; Molkentine, D.; Giri, U.; Milas, L.; Raju, U., A novel Chk inhibitor, XL-844, increases human cancer cell radiosensitivity through promotion of mitotic catastrophe. *Invest. New Drugs* **2011,** *29*, 514-22; (b) Parsels, L. a.; Morgan, M. a.; Tanska, D. M.; Parsels, J. D.; Palmer, B. D.; Booth, R. J.; Denny, W. a.; Canman, C. E.; Kraker, A. J.; Lawrence, T. S.; Maybaum, J., Gemcitabine sensitization by checkpoint kinase 1 inhibition correlates with inhibition of a Rad51 DNA damage response in pancreatic cancer cells. *Mol. Cancer Ther.* **2009,** *8*, 45-54.

52. Takai, H.; Tominaga, K.; Motoyama, N.; Minamishima, Y. A.; Nagahama, H.; Tsukiyama, T.; Ikeda, K.; Nakayama, K.; Nakanishi, N.; Nakayama, K., Aberrant cell cycle checkpoint function and early embryonic death in Chk1(-/-) mice. *Gene. Dev.* **2000,** *14*, 1439-47.

53. Ciminoa, G.; Rosaa, S. D.; Stefanoa, S. D.; Mazzarellab, L.; Pulitia, R.; Sodano, G., Isolation and X-ray crystal structure of a novel bromo-compound from two marine sponges. *Tetrahedron Lett.* **1982,** *23*, 767-8.

54. Sharma, V.; Tepe, J. J., Potent inhibition of checkpoint kinase activity by a hymenialdisine-derived indoloazepine. *Bioorg. Med. Chem. Lett.* **2004,** *14*, 4319-21.

55. Castedo, M.; Perfettini, J. L.; Roumier, T.; Yakushijin, K.; Horne, D.; Medema, R.; Kroemer, G., The cell cycle checkpoint kinase Chk2 is a negative regulator of mitotic catastrophe. *Oncogene* **2004,** *23*, 4353-61.

56. Qin, Y.; He, Q. F.; Chen, W., Synthesis of 2-substituted endo-hymenialdisine derivatives. *Tetrahedron Lett.* **2007,** *48*, 1899-901.

57. Sharma, V.; Lansdell, T. A.; Jin, G.; Tepe, J. J., Inhibition of cytokine production by hymenialdisine derivatives. *J. Med. Chem.* **2004,** *47*, 3700-3.

58. Meijer, L.; Thunnissen, A.-M.; White, A.; Garnier, M.; Nikolic, M.; Tsai, L.-H.; Walter, J.; Cleverley, K.; Salinas, P.; Wu, Y.-Z.; Biernat, J.; Mandelkow, E.-M.; Kim, S.-H.; Pettit, G., Inhibition of cyclin-dependent kinases, GSK-3β and CK1 by hymenialdisine, a marine sponge constituent. *Chem. Biol.* **2000,** *7*, 51-63.

59. Tasdemir, D.; Mallon, R.; Greenstein, M.; Feldberg, L. R.; Kim, S. C.; Collins, K.; Wojciechowicz, D.; Mangalindan, G. C.; Concepción, G. P.; Harper, M. K.; Ireland, C. M., Aldisine alkaloids from the Philippine Sponge Stylissa massa are potent inhibitors of mitogen-activated protein kinase kinase-1 (MEK-1). *J. Med. Chem.* **2002,** *45*, 529-32.

CHAPTER 3

SYNTHESIS AND KINASE PROFILING OF NOVEL BENZOAZEPINONE BASED ANALOGS OF HMD

3.1. Introduction

Exploration of the structure activity relationship (SAR) is an essential undertaking in the field of drug discovery. SAR enables the optimization of the structure for activity of the lead molecule towards attaining the desired potency and selectivity for a particular target protein.[1] Natural products, HMD and DBH, have been the structures of the interest for many research groups who have prepared different analogs of the natural products[2] and have shown that small changes in the structure can make the analogs more potent for certain CDKs or GSK3β[3], ChK1[4] or ChK2[5].

We have shown the synthesis of the indoloazepinone and 2-arylpyrroloazepinone derivatives of the natural product in the previous chapters along with the kinase profiling of these derivatives. A glance at these molecules (Figure 3.1) reveals one common feature among others. These derivatives have pyrrolic or indolic nitrogen atom. The study of the H-bond interaction in the crystal structure of ChK2 and DBH reveals that this N-atom is present inside the binding pocket of the protein and is projected towards the peptide chain. However, unlike the other N-atoms in the molecules, which are involved in the donaptor interaction with different residues in the binding pocket, this N-atom does not seem to have any polar residue in its vicinity to establish any interaction. This raises the question on the importance of having a hetero-atom at this site.

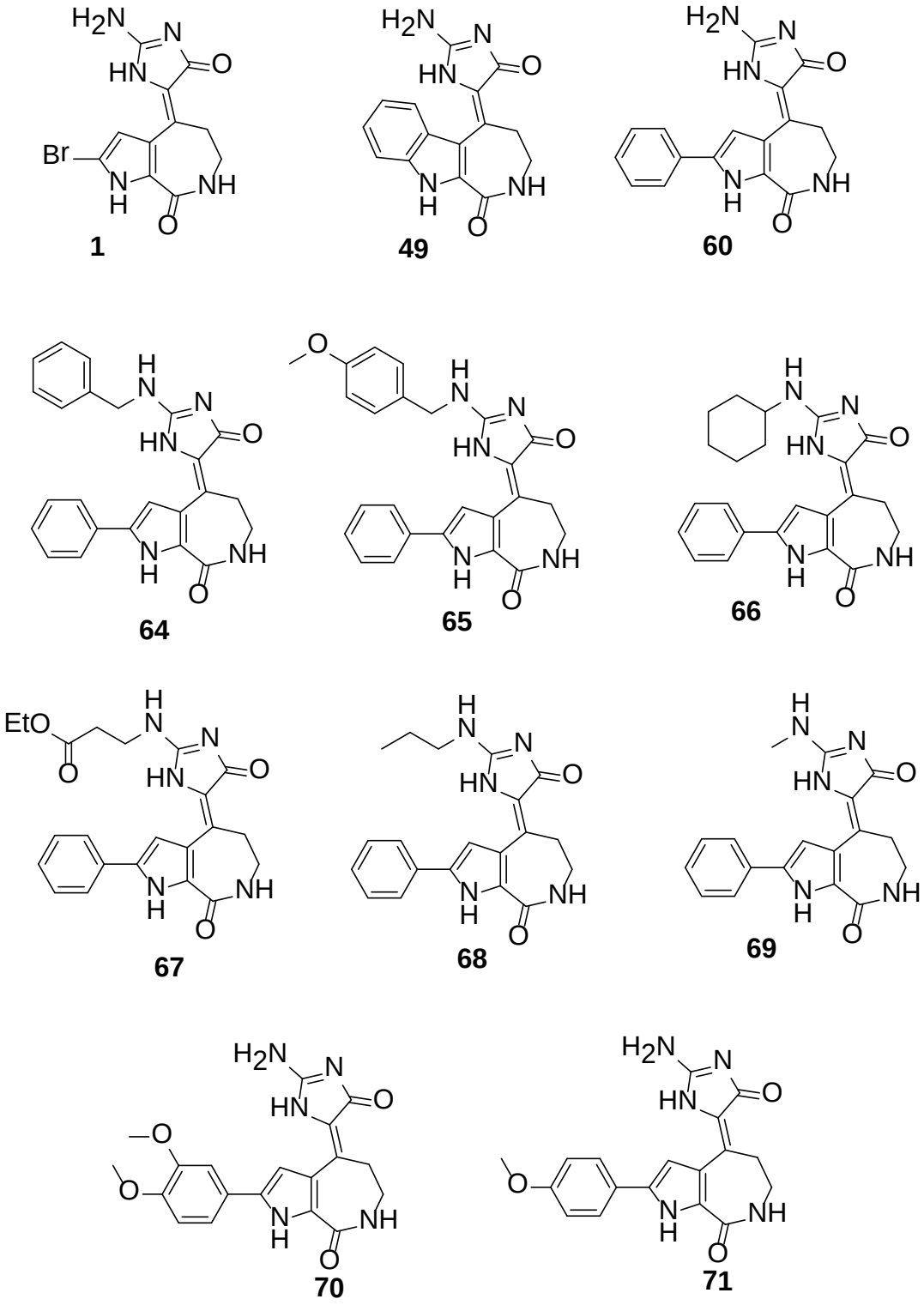

Figure 3.1. HMD and its analogs

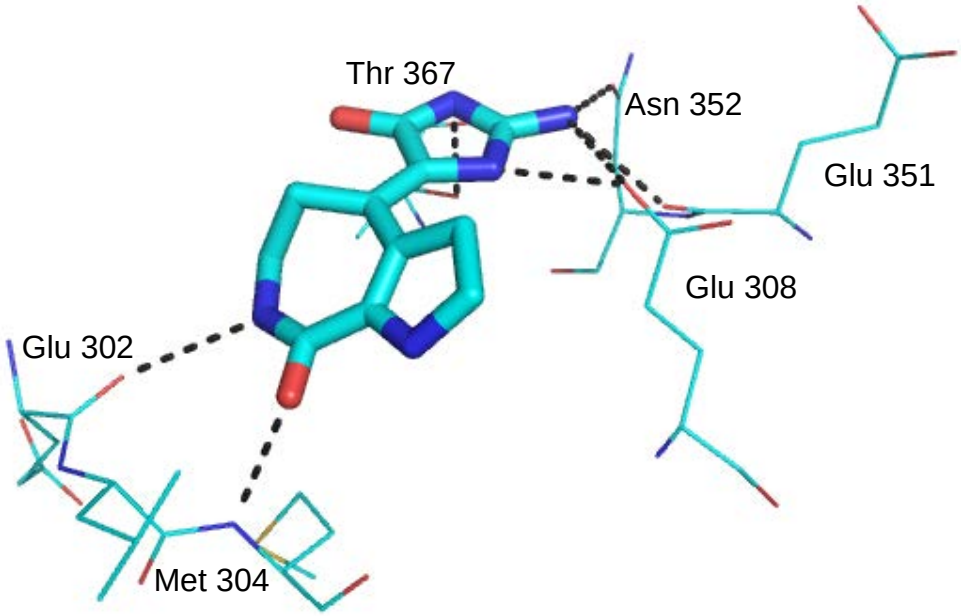

Figure 3.2: Crystal structure of DBH in ATP binding pocket of ChK2

Previously we synthesized compound **81**. In compound **81** the indolic N-atom was protected with a methyl group. This compound lacked the ability to inhibit ChK2.

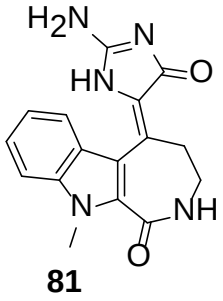

81

Figure 3.3: N-methylated indoloazepinone derivative of HMD

In order to establish the importance of this N-atom and to comprehend the loss of the activity of compound **81,** we were interested in synthesizing another class of HMD analogs. We wanted to replace the pyrrole ring in these molecules with the phenyl

ring and prepare the benzoazepinone compound **83**. In these molecules instead of protecting the N-atom, we replaced the pyrrole ring with the phenyl ring. The kinase profiling of this class of compounds will address the loss of the activity of compound **81**, and importance of the N-atom.

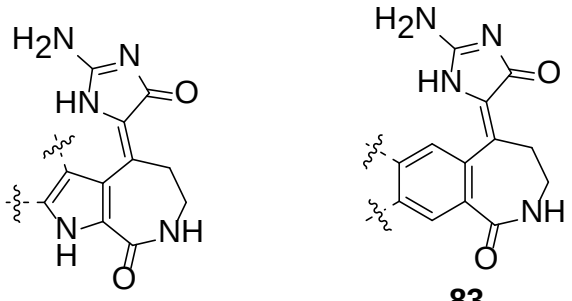

82 **83**

Figure 3.4: Proposal for the new analog

On the route to achieve the synthesis of benzoazepinone analogs, we attempted the synthesis of the following molecules with different substitutions on the phenyl ring.

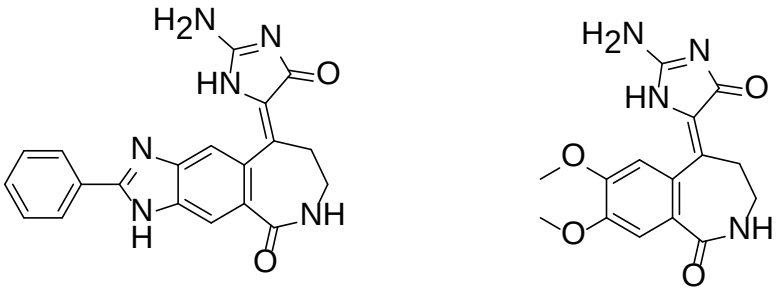

84 **85**

.

Figure 3.5: Benzoazepinone analogs of HMD

3.2. Efforts towards synthesis of new analogs of the natural products

3.2.1. Efforts towards synthesis of compound 84

In order to synthesize compound **84**, we envisioned to use the same synthetic approach that we used for the synthesis of HMD and considered to use compound **86** as the key intermediate. Compound **86** could be prepared by intramolecular Friedal-Craft reaction of compound **87,** which can be prepared from commercially available compound **88** as shown in scheme 3.1.

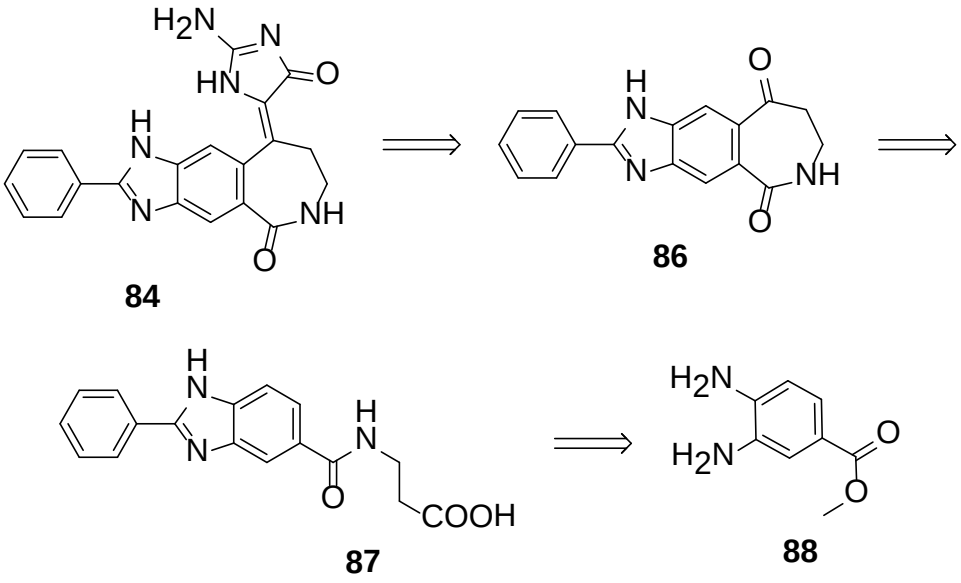

Scheme 3.1. Retrosynthetic analysis for compound 84

The synthesis started with the oxidative condensation of compound **88** with benzaldehyde giving compound **89.** Compound **89** was hydrolyzed and condensed with β-alanine ethyl ester in presence of EDCI to yield compound **91.** Basic hydrolysis of compound **91** afforded the compound **87**.

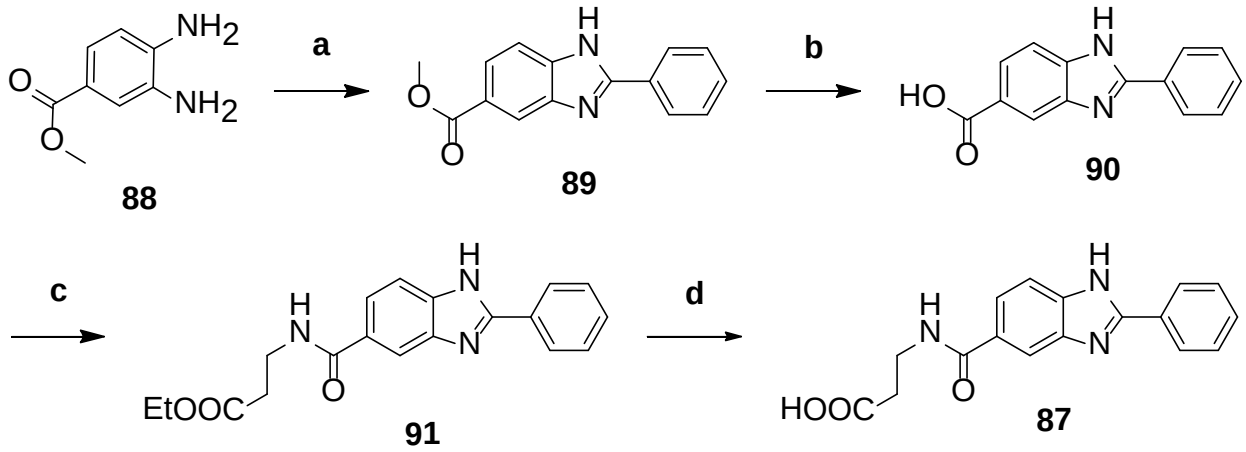

Scheme 3.2. Synthesis of compound 87

Reactions and conditions: (a) PhCHO, TsOH, PhMe, 18h, 110^{o}C, 13% (b) KOH, MeOH, H_2O, reflux, 14h, 96% (c) $H_2NCH_2CH_2CO_2Et.HCl$, EDCI, DMAP, DCM, 0^{o}C-rt, 81% (d) LiOH, EtOH, H_2O, rt, 14h, 91%

In the next step compound **87** was heated with phosphorous pentoxide under acidic conditions or treated with aluminum chloride but conversion to compound **86** was not observed.

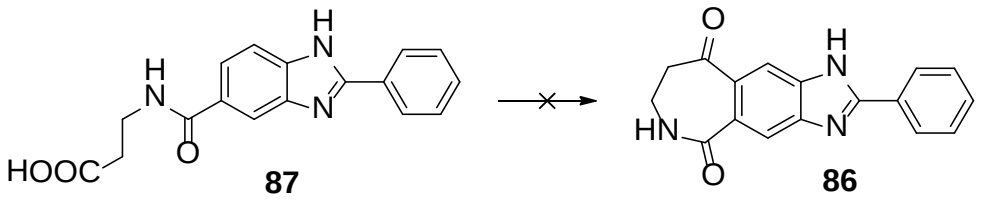

Scheme 3.3. Intramolecular Friedel-Craft reaction of compound 87

Reactions and conditions: P_2O_5, $MeSO_3H$ or P_2O_5, PPA or $AlCl_3$, DCM, reflux

The aromatic ring in focus was part of the benzimidazole ring system. The phenyl ring was thought to be lacking the electron richness sufficient enough to carry out this reaction. We were attempting to carry out the Friedel-Craft reaction ortho to an electron withdrawing group, and we were trying to make a seven-membered ring with potentially 6-atoms bearing the sp^2-character. This made us to think that Friedel-Craft reaction was not be the best strategy for these molecules and we opted to use an alternate strategy.

We envisioned that the compound **86** can be prepared by Claisen condensation of compound **92,** which can be prepared by reaction of β-alanine ethyl ester with compound **93.** The compound **93** could be prepared from commercially available compound **94.**

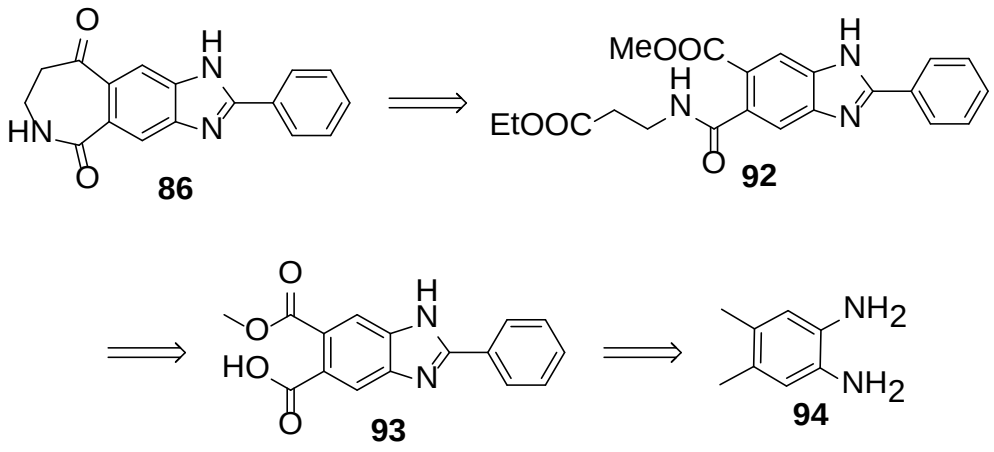

Scheme 3.4. Retrosynthetic analysis of alternate approach to compound 86

In this scheme, the synthesis of compound **93** started with the oxidative condensation of the compound **94** with benzaldehyde giving compound **95**. The compound **95** was oxidized to dicarboxylic acid **96**. The dicarboxylic acid **96** was

converted to the anhydride **97** using thionyl chloride. Then the anhydride ring of the compound **97** was opened with methanol giving half ester **93** as shown in Scheme 3.5.

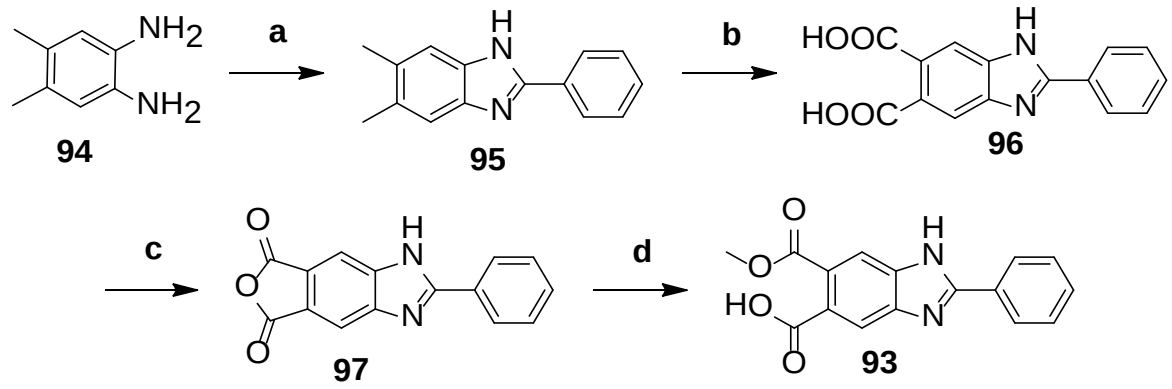

Scheme 3.5. Synthesis of compound 93

Reactions and conditions: (a) PhCHO, $Na_2S_2O_5$, xylene, 140^{o}C, 18h, 84% (b) $KMnO_4$, ^{t}BuOH, H_2O, 70^{o}C, 5h, 60% (c) $SOCl_2$, reflux, 13h, 95% (d) MeOH, reflux, 14h, 62%

In order to prepare compound **92**, the compound **93** was reacted with β-alanine ethyl ester. However, it was found that compound **92** was unstable and would undergo elimination of methanol to produce compound **98** as shown in scheme 3.6.

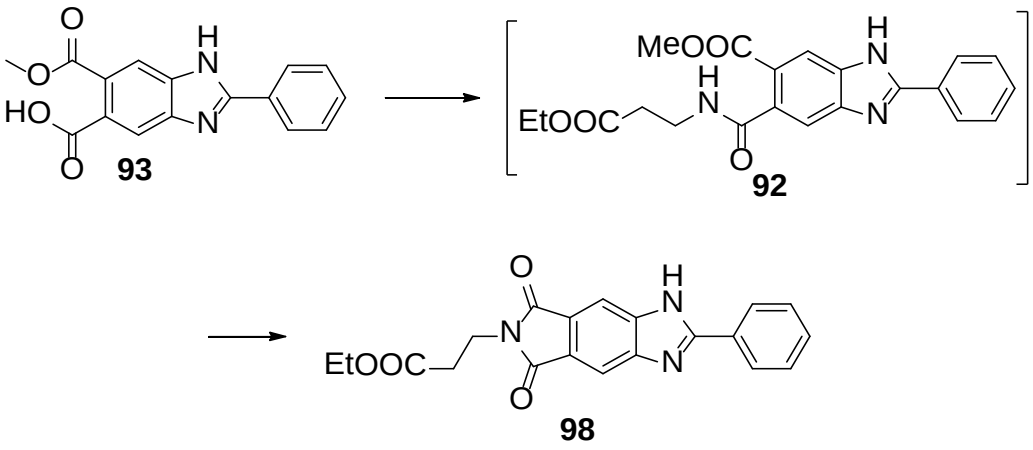

Scheme 3.6. Reaction of compound 93 with β-alanine ethyl ester

Reactions and conditions: $H_2NCH_2CH_2COOEt.HCl$, EDCI, DMAP, DCM, rt, 15h 31%

In order to circumvent this problem, the N-atom was protected with PMB-group. The β-alanine ethyl ester was reacted with p-anisaldehyde to give compound **99** scheme 3.7.

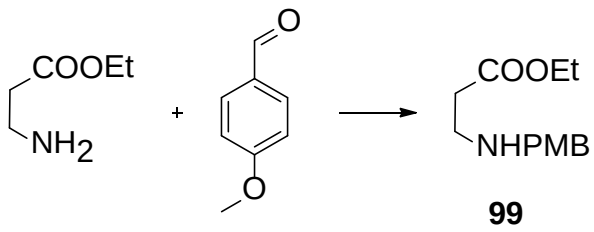

Scheme 3.7. Protection of β-alanine ethyl ester with PMB-group

Reactions and conditions: (i) Benzene, reflux, 48h, (ii) $NaBH_4$, EtOH, rt, 48h 54%.

The PMB-protection was expected to eliminate the formation of the phthalimide **98** so the compound **99** was reacted with compound **93** yielding compound **100** as shown in scheme 3.8.

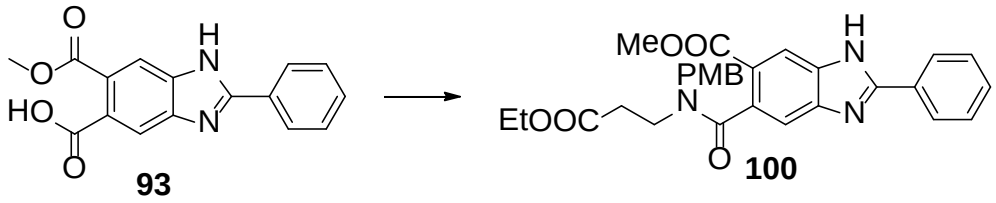

Scheme 3.8. Synthesis of compound 99

Reactions and conditions: (a) **98**, EDCI, DMAP, DCM, rt, 14h 57%

In the next step compound **100** was subjected to Clainsen condensation; however the condensation could not be achieved.

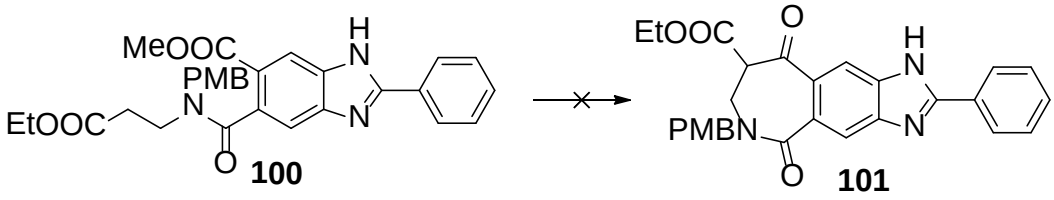

Scheme 3.9. Claisen condensation reaction with compound 100

Reactions and conditions: NaOMe, MeOH, reflux, 14 h or NaH, DMF, rt, 48h

Although we eliminated the possibility of formation of the phthalimide, we made the nitrogen atom very congested with the substituent groups. In our opinion this might have made it difficult for the enolate ion to attain the correct orientation to attack the methyl ester and yield the desired product. At this stage we considered changing the substituents on the aromatic ring, so that it can be more electron rich. We decided to continue the effort of making benzoazepinone based HMD-analogs with a more electron right the aromatic ring of dimethoxy phenyl ring.

Figure 3.6: Benzimidazole ring (left) and dimethoxy phenyl ring (right)

3.2.2. Efforts towards synthesis of compound 85

In order to synthesize compound **85** we planned to apply a different approach. The approach involved the generation of 7-membered azepinone ring by ring expansion of the 6-membered dihydronaphthalenone compound **104**.

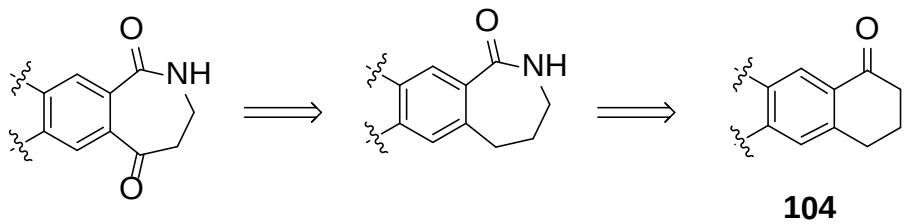

102 **103** **104**

Scheme 3.10. Strategy of benzoazepindione synthesis

It is considered that the azepindione type compounds can be prepared from azapinone **103**, which can be prepared by Schmidt reaction of the compound **104**.

In this synthesis, molecule **105** was considered to be the key intermediate and can be prepared by benzylic oxidation of the compound **106,** which in turn can be prepared by ring expansion of the compound **107** via Schmidt rearrangement. The compound **107** can be obtained from compound **108**.

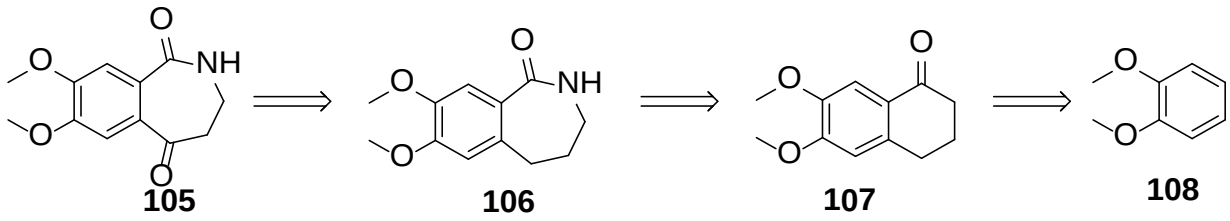

Figure 3.7: Retrosynthethic considerations for synthesis of compound 105

The synthesis started with the reaction of the compound **108** with succinic anhydride giving compound **109**. Hydride reduction of the ketone on compound **109** gave compound **110**. Compound **110** was subjected to Friedel-Craft acylation to yield compound **107**.

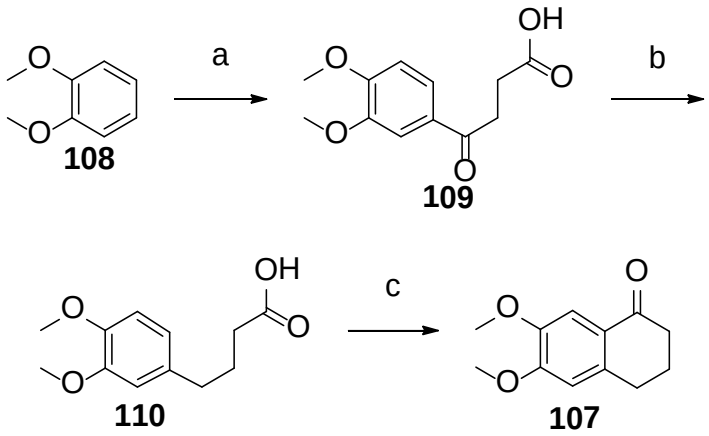

Scheme 3.11. Synthesis of compound 107

Reactions and conditions: (a) Succinic anhydride, $AlCl_3$, DCM, reflux, 4h, 90% (ii) Et_3SiH, TFA, 15min, rt, 91% (3) TFAA, TFA, 1h, rt, 93%

In the next step of the synthesis, ring expansion was carried out to generate azepinone ring utilizing Schmidt rearrangement. In this reaction compound **107** was treated with sodium azide under acidic conditions yielding compound **106** as shown in scheme 3.12.

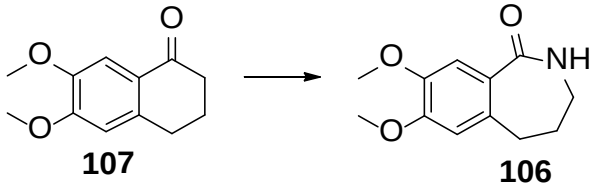

Scheme 3.12. Schmidt rearrangement

Reactions and conditions: NaN_3, $MeSO_3H$, 48h, rt, 52%

The next step was to oxidize the benzylic methylene of compound **106** to carbonyl group to obtain compound **105**. The oxidation of this benzylic site of azepinone ring again proved challenging. A number of oxidants including H_5IO_6, $FeCl_3/^tBuOOH$, $CrO_3/^tBuOOH$, H_5IO_6/CrO_3, AIBN/^{t}BuOOH, CAN, NBS/$CaCO_3$, PCC/^{t}BuOOH, IBX/Oxone and DDQ did not give any conversion or gave little conversion at all. Sodium bismuthate gave better conversion in the initial screening. The optimization of the reaction conditions led to the increase of the reaction yield to 41% of compound **105**.

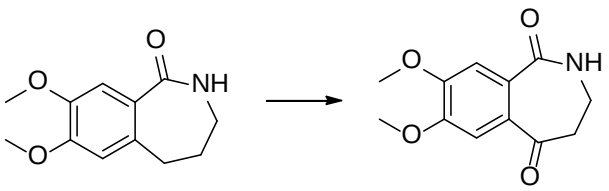

106 **105**

Scheme 3.13. Oxidation of compound 106

Reactions and conditions: $NaBiO_3$, AcOH, H_2O, 72h, reflux, 41%

Once compound **105** was prepared, it was the time to complete the synthesis of the HMD analog. In this regard, compound **105** was reacted with com **42** using titanium tetrachloride and then with ammonium hydroxide yielding the product **85**.

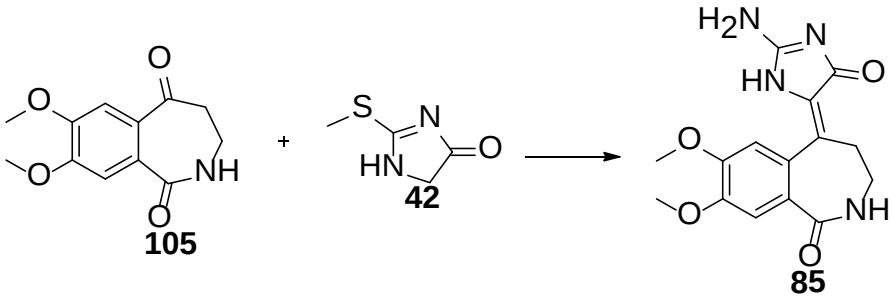

Scheme 3.14. Completion of the synthesis

Reactions and conditions: (i) $TiCl_4$, py, THF, -10^{o}C, rt or $BF_3.OEt_2$, py, THF, -10^{o}C, rt (ii) NH_4OH, THF, 110^{o}C, 14hr

The kinase profiling of this compound will be carried out in the short while.

3.3. Experimental section

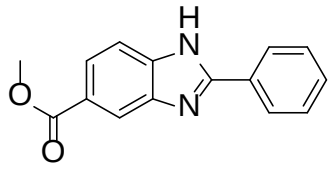

Methyl 2-phenyl-1H-benzo[d]imidazole-5-carboxylate(89):

Compound **88** (1g, 6mmol) was dissolved in toluene (30mL) in a 100 mL round bottom flask. TsOH (30mg, 0.17mmol) and benzaldehyde (0.62mL, 6.1mmol) were added to the reaction mixture. The reaction mixture was refluxed for 18 hours at 110^{o}C. Then the mixture was cooled to room temperature and washed with 10% $NaHCO_3$ solution (100mL x 3) and brine (100mL). The crude material was purified by column chromatography (silica 3:1 Dichloromethane: ethyl acetate) affording compound **89** (200mg, 13%). ^{1}H NMR (600MHz, DMSO-d_6+drop of CF_3COOH) δ 8.3 (1H, m), 8.21 (2H, dd, J=8.5, 1.5 Hz), 8.05 (1H, dd, J=8.5, 1.5 Hz), 7.89 (1H, d, J= 8.5 Hz), 7.69-7.74 (3H, m), 3.90 (3H, s); ^{13}C NMR (150MHz, DMSO-d_6+drop of CF_3COOH) δ 164.8, 152.0, 136.6, 133.5, 133.3 (s), 129.7 (s), 128.0 (s), 126.5, 126.0 (s), 124.3, 115.8 (s), 114.5 (s), 52.5 (t).

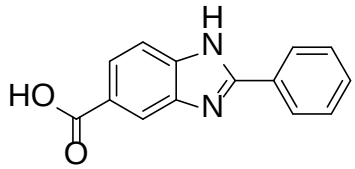

2-phenyl-1H-benzo[d]imidazole-5-carboxylic acid (90):

In a 250 mL round bottom flask, compound **89** (1.5g, 5.95mmol) was dissolved in methanol (20mL). KOH (336mg, 6mmol) was dissolved in water (5 mL) and this

aqueous solution of KOH was added to the reaction mixture. The mixture was refluxed for 14 hours. Then the temperature of the flask was allowed to cool down to room temperature and the solvent was removed. The residue thus obtained was dissolved in water (50mL) and this aqueous solution was acidified by 1N HCl to pH=1. Then the reaction mixture was cooled 10^{o}C and the suspension of the product was stirred for 15 minutes and then collected by filtration and dried in vacuo affording compound **90** (1.35g, 96%). ^{1}H NMR (500MHz, DMSO-d_6) δ 8.36 (2H, m), 8.30 (1H, s), 8.04 (1H, d, J=8 Hz), 7.86 (1H, d, J= 9 Hz), 7.69 (3h, m); ^{13}C NMR (125 MHz, DMSO-d_6) δ 166.9, 151.5, 136.8, 132.8(s), 132.9, 129.5(s), 128.0(s), 127.3, 125.9(s), 124.7, 115.8(s), 114.2 (s).

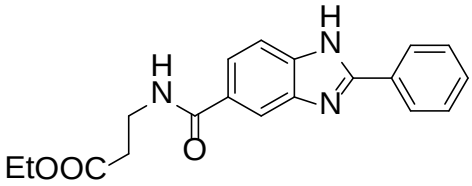

Ethyl 3-(2-phenyl-1H-benzo[d]imidazole-5-carboxamido)propanoate(91):

Compound **90** (600mg, 2.52mmol) was suspended in DCM (50mL). The reaction mixture was cooled to 0^{o}C and β-alanine ethyl ester (318mg, 2.71mmol), DMAP (540mg, 4.42mmol) and N-(3-dimethylaminopropyl)-N-ethylcarbodiimide (EDCI.HCl) (600mg, 3.13mmol) were added to the stirring solution. The reaction mixture was stirred at 0^{o}C for 4h and then allowed to reaction to warm up to room temperature over 20h. Then the contents of the reaction mixture were transferred to separatory funnel and washed with sat. $NaHCO_3$ soln. (100mL), water (100mL), sat. NH_4Cl

soln. (100mL) and brine (100mL). Then the organic layer was collected and dried over Mg_2SO_4 (1g). Then the solvent was removed and the residue was dried in *vacuo* yielding compound **91** (659mg, 81%). ^{1}H NMR (600MHz, DMSO-d_6+drop of CF_3COOH) δ 8.22 (3H, m), 8.02 (1H, dd, J=8.5, 1.5bHz), 7.90 (1H, d, J= 8.5 Hz), 7.73-7.77 (3H, m), 4.07 (2H, q, J=7.1 Hz), 3.54 (2H, q, J=7.0 Hz), 2.61 (2H, t, J=7.0 Hz), 1.17 (3H, t, J=7.1 Hz); ^{13}C NMR (150MHz, DMSO-d_6+drop of CF_3COOH) δ 171.3, 165.5, 151.0, 14.1 (t), 133.6, 132.2, 132.1 (s), 129.8 (s), 128.3 (s), 125.1 (s), 123.4, 114.0 (s), 113.4 (s), 60.0 (d), 35.8 (d), 33.8 (d).

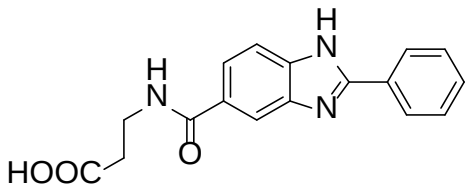

3-(2-phenyl-1H-benzo[d]imidazole-5-carboxamido)propanoic acid (87):

In a 250 mL round bottom flask, compound **91** (659g, 1.95mmol) was dissolved in methanol (30mL). KOH (150mg) was dissolved in water (5mL) and this aqueous solution of KOH was added to the reaction mixture. The mixture was refluxed for 14 hours. Then the reaction mixture was allowed to cool down to room temperature and the solvent was removed. The residue thus obtained was dissolved in water (50mL) and this aqueous solution was acidified by 1N HCl to pH=1. Then the reaction mixture was cooled 10^{o}C and the suspension of the product was stirred for 15 minutes. The desired product was collected by filtration and dried in vacuo affording compound **87** (550 mg, 91%). ^{1}H NMR (500MHz, DMSO-d_6) δ 8.79 (1H, t), 8.32 (2H, m), 8.24 (1H, s), 7.96 (1H, d, J=8 Hz), 7.82 (1H, d, J=8 Hz), 7.71 (3H, m), 3.50

(2H, q), 2.55 (2H, t); ^{13}C NMR (125 MHz, DMSO- d_6) δ 173.6, 166.1, 151.06, 134.7, 134.1, 132.8, 132.6(s), 130.3(s), 129.0(s), 125.6(s), 124.0, 114.4(s), 114.0(s), 36.5(d), 34.5(d).

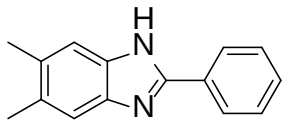

5,6-dimethyl-2-phenyl-1H-benzo[d]imidazole (95):

Compound **94** (1, 7.35mmol) was dissolved in xylene (10mL) in 100 mL round bottom flask. Benzaldehyde (0.75mL, 7.35mmol) and sodium hydrogensulfite (1.4g, 7.6mmol) were added to the reaction mixture. The reaction mixture was refluxed at 140^{O}C for 18 hours. Then the reaction mixture was allowed to cool down to room temperature and the solvent was removed. The residue thus obtained was subjected to purification by column chromatography (hexane:ethyl acetate 1:1) to affor **95** (1.37g, 84%). ^{1}H NMR (500MHz, DMSO- d_6) δ 8.14(2H,d, J=2 Hz), 7.47(2H,m), 7.42 (3H,m), 2.31(6H,d, J=10 Hz); ^{13}C NMR (125 MHz, DMSO- d_6) δ 150.3, 130.4, 129.4(s), 128.8(s), 126.1(s), 20.0(t).

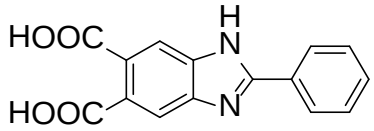

2-phenyl-1H-benzo[d]imidazole-5,6-dicarboxylic acid (96):

The compound **95** (220mg, 1mmol) was dissolved in a mixture of H_2O/^{t}BuOH (1:1, 30mL) in a 100 mL round bottom flask. The reaction mixture was warmed up to

70^{O}C. At this temperature a solution of potassium permanganate (1.58g, 10mmol) in water (30mL) was added to the reaction mixture in drop-wise manner over a period of 5 hours. The reaction mixture was heated at 70^{O}C for one more hour. Then the reaction mixture was allowed to cool down to room temperature and the solvent was removed. Then anhydrous sodium sulfite (630mg, 5mmol) was added to the reaction mixture to decompose excess of potassium permanganate present in the reaction mixture. The reaction mixture was stirred for more 30 minutes to complete the decomposition. Then, in order to remove insoluble by-products, the reaction mixture was filtered and the residue was washed the residue with hot water (50mL). The filterate and aqueous washing were combined and cooled to 0^{O}C. The filterate was acidified with HCl to pH 2 resulting in the precipitation of the desired product. The precipitate was filtered and dried *in vacuo* affording **96** (130mg, 59%). ^{1}H NMR (500MHz, DMSO- d_6) δ 8.23(2H,d, J=7.5 Hz), 7.85(2H, s), 7.55 (3H, m); ^{13}C NMR (125 MHz, DMSO- d_6) δ 169.0, 154.5, 130.7(s), 129.3, 129.1(s), 128.8, 127.5, 126.9(s).

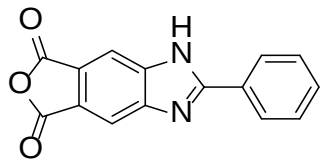

2-phenyl-1H-isobenzofuro[5,6-d]imidazole-5,7-dione (97):

Compound **96** (670mg, 2.53mmol) was placed in a 100mL round bottom flask and thionyl chloride (15mL) was added to the flask at room temperature. The reaction mixture was then refluxed for 13 hours. At this point, the reaction mixture was cooled

down and the excess of thionyl chloride was removed using rotary evaporator. In order to ensure complete removal of thionyl chloride, benzene (10mL) was added to the reaction mixture, the mixture was stirred for 5 minutes. Then the solvent was removed and the residue was dried *in vacuo* affording **97** (600mg, 95%). ^{1}H NMR (500MHz, DMSO- d_6) δ 8.34(2H, m), 8.24(2H,s), 7.61 (3H,m); ^{13}C NMR (125 MHz, DMSO- d_6) δ 163.6, 156.7, 131.6(s), 129.2(s), 128.2, 127.4(s), 124.6, 112.8.

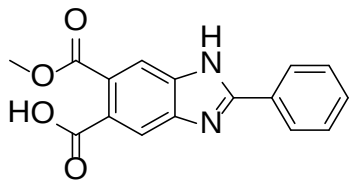

6-(methoxycarbonyl)-2-phenyl-1H-benzo[d]imidazole-5-carboxylic acid (93):

Added compound **97** (500mg, 1.89mmol) dissolved in methanol (15ml) in a 250 mL round bottom flask. The reaction mixture was refluxed for 14 hours. Then allowed the temperature of the reaction mixture to drop down to room temperature. Then the solvent was removed and the residue was dried *in vacuo* affording **93** (350mg, 62%). ^{1}H NMR (500MHz, DMSO- d_6) δ 8.34(2H, m), 8.05(1H,s), 7.92 (1H, s), 7.65 (3H,m), 3.82 (3H, s); ^{13}C NMR (125 MHz, DMSO- d_6) δ 168., 167.8, 153.4, 133.3, 132.2, 129.5, 129.4, 129.1, 128.7, 128.5, 127.8, 127.6, 115.7, 115, 52.53(t).

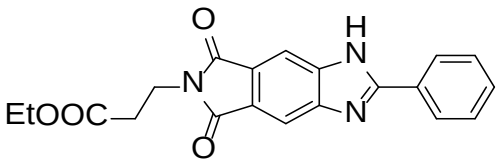

Ethyl 3-(5,7-dioxo-2-phenylimidazo[4,5-f]isoindol-6(1H,5H,7H)-yl)propanoate (98): Compound **93** (340mg, 1.15mmol) was dissolved in dichloromethane (15mL). Cooled the reaction mixture to 0^{o}C and added β-alanine ethyl ester (178mg, 1.16mmol), EDCI (240mg, 1.25mmol) and DMAP (150mg, 1.23mmol) to the stirring reaction mixture. Stirred the mixture for 15 hours, allowing the reaction temperature to gradually rise to room temperature. Then the contents of the reaction mixture were transfer to separatory funnel and washed with sat. $NaHCO_3$ soln. (100mL), water (100mL), sat. NH_4Cl soln. (100mL) and brine (100mL). Then the organic layer was collected and dried over Mg_2SO_4 (1g). Purified the product by column chromatography (silica, EtOAc) to give **98** (130mg, 31%). ^{1}H NMR (500MHz, DMSO-d_6) δ 8.19(2H, m), 7.97(2H,br), 7.55 (3H,m), 4.02 (2H,q, J=7 Hz), 3.80(2H,t, J=7 Hz), 2.65 (2H,t, J=7 Hz), 1.10(3H,t, J=7 Hz); ^{13}C NMR (125 MHz, DMSO- d_6) δ 170.61, 167.72, 155.20, 130.96, 129.18, 128.99, 126.85, 125.74, 60.17, 33.61, 32.63, 13.94.

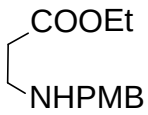

Ethyl 3-(4-methoxybenzylamino)propanoate (99):

Dissolved p-methoxybenzaldehyde (4.4mL, 32.68mmol) in benzene (25mL) in a 100 mL round bottom flask. Added β-alanine ethyl ester (5g, 31.7mmol) to the reaction mixture and refluxed for 48 hours. Then the reaction mixture was cooled to room temperature and sodium borohydride (1.2g, 31mmol) was added to the reaction mixture. Methanol (5mL) was added to the reaction mixture in dropwise mannder and the reaction mixture was stirred for 48 hours at room temperature. Then the solvent was removed and crude product was purified by column chromatography (silica, EtOAc) to give **99** (4.2g, 54%). ^{1}H NMR (500MHz, $CDCl_3$) δ 7.20(2H,d, J=8Hz), 6.82 (2H,d, J=8Hz), 4.11 (2H,q, 7Hz), 3.76 (3H,s), 3.70 (2H,s), 2.85 (2H,t, J=7Hz), 2.48 (2H,t, J=7Hz), 1.23(3H,t, J=7Hz); ^{13}C NMR (125 MHz, $CDCl_3$) δ 172.6, 158.6, 132.3, 129.2(s), 113.8(s), 60.4(d), 55.2(t), 53.1(d),44.4(d), 34.7(d), 14.2(t).

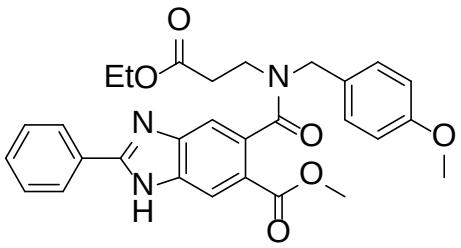

Methyl 5-((3-ethoxy-3-oxopropyl)(4-methoxybenzyl)carbamoyl)-2-phenyl-1H-benzo[d]imidazole-6-carboxylate (100):

Compound **93** (100mg, 0.34mmol) was dissolved in dichloromethane (15mL). Cooled the reaction mixture to 0^{o}C and added **99** (80.58mg, 0.34mmol), EDCI (96mg, 0.5mmol) and DMAP (61mg, 0.5mmol) to the stirring reaction mixture. Stirred the mixture for 14 hours, allowing the reaction temperature to gradually rise to room temperature. Then the contents of the reaction mixture were transfer to separatory funnel and washed with sat. $NaHCO_3$ soln. (100mL), water (100mL), sat. NH_4Cl soln. (100 mL) and brine (100mL). Then the organic layer was collected and dried over Mg_2SO_4 (1g). Purified the product by column chromatography (silica, Hexanes: ethyl acetate 1:1) to give **100** (100mg, 57%). ^{1}H NMR and ^{13}C NMR (125 MHz, DMSO- d_6) showing a mixture of rotamers. MS (ES) m/z: M^{+} 515

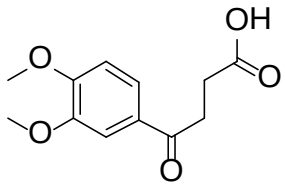

4-(3,4-dimethoxyphenyl)-4-oxobutanoic acid (109):

Suspended aluminum chloride (800mgs, 6mmol) in dichloromethane in 100mL round bottom flask. Added veratrole **108** (0.64mL, 5mmol) and succinic anhydride (600mgs, 6mmol) to the reaction mixture. Then refluxed the reaction mixture for 4 hours. Then allowed the reaction mixture to cool to room temperature and transferred the contents of the reaction flask to separatory flask. Washed the organic layer using 10% HCl soln. (150mL) and brine soln. (150mL). Then collected the organic fraction of the separatory flask and dried it over Mg_2SO_4 (1g), removed the solvent **109** (1g, 90%). ^{1}H NMR (500MHz, $CDCl_3$) δ 7.59 (1H, dd, J=2, 6 Hz), 7.50 (1H, d, J=2 Hz), 6.86 (1H, d, J=6 hz), 3.92 (3H, s), 3.90 (3H, s), 3.26 (2H, t, J=7 Hz), 2.77 (2H, t, J=7 Hz); ^{13}C NMR (125 MHz, $CDCl_3$) δ 196.43, 178.80, 153.45, 149.01, 129.57, 122.70 (s), 110.06(s), 110.01(s), 56.03(t), 55.93(t), 32.63(d), 28.17(d).

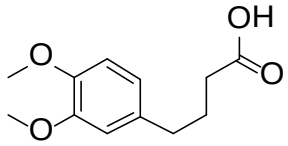

4-(3,4-dimethoxyphenyl)butanoic acid (110):

Dissolved **109** (395 mgs, 1.66mmol) in trifluoroacetic acid (7ml) in 50 mL round bottom flask. Vigorously stirred the reaction mixture and in drop-wise manner added triethyl silane (0.8ml, 5mmol) to the reaction mixture. Stirred the reaction mixture for

15 minutes, and then concentrated *in vacuo* to obtain dark brown oil. The oil was dissolved in 10% aqueous KOH (50mL). The aqueous solution was transferred to separatory flask, then it was acidified with HCl and the product was extracted using DCM (50 mL x 3). The DCM fractions were combined, dried over magnesium sulfate and the solvent was removed to yield **110** (334mgs, 91%). ^{1}H NMR (300MHz, $CDCl_3$) δ 6.81 (3H, m), 3.89 (3H, s), 3.88(3H, s), 2.65(2H, t, J=8 Hz), 2.39(2H, t, J=8 Hz), 1.98(2H, m), ^{13}C NMR (75MHz, $CDCl_3$) δ179.94, 148.69, 147.17, 133.74, 120.31(s), 111.66(s), 111.19(s), 55.81(t), 55.71(t), 34.47(d), 33.18(d), 26.28(d).

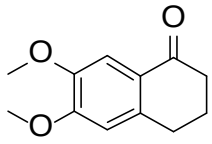

6,7-dimethoxy-3,4-dihydronaphthalen-1(2H)-one (107):

Dissolved **110** (7g, 31.2mmol) in trifluoroacetic acid (40mL) at room temperature in 100 mL round bottom flask. Added trifluoroacetic anhydride (50mL) to the reaction mixture and stirred for 30 minutes at room temperature. Then the reaction mixture was concentrated *in vacuo* and the residue thus obtained was dissolved in 10% aqueous KOH (100mL). The aqueous solution was transferred to separatory flask, then it was acidified with HCl and the product was extracted using DCM (50 mL x 3). The DCM fractions were combined, dried over magnesium sulfate and the solvent was removed and residue was dried *in vacuo* affording **107** (6g, 93%). ^{1}H NMR (500MHz, $CDCl_3$) δ 7.41 (1H, s), 6.58 (1H, s), 3.83 (3H, s), 3.81 (3H, s), 2.79(2H, t, J=7 Hz), 2.48(2H, t, J=7 Hz), 2.01 (2H, m); ^{13}C NMR (125 MHz, $CDCl_3$) δ 196.92,

153.25, 147.67, 125.58, 110.00(s), 108.22(s), 55.79(t), 55.73(t), 38.30(d), 29.21(d), 23.41(d).

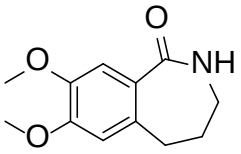

7,8-dimethoxy-2,3,4,5-tetrahydro-1H-benzo[c]azepin-1-one (106):

Dissolved **107** (3.7g, 17.94mmol) in methanesulfonic acid (30mL) in 100 mL round bottom flask. The reaction mixture was cooled to 0^{o}C in ice-bath and sodium azide (1.6g, 24mmol) was slowly added to the reaction mixture over 15 minutes. Stirred the contents of the reaction flask for two days and allowed the temperature to rise back to room temperature. Then cooled the reaction mixture in ice-bath and neutralized the acid with 10% $NaHCO_3$ solution. The reaction mixture was transferred to the separatory flask and extracted the organic compounds from this aqueous solution using DCM (100mL x 3). Combined the DCM fractions and dried these over Mg_2SO_4 (1g). Removed the solvent and purified the product by column chromatography (silica, ethyl acetate) affording **106** (2.7g, 68%) ^{1}H NMR (500MHz, $CDCl_3$) δ 7.21(1H, s), 6.63(1H, s), 3.88(3H, s), 3.86 (3H, s), 3.10 (2H, q, J=6 Hz), 2.76 (2H, t, J=6 Hz), 1.97(2H, m); ^{13}C NMR (125 MHz, $CDCl_3$) δ 174.20 , 150.92, 147.62, 132.07, 126.79, 111.61(s), 111.47(s), 55.96(t), 55.87(t), 39.73(d), 30.73(d), 30.12(d).

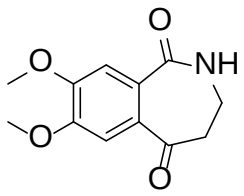

7,8-dimethoxy-3,4-dihydro-1H-benzo[c]azepine-1,5(2H)-dione (105):

Dissolved **106** (1g, 4.52mmol) in acetic acid (20mL) and water (20mL). Added sodium bismuthate (15g, 72mmol) to the reaction mixture in three equal portions at intervals of 24 hours and refluxed the reaction mixture for a total of 72 hours. Then allowed the reaction mixture to cool down to room temperature and filtered to remove the insoluble residue. The residue was discarded and the acetic acid was removed from the filterate giving black organic mixture, which was dissolved in ethyl acetate (200mL). The ethyl acetate solution was transferred to a separatory flask and washed with 10% $NaHCO_3$ (100mL) and brine (100mL). The organic layer was, then, dried over Mg_2SO_4 and solvent was removed. In the last step purified the crude product by column chromatography (silica, ethyl acetate) affording **105** (436mgs, 41%). ^{1}H NMR (500MHz, $CDCl_3$) δ 7.41(s, 1H), 7.26(1H, s), 3.95 (3H, s), 3.92 (3H, s), 3.48 (2H, q, J=5Hz), 2.93 (2H, t, J=5Hz) ^{13}C NMR (125 MHz, $CDCl_3$) δ 200.30, 170.52, 152.71, 151.51, 129.23, 126.32, 112.68(s), 110.87(s), 56.34(t), 56.21(t), 45.90(d), 37.01(d); IR (film) 3314(br) 1719, 1653 cm^{-1}; MS (ES+) m/z: 235.1 (M)+; m.p. 188^{o}C; HRMS (ES+) calcd for $C_{12}H_{14}NO_4$ $[M+H]^+$ 236.0923, found 236.0929.

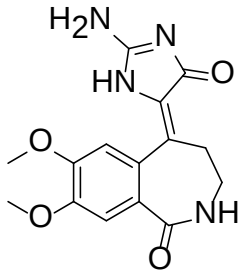

7,8-dimethoxy-3,4-dihydro-1H-benzo[c]azepine-1,5(2H)-dione (85):

Dissolved **105** (150mg, 0.638mmol) was dissolved in THF (50 mL) and compound **42** (166mg, 1.275mmol) was added to the reaction flask. The reaction mixture was cooled to 0°C and 1M solution of $TiCl_4$ in DCM (2.55mL, 2.55mmol) was added to the reaction mixture in drop-wise manner. The reaction mixture was stirred for 30 minutes and then pyridine (0.4mL, 5.1mmol) was added to the reaction mixture in drop-wise manner over 15 minutes. Then the reaction mixture was stirred for an additional 14 hours allowing it to gradually warm to room temperature. At this point saturated NH_4Cl solution (40mL) was added to the reaction mixture and contents of the flask were transferred to the separatory funnel, the organic layer was obtained and the solvent was removed, the residue was passed through a short silica plug using EtOAc. The solvent was removed and the residue was then transferred to the sealed tube. THF (2mL) and ammonium hydroxide (5mL) were added to the sealed tube. The resulting mixture was heated at 90°C for 18 hours and then allowed to cool down to room temperature. Then the reaction mixture was concentrated and crude material was purified by column chromatography (silica, MeOH/DCM 1:4) affording 70 (35mg, 17%). ^{1}H NMR (500MHz, $CDCl_3$) δ 7.25 (1 H, s), 6.93 (1 H, s), 3.83 (3 H, s), 3.81 (3 H, s), 3.14 (4 H, br); ^{13}C NMR (125 MHz, DMSO-d_6+ a drop of

CF_3COOH) δ 170.43, 163.3, 154.9, 151.4, 150.2, 133.9, 128.2, 126.4, 125.5, 112.8 (s), 112.21 (s), 56.2 (t), 56.1 (t), 38.1 (d), 35.4 (d); IR (KBr): 3409, 3298, 1722, 1707, 1682, 1644, 1205, 1181 cm^{-1}; MS (ES) m/z: 317.1 $[M+H]^+$; m.p. decomposes over 250°C; HRMS (ES+): m/z calcd for $C_{15}H_{17}N_4O_4$ $[M+H]^+$ 317.1250, found 317.1252.

References

3.4. References

1. Peltason, L.; Bajorath, J., SAR index: Quantifying the nature of structure - activity relationships. *J. Med. Chem.* **2007,** *50*, 5571-8.

2. (a) Chacun-Lefèvre, L.; Joseph, B.; Mérour, J.-Y., Synthesis and reactivity of azepino[3,4-b]indol-5-yl trifluoromethanesulfonate. *Tetrahedron* **2000,** *56*, 4491-9; (b) Mangu, N.; Spannenberg, A.; Beller, M.; Tse, M.-K., Synthesis of novel annulated hymenialdisine analogues via palladium-catalyzed cross-coupling reactions with aryl boronic acids. *Synlett* **2009,** *2010*, 211-4; (c) Qin, Y.; He, Q. F.; Chen, W., Synthesis of 2-substituted endo-hymenialdisine derivatives. *Tetrahedron Lett.* **2007,** *48*, 1899-901.

3. Wan, Y.; Hur, W.; Cho, C. Y.; Liu, Y.; Adrian, F. J.; Lozach, O.; Bach, S.; Mayer, T.; Fabbro, D.; Meijer, L.; Gray, N. S., Synthesis and target identification of hymenialdisine analogs. *Chem. Biol.* **2004,** *11*, 247-59.

4. Parmentier, J.-G.; Portevin, B.; Golsteyn, R. M.; Pierré, A.; Hickman, J.; Gloanec, P.; De Nanteuil, G., Synthesis and CHK1 inhibitory potency of hymenialdisine analogues. *Bioorg. Med. Chem. Lett.* **2009,** *19*, 841-4.

5. Sharma, V.; Tepe, J. J., Potent inhibition of checkpoint kinase activity by a hymenialdisine-derived indoloazepine. *Bioorg. Med. Chem. Lett.* **2004,** *14*, 4319-21.

CHAPTER 4

SYNTHESIS OF 1,2,4-TRIAZOLINES AND TRIAZOLES UTILIZING OXAZOLONES

4.1. Introduction

The diversity oriented synthesis of small molecule libraries has plays an important role in the development of new pharmaceutical agents.[1] The strategies that allow the production of library of molecules with considerable structural variation hold importance in the field of drug discovery as screening of these libraries leads not only to identification of new drug candidates, but also to new therapeutic protein targets, which could be regulated by small molecules.

The oxazolone template has been a scaffold of interest for many research groups for the synthesis of β-lactams,[2] pyrroles,[3] pyrrolines[4] and imidazoles.[5] Our group has also exploited the oxazolone template as a pivotal scaffold to access a wide range of heterocyclic compounds and natural products, including imidazolines, imidazolones, dihydropyrrolines, alkoxypyrrolidinones, dihydro- imidazolones and oxazoles.[6]

Oxazolones are unique in that these templates contain multiple reactive sites capable of yielding a wide range of diverse products by minor manipulations of the reaction conditions or reaction substrates.[7] Based on these previous observations, we anticipated that oxazolones could be ideal substrates to access libraries of triazoline and triazole compounds.

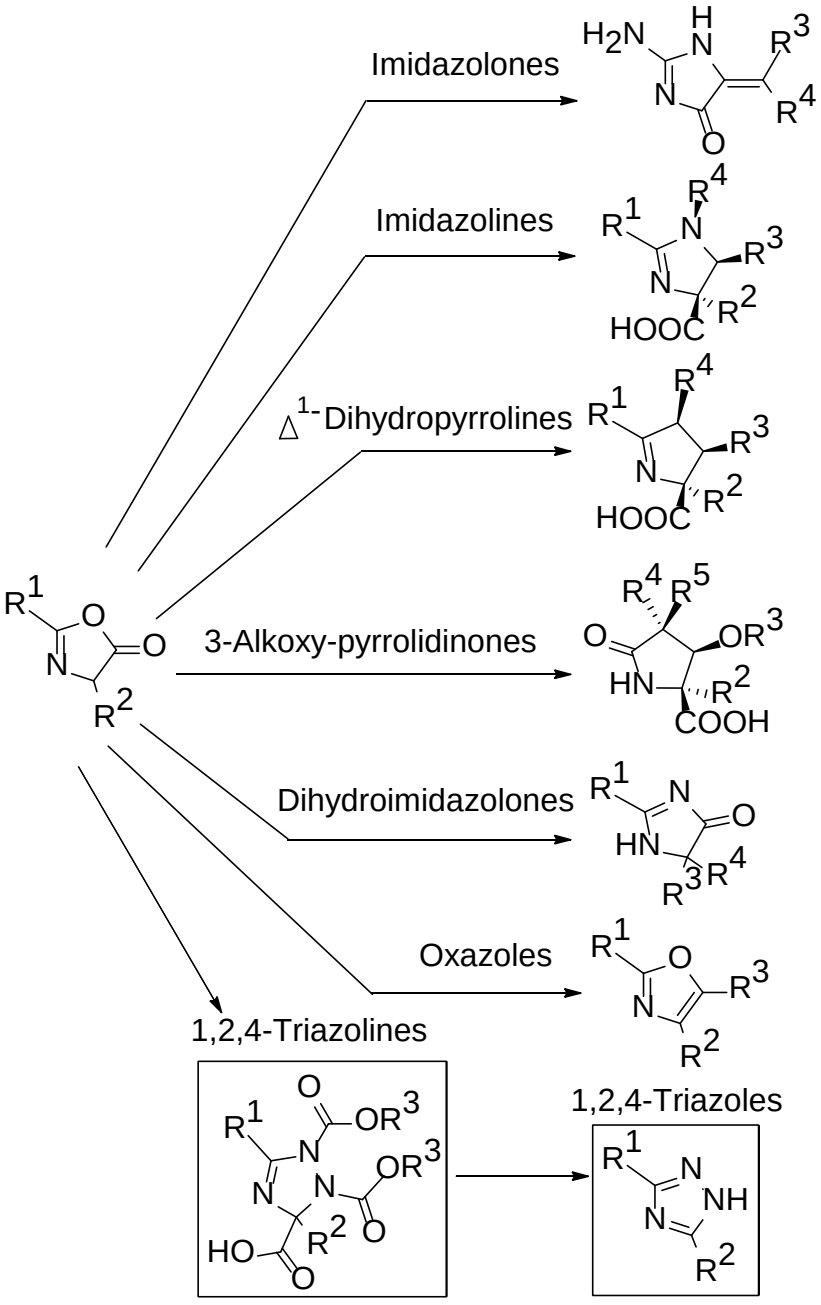

Scheme 4.1. Oxazolone as template for synthesis of heterocycles

The 1,2,4-triazoline core belongs to an underutilized class of heterocycles whose biological properties remain largely unexplored. There are only a handful of the examples of syntheses of 1,2,4-triazolines with quaternary C-3 carbon containing alkoxy

carbonyl or carboxyl moieties. Kolasa and Miller[8] have reported three examples of the triazoline synthesis from α-amino acids utilizing the Mitsunobu reaction conditions. Ibata and Hassner[9] have utilized oxazoles and thiazoles for the synthesis of this triazoline motif. Anderson and Watt[10] have showed the generation of triazoline adduct along with Michael-type addition product upon the reaction of imidazopyridine with azodicarboxylates. Similarly, Tsuge and coworkers[11] have utilized the azodicarboxylate compounds with N-[(trimethylsilyl) methyl] iminium triflates to synthesize the imidazolines and the triazolines. However, the cycloaddition of oxazolone with azodicarboxylate compounds was unprecedented. We envisioned that oxazolone could be used for the synthesis of triazoline compound through cycloaddition reaction with azodicarboxylate compounds.

4.2. Cycloaddition of oxazolone with azodicarboxylate compounds

4.2.1. Scope of the catalyst

As in our previously reported cycloaddition reactions of oxazolones, a Lewis acid was required for the cycloaddition reaction to take place. Therefore, to check the possibility of the reaction to take place, we reacted 4-methyl-2-phenyloxazol-5(4H)-one (**111**) with diethyl azodicarboxylate (DEAD) in dichloromethane at room temperature using a range of catalysts. The reaction was analyzed at the after 4 hours and 9 hours of stirring the reaction mixture. To our delight, the reaction yielded the product at room temperature and did not require a catalyst. The catalyst caused to the lowering of the reaction yield in the given reaction time.

Table 4.1. Catalyst scope

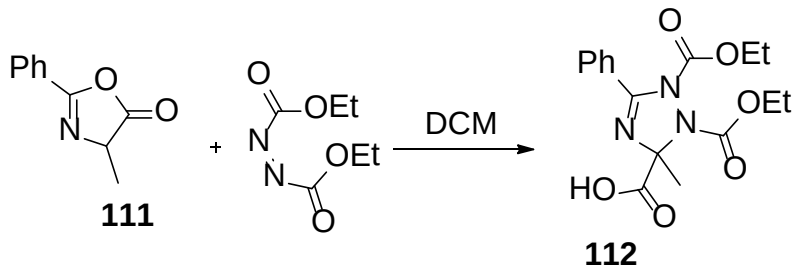

	Catalyst	Reaction Time (hr)	Yield (%)		Reaction Time (hr)	Yield(%)
1	No catalyst	4hr	58		9hr	75
2	TMS-Cl	4hr	70		9hr	75
3	AgOAc	4hr	16		9hr	20
4	$AlCl_3$	4hr	21		9hr	33
5	$Cu(OAc)_2$	4hr	8			
6	Mg_2SO_4	4hr	10			

4.2.2. Solvent scope

Next the scope of the solvent was evaluated. The reaction was carried out in a range of solvents including acetonitrile, benzene, diethyl ether and tetrahydrofuran for a period of 9 hours at room temperature and the reaction was evaluated for the yield (Table 4.2). Among the solvent evaluated in this scope, diethyl ether gave the lowest yield of the product in the given reaction time. Acetonitrile was found to be the superior solvent for this reaction.

Table 4.2. Solvent scope

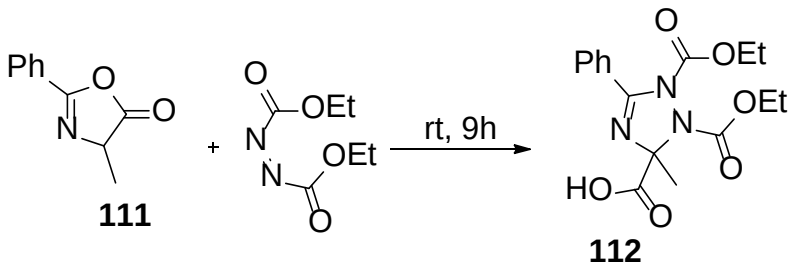

	Solvent	Yield (%)
1	MeCN	94
2	DCM	75
3	C_6H_6	22
4	THF	26
5	Et_2O	15

The reaction was then examined in acetonitrile for the conversion of the reactant into product over time. The reaction was carried out for 5, 6, 7,8, 9, 10, 11, 12, 18, 24 and 30 hours and then evaluated for the conversion. The examination revealed that the compound **111** was quantitatively converted into compound **113** in 11 hours (Table 4.3).

Table 4.3. Optimization of reaction time

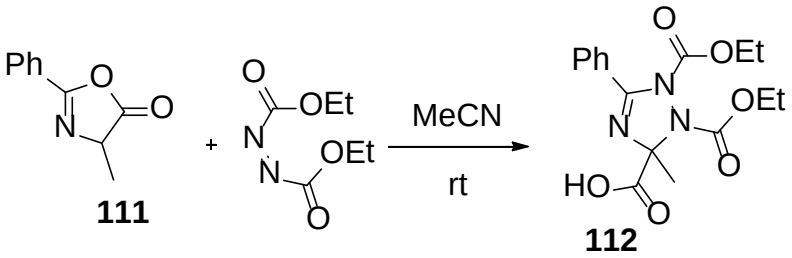

	Reaction time (h)	Yield (%)
1	5	55%
2	6	67
3	7	82
4	8	89
5	9	93
6	10	99
7	11	100
8	12	100
9	18	100
10	24	94
11	30	97

4.2.3. Reaction scope

The scope of the reaction was evaluated for commercially available azodicarboxylate compounds and the range of the substituents on the oxazolone.

Table 4.4. Scope of the reaction

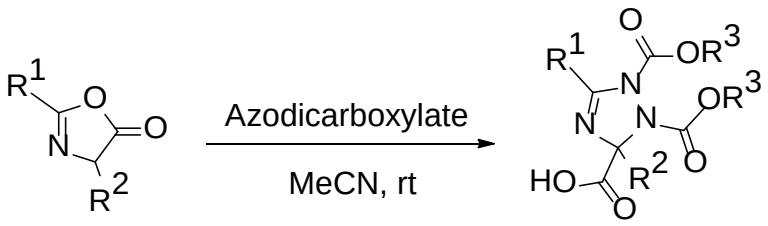

	Substrate	R^1	R^2	Azo-dicarboxylate	Product	Reaction time (h)	Yield (%)
1	**111**	Ph	Me	DEAD	**112**	11	100
2	**111**	Ph	Me	DIAD	**113**	11	99
3	**111**	Ph	Me	PTAD	**114**	4	85*
4	**115**	p-NO_2-C_6H_4	Me	DEAD	**116**	22	50**
5	**117**	p-F-C_6H_4	Me	DEAD	**118**	11	98
6	**119**	p-MeO-C_6H_4	Me	DEAD	**120**	11	85
7	**121**	Ph	Bn	DEAD	**122**	11	82
8	**123**	Ph	iPr	DEAD	**124**	22	95**
9	**125**	Ph	Indolyl-3-methyl	DEAD	**126**	22	94**

* Isolated as TMS-methyl ester (**127**).

** Yields of 89%, 84% and 82% were obtained for entries 4, 8 and 9 respectively, when the reaction was carried out at room temperature for 9 hours in dichloromethane using 2 equivalents of DEAD.

Although the diisopropyl azodicarboxylate (DIAD) is sterically more demanding than DEAD, the reaction with DIAD proceeded smoothly leading to the excellent yield of the triazoline product **113** (Table 4.4, entries 2). Similarly, 4-phenyl-1,2,4-triazoline-3,5-dione (PTAD) also rendered the triazoline product **114** in excellent yield (Table 4.4, entry 3).

Different oxazolones were prepared from *N*-acyl amino acids, using trifluoroacetic anhydride as dehydrating agent, and were subsequently evaluated for their reactivity with azodicarboxylates.

Different aromatic groups incorporated at the R^1 position included a phenyl, p-methoxy phenyl, p-fluoro phenyl and p-nitro phenyl moiety. The reaction of the oxazolones with azodicarboxylates proceeded in very good yields for p-methoxy phenyl and p-fluoro phenyl moieties (Table 4.4, entries 5, 6). As anticipated, the reaction proceeded significantly slower when the oxazolones were substituted by the electron withdrawing p-nitro phenyl group (Table 4.4, entry 4). Switching to a less polar solvent such as dichloromethane increased the yield in this case.

The reaction was also amendable to changes at the R^2 position in most cases. The R^2 position was substituted with R^2 being a methyl, benzyl and isopropyl (Table 4.4, entries 1, 7-9), which all provided the triazoline product in very good yields.

However, the reaction proceeded slower in presence of bulky groups such as an isopropyl group, and required more time for completion (24hrs).

Additional structural confirmation was established by X-ray crystallography. The crystals of compound **124** (Table 4.4, entry 8) were grown from dichloromethane-hexane solution and analyzed by single crystal X-ray crystallography (crystal structure presented in the experimental section).

4.2.4. Proposed reaction mechanism

The reaction is believed to proceed via electrophilic attack of oxazolone to azodicarboxylate leading to the formation of dipolar intermediate **129**. This intermediate then undergoes ring opening and generates a nitrilium intermediate **130**. This intermediate leads to the cycloadduct upon nucleophilic attack by the other nitrogen of azodicarboxylate via a 5-endo-dig type ring closure (Scheme 4.2)**.**

4.3. Synthesis of triazoles

Although little is known about the biological properties of triazolines, the 1,2,4-triazole moiety constitutes the core structure of a wide range of compounds. These compounds

have been shown to possess antiviral, anticancer, anti-inflammatory, anticonvulsant properties.[12]

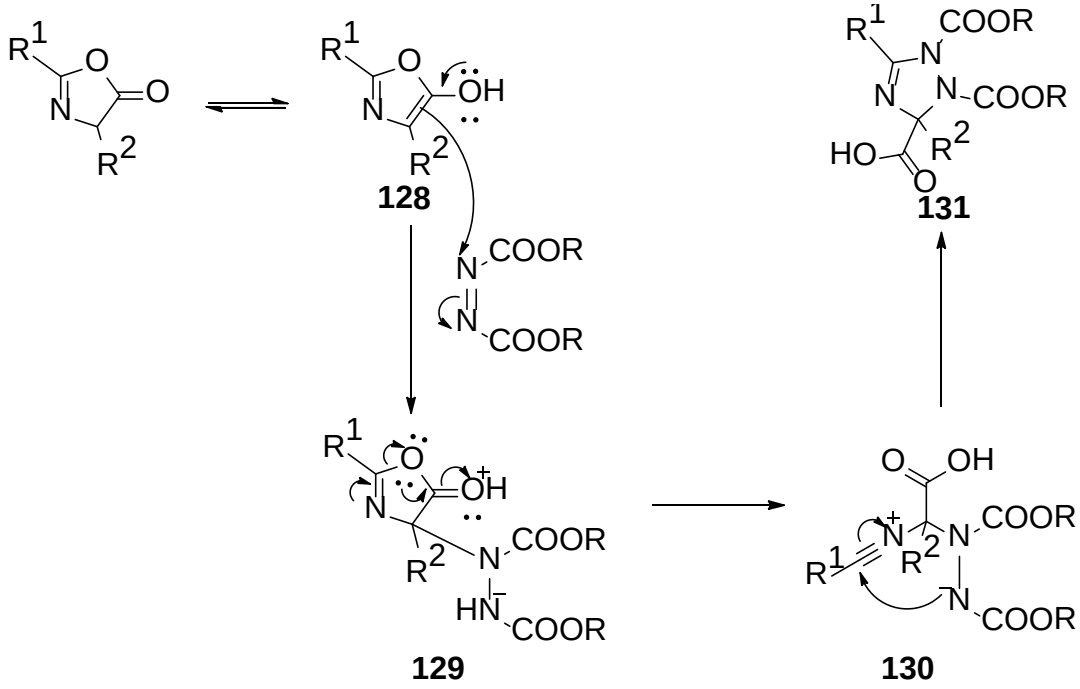

Scheme 4.2. Proposed mechanism of triazoline formation

In addition this core is also a part of antiviral, anti-asthmatic, antifungal, antibacterial and hypotonic drugs.[13] The 1,2,4-triazolines produced in the cycloaddition of the oxazolone compounds and diazocarboxylates were found to be excellent precursors to prepare the triazoles.

The triazolines prepared were readily converted into their corresponding triazoles, by decarboxylation and aromatization. This conversion was achieved in one step in excellent yield using alcoholic sodium hydroxide under refluxing conditions for 2 hours (

Table **4.5**).

Table 4.5. Conversion of triazoline to triazole

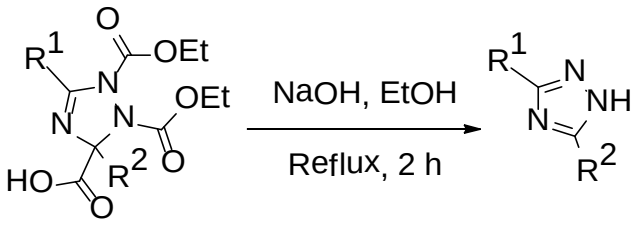

	R^1	R^2	Product	Yield (%)
1	Ph	Me	**132**	82
2	p-NO_2-C_6H_4	Me	**133**	74
3	p-F- C_6H_4	Me	**134**	84
4	Ph	Indolyl-3-Methyl	**135**	83

Crystals of compound **132** were grown from dichloromethane solution and the structure of compound **132** was confirmed by single crystal X-ray crystallography (X-ray structure is presented in the experimental section).

4.4. Experimental Section

General procedure for synthesis of oxazolones:

N-benzoyl amino acid was suspended in anhydrous dichloromethane in a round bottom flask under nitrogen. 1.3 equivalents of TFAA were added to the reaction mixture and it was stirred for 1.5 h at room temperature. Then the contents of the flask were poured into a separating funnel and washed with aqueous sodium bicarbonate solution three times. Subsequently, the reaction mixture was washed with brine, dried over sodium sulfate and placed on a rotary evaporator to evaporate the solvent. Residual solvent was removed *in vacuo* and the oxazolone formed were used in the next reaction. Previously reported oxazolones (**111, 115, 119, 121, 123, and 125**) were matched with their reported data.[14]

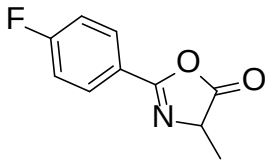

2-(4-fluorophenyl)-4-methyloxazol-5(4H)-one (117): ^{1}H NMR (500 MHz, $CDCl_3$) δ 7.93 (2H, m), 7.10 (2H, m), 4.38 (2H, q, J= 7 Hz), 1.51 (3H, d, J= 7 Hz); ^{13}C NMR (125 MHz, $CDCl_3$) δ 178.5, 166.4, 164.4, 164.3, 160.6, 130.2 (s), 130.1 (s), 128.1, 128.0, 122.1, 122.0, 116.1 (s), 116.0 (s), 60.9 (s), 16.7 (t); IR (NaCl, neat): 3290, 1734, 1705, 1631cm^{-1}; MS (ES+) m/z: 194.1 $[M+H]^+$; mp 128-130^{o}C; HRMS (ES+) calcd for $C_{10}H_9NO_2F$ $[M+H]^+$ 194.0617, found 194.0624.

General procedure for the cycloaddition reactions:

Oxazolone (0.5-0.8 mmol) was dissolved in 10mL of MeCN in a 20mL scintillation vial. One equivalent of the azodicarboxylate was added to solution. The reaction mixture was stirred at room temperature for 4-22 hours. The contents of the vial were, then, transferred into a separating funnel containing aqueous sodium bicarbonate and dichloromethane. The product was extracted into the aqueous bicarbonate layer and the dichloromethane layer was discarded. The aqueous sodium bicarbonate layer was acidified with HCl, and the product extracted with dichloromethane (40mL x 4). The dichloromethane fractions were combined and dried over sodium sulfate. The organic solvent was removed using a rotary evaporator to provide the product, which was further dried over vacuum and analyzed.

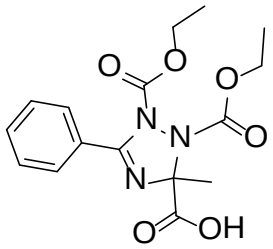

1,2-bis(ethoxycarbonyl)-3-methyl-5-phenyl-2,3-dihydro-1H-1,2,4-triazole-3-carboxylic acid (112): ^{1}H NMR (500 MHz, $CDCl_3$) δ 7.77 (2H, d, J= 7 Hz), 7.44 (1H, t, J= 7 Hz), 7.36 (2H, t, J= 7 Hz), 4.18 (2H, m), 4.10 (2H, m), 1.76 (3H, s), 1.21 (3H, t, J= 7 Hz), 1.02 (3H, t, J= 7 Hz); ^{13}C NMR (125 MHz, $CDCl_3$) δ 171.5, 158.8, 154.3, 152.8, 131.7 (s), 129.7 (s), 128.6, 127.7 (s), 90.2, 63.9 (d), 62.8 (d), 22.6 (t), 14.1 (t),

13.7 (t); IR (NaCl, neat): 1759, 1700,1631 cm^{-1}; MS (ES+) m/z: 350.1 $[M+H]^+$; HRMS (ES+) calcd for $C_{16}H_{20}N_3O_6$ $[M+H]^+$ 350.1352, found 350.1354.

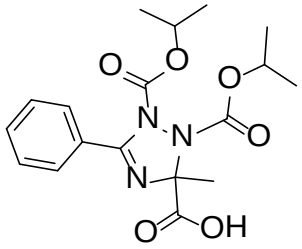

1,2-bis(isopropoxycarbonyl)-3-methyl-5-phenyl-2,3-dihydro-1H-1,2,4-triazole-3-carboxylic acid (113): ^{1}H NMR (500 MHz, $CDCl_3$) δ 7.78 (2H, d, J= 7 Hz), 7.45 (1H, t, J= 7 Hz), 7.37 (2H, t, J= 7 Hz), 4.98 (1H, m), 4.83 (1H, m), 1.78 (3H, s), 1.24 (3H, d, J= 6 Hz), 1.20 (3H, d, J= 6 Hz), 1.08 (3H, d, J= 6 Hz), 0.98 (3H, d, J= 6 Hz). ^{13}C NMR (125 MHz, $CDCl_3$) δ 172.3, 159.4, 153.5, 152.3, 131.7 (s), 129.8 (s), 128.7, 127.7 (s), 89.7, 72.4 (s), 71.2 (s), 22.6 (t), 21.9 (t), 21.5 (t), 21.4 (t), 21.2 (t). IR (NaCl, neat): 1761, 1705, 1653, 1630 cm^{-1}. MS (ES) m/z: $[M+H]^+$ 378.1 mp48^{o}C. HRMS (ES+) calcd for $C_{18}H_{24}N_3O_6$ $[M+H]^+$: 378.1665 found: 378.1667.

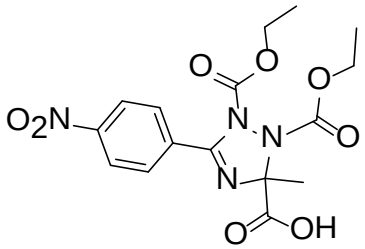

1,2-bis(ethoxycarbonyl)-3-methyl-5-(4-nitrophenyl)-2,3-dihydro-1H-1,2,4-triazole-3-carboxylic acid (116): ^{1}H NMR (500 MHz, $CDCl_3$) δ 8.19 (2H, d, J= 7 Hz), 7.95 (2H, d, J= 7 Hz), 4.22 (2H, q, J= 7 Hz), 4.12 (2H, q, J= 7 Hz), 1.78 (3H, s), 1.23 (3H, t, J= 7 Hz), 1.06 (3H, t, J= 7 Hz); ^{13}C NMR (125 MHz, $CDCl_3$) δ 171.7, 157.5, 154.1, 152.6, 149.6, 130.8 (s), 122.9 (s), 90.5, 64.5 (d), 63.2 (d), 22.5 (t), 14.1 (t), 13.8 (t); IR (NaCl, neat): 3100(br), 1761, 1653, 1599, 1527cm^{-1}; MS (ES+) m/z: 395.1 $[M+H]^+$; mp 134-136^{o}C; HRMS (ES+) calcd for $C_{16}H_{19}N_4O_8$ $[M+H]^+$ 395.1203, found 395.1212.

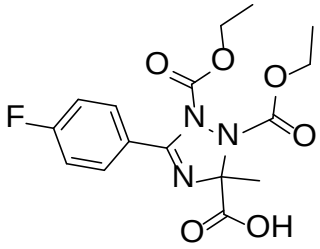

1,2-bis(ethoxycarbonyl)-5-(4-fluorophenyl)-3-methyl-2,3-dihydro-1H-1,2,4-triazole-3-carboxylic acid (118): ^{1}H NMR (500 MHz, $CDCl_3$) δ 7.80 (2H, m), 7.04 (2H, m), 4.20 (2H, q, J= 7 Hz), 4.12 (2H, q, J= 7 Hz), 7.73 (3H, s), 1.22 (2H, t, J= 7 Hz), 1.06 (2H, t, J= 7 Hz); ^{13}C NMR (125 MHz, $CDCl_3$) δ 171.7, 165.9, 163.9, 158.1, 154.0, 152.7, 132.2(s), 132.1 (s), 124.5, 124.4, 155.1 (s), 155.0 (s), 89.8, 64.1 (d), 62.9 (d),

22.4 (t), 14.1 (t), 13.7 (t); IR (NaCl, neat): 3200(br), 1759, 1633, 1604, 1510 cm^{-1}; MS (ES+) m/z: 368.1 $[M+H]^+$; mp 46-48^oC; HRMS (ES+) calcd for $C_{16}H_{19}N_3O_6F$ $[M+H]^+$ 368.1258, found 368.1264.

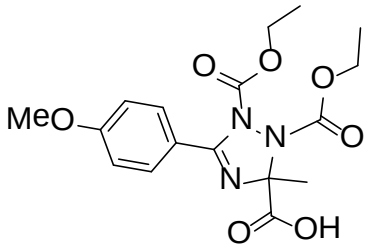

1,2-bis(ethoxycarbonyl)-5-(4-methoxyphenyl)-3-methyl-2,3-dihydro-1H-1,2,4-triazole-3-carboxylic acid (120): ^1H NMR (500 MHz, $CDCl_3$) δ 7.75 (2H, d, J= 7 Hz), 6.86 (2H, d, J= 7 Hz), 4.20 (2H, q, J= 7 Hz), 4.11 (2H, q, J= 7 Hz), 3.80 (3H, s), 1.76 (3H, s), 1.22 (3H, t, J= 7 Hz), 1.08 (3H, t, J= 7 Hz); ^{13}C NMR (125 MHz, $CDCl_3$) δ 171.8, 162.5, 158.7, 154.0, 153.0, 131(s), 120.4, 113.1 (s), 89.4, 63.9 (d), 62.8 (d), 55.3 (t), 22.4 (t), 14.1 (t), 13.7 (t); IR (NaCl, neat): 3200 (br), 1757, 1718, 1624, 1608, 1512cm^{-1}; MS (ES+) m/z 380.1 $[M+H]^+$; mp 42-44^oC; HRMS (ES+) calcd for $C_{17}H_{22}N_3O_7$ $[M+H]^+$ 380.1458, found 380.1461.

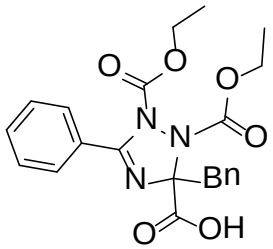

3-benzyl-1,2-bis(ethoxycarbonyl)-5-phenyl-2,3-dihydro-1H-1,2,4-triazole-3-carboxylic acid (122): ^{1}H NMR (500 MHz, $CDCl_3$) δ 7.67 (2H, d, J= 7 Hz), 7.45 (1H, t, J= 7 Hz), 7.35 (2H, t, J= 7 Hz), 7.29 (2H, d, J= 7 Hz), 7.21 (2H, , J= 7 Hz), 7.15 (1H, t, J= 7 Hz), 4.28 (2H, m), 3.73 (1H, m), 3.70 (1H, m), 3.64 (1H, d, J= 14 Hz), 3.44 (1H, d, J= 14 Hz), 1.29 (3H, t, J= 7 Hz), 0.91 (3H, t, J= 7 Hz); ^{13}C NMR (125 MHz, $CDCl_3$) δ 171.7, 159.8, 154.9, 151.4, 133.6, 131.5 (s), 131.2 (s), 129.2 (s), 128.8, 127.7 (s), 127.6 (s), 126.8 (s), 93.0, 63.4 (d), 63.0 (d), 40.7 (d), 14.1 (t), 13.4 (t); IR (NaCl, neat): 3200 (br), 1757, 1718, 1686, 1635 cm^{-1}; MS (ES+) m/z: 426.2 $[M+H]^+$; mp 61-64^{o}C; HRMS (ES+) calcd for $C_{22}H_{24}N_3O_6$ $[M+H]^+$ 426.1665, found 426.1666.

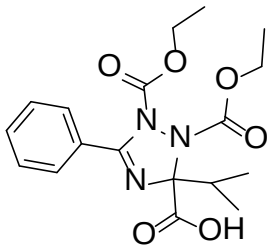

1,2-bis(ethoxycarbonyl)-3-isopropyl-5-phenyl-2,3-dihydro-1H-1,2,4-triazole-3-carboxylic acid (124): ^{1}H NMR (500 MHz, $CDCl_3$) δ 7.77 (2H, d, J= 7 Hz), 7.45 (1H, t, J= 7 Hz), 7.35 (2H, t, J= 7 Hz), 4.15 (4H, m), 2.62 (1H, m), 1.20 (3H, t, J= 7 Hz), 1.05 (6H, q, J= 7 Hz), 0.91 (3H, d, J= 7 Hz); ^{13}C NMR (125 MHz, $CDCl_3$) δ 171.6, 158.7,

155.5, 152.4, 131.6 (s), 129.6 (s), 128.6, 127.7 (s), 96.1, 63.7 (d), 62.9 (d), 33.1 (s), 17.2 (t), 16.2 (t), 14.0 (t), 13.8 (t); IR (NaCl, neat): 1759, 1635cm^{-1}; MS (ES+) m/z 378.1 $[M+H]^+$; mp 98-99^{o}C; HRMS (ES+) calcd for $C_{18}H_{24}N_3O_6$ $[M+H]^+$ 378.1665, found 378.1665.

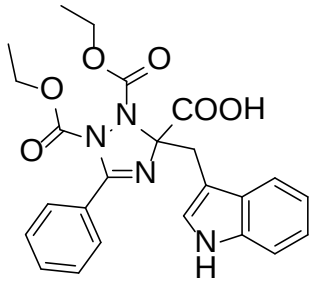

3-((1H-indol-3-yl)methyl)-1,2-bis(ethoxycarbonyl)-5-phenyl-2,3-dihydro-1H-1,2,4-triazole-3-carboxylic acid (126): ^{1}H NMR (500 MHz, $CDCl_3$) δ 8.28 (1H, br), 7.68 (1H, d, J= 7 Hz), 7.60 (2H, d, J= 7 Hz), 7.37 (1H, t, J= 7 Hz), 7.27 (2H, d, J= 7 Hz), 7.15 (1H, d, J= 7 Hz), 7.06 (2H, m), 7.01 (1H, d, J= 2 Hz), 4.25 (2H, m), 3.69 (2H, s), 3.45 (1H, m), 2.96 (1H, m), 1.26 (3H, t, J= 7 Hz), 0.59 (3H, t, J= 8 Hz); ^{13}C NMR (125 MHz, $CDCl_3$) δ 171.2, 159.7, 154.8, 152.3, 135.6, 131.5 (s), 129.3 (s), 128.7, 128.4, 127.7 (s), 124.5 (s), 121.5 (s), 119.4 (s), 119.2 (s), 110.8 (s), 107.3, 93.4, 63.2 (d), 62.9 (d), 30.4 (d), 14.2(t), 13.1 (t); IR (NaCl, neat): 3391, 2984, 1753, 1633, 1458,1327, 1259cm^{-1}; MS (ES+) m/z: 465.2 $[M+H]^+$; mp 97-99^{o}C; HRMS (ES+) calcd for $C_{24}H_{25}N_4O_6$ $[M+H]^+$: 465.1774 found: 465.1776.

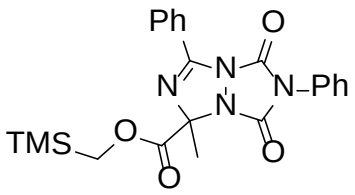

(Trimethylsilyl)methyl 1-methyl-5,7-dioxo-3,6-diphenyl-1,5,6,7-tetrahydro-[1,2,4]triazolo[1,2-a][1,2,4]triazole-1-carboxylate (127): 4-methyl-2-phenyloxazol-5(4H)-one (**1**, 175mg, 1mmol) was dissolved in 10mL of acetonitrile in a 20mL scintillation vial and PTAD (175mg, 1mmol) was added to the reaction mixture. The addition of PTAD turned the solution scarlet red in color. The reaction mixture was stirred for 4 hours, which lead to the disappearance of the color. At this point the reaction mixture was cooled to 0^{o}C and (trimethylsilyl)diazomethane (1.5mL, 3mmol) was added to the solution in drop-wise manner. The reaction mixture was stirred for 15 minutes and then methanol (3mL) was added in drop wise manner. The reaction was further stirred at 0^{o}C for 3 hour and then the reaction temperature was allowed to come to ambient temperature. Subsequently, the reaction mixture was concentrated to minimal residue and purified column chromatography (silica, ethyl acetate/hexanes 1:4) to obtain (trimethylsilyl)methyl 1-methyl-5,7-dioxo-3,6-diphenyl-1,5,6,7-tetrahydro-[1,2,4]triazolo[1,2-a][1,2,4]triazole-1-carboxylate as viscous liquid (370 mg, 85%).

^{1}H NMR (500 MHz, $CDCl_3$) δ 8.06 (1H, d, J= 7 Hz), 7.58 (1H, t, J= 7 Hz), 7.46 (6H, m), 7.38 (1H, t, J= 7 Hz), 4.09 (1H, d, J= 14 Hz), 3.85 (1H, d, J= 14 Hz) , 2.06 (3H, s), 0.07 (9H, s); ^{13}C NMR (150MHz, -10^{o}C) (CD_3OD) δ 167.5, 153.7, 153.5, 148.1, 133.3 (s), 130.9, 130.3 (s), 129.2 (s), 128.7 (s), 128.4 (s), 125.9 (s), 125.0, 90.8, 60.9 (d), 23.4 (t),

-3.2 (t); IR (NaCl, neat): 1794, 1740, 1616, 1500, 1450, 1398, 1329, 1251cm^{-1}; MS (ES) m/z: 437.2 $[M+H]^+$; HRMS (ES+) calcd for $C_{22}H_{25}N_4O_4Si$ $[M+H]^+$, 437.1645 found 437.1653.

General procedure for conversion of triazolines to triazoles:

The triazoline (0.5-1mmol) was dissolved in 25 mL ethanol in 100mL round bottom flask. Four equivalents of sodium hydroxide were added to this solution and the solution was heated to reflux for 2 hours. The temperature of the flask was, then, allowed to cool down to room temperature. The excess base in the solution was neutralized with aqueous HCl. The ethanol was removed on a rotary evaporator and the residue was dissolved in ethyl acetate. The ethyl acetate solution was washed with brine and dried over sodium sulfate. Subsequently, the ethyl acetate was removed on a rotary evaporator and crude product was purified by column chromatography (silica, ethyl acetate) to obtain the triazole.[15]

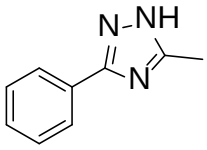

Synthesis of 5-methyl-3-phenyl-1H-1,2,4-triazole (132): ^{1}H NMR (500 MHz, $CDCl_3$) δ 7.95 (2H, d, J= 7 Hz), 7.42 (3H, m), 2.45 (3H, s); ^{13}C NMR(150MHz, -10^{o}C) (CD_3OD) δ 162.7, 155.5, 131.7, 130.6(s), 1129.8(s), 127.2 (s), 11.6 (t); IR (NaCl, neat): 3500 (br),

1700, 1720cm^{-1}; MS (ES) m/z: 159.1 $(M)^{+}$; mp 144-145^{o}C; HRMS (ES+) calcd for $C_9H_{10}N_3$ $[M+H]^{+}$ 160.0875, found 160.0880.

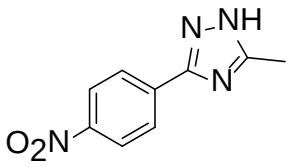

5-methyl-3-(4-nitrophenyl)-1H-1,2,4-triazole(133):

^{1}H NMR (600MHz, CD_3OD) δ 8.31 (2H, d, J= 9 Hz), 8.21 (2H, d, J= 9 Hz), 2.51 (3H, s); ^{13}C NMR (150 MHz, CD_3OD) δ 149.6, 138.0, 129.9, 128.0, 125.0, 11.7; IR (NaCl, neat): 3034 (br), 1603, 1508cm^{-1}; MS (ES+) m/z: 205.1 $[M+H]^{+}$; mp 232-234^{o}C; HRMS (ES+) calcd for $C_9H_9N_4O_2$ $[M+H]^{+}$ 205.0726, found 205.0726.

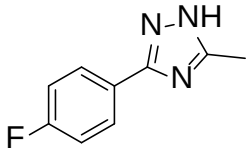

3-(4-fluorophenyl)-5-methyl-1H-1,2,4-triazole(134):

^{1}H NMR (600MHz, CD_3OD) δ 7.96 (2H, dd, J= 5 Hz, 7 Hz), 7.15 (2H, t, J= 9Hz), 2.49 (3H, s); ^{13}C NMR (150MHz, CD_3OD) δ 165.8, 164.1, 160.7, 156.9, 129.4, 129.3, 127.8, 127.7, 116.7, 116.6, 11.9; IR (NaCl, neat): 3055 (br), 1603, 1560, 1533, 1473, 1219 cm^{-}

^{1}; MS (ES) m/z: 178.1 $[M+H]^{+}$; mp279-283^{o}C; HRMS (ES+) calcd for $C_9H_9FN_3$ $[M+H]^{+}$ 178.0781, found 178.0783.

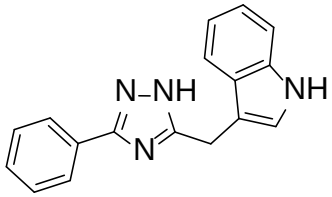

3-((3-phenyl-1H-1,2,4-triazol-5-yl)methyl)-1H-indole(135):

^{1}H NMR (600MHz, CD_3OD) δ 7.98 (2H, d, J= 7 Hz), 7.44 (4H, m), 7.34 (1H, d, J= 8 Hz), 7.17 (1H, s), 7.08 (1H, t, J= 7 Hz), 6.98 (1H, t, J= 7 Hz), 4.30 (2H, s); ^{13}C NMR (226MHz, CD_3OD) δ 160.8, 138.3, 131.2, 130.8, 129.8, 128.3, 127.4, 124.5, 122.6, 120.0, 119.2, 112.4, 110.5, 24.2; IR (NaCl, neat): 3333, 3128 (br), 1558, 1471cm^{-1}; MS (ES+) m/z: 275.1 $[M+H]^{+}$; mp 241-243^{o}C; HRMS (ES+) calcd for $C_{17}H_{15}N_4$ $[M+H]^{+}$ 275.1297, found 275.1307.

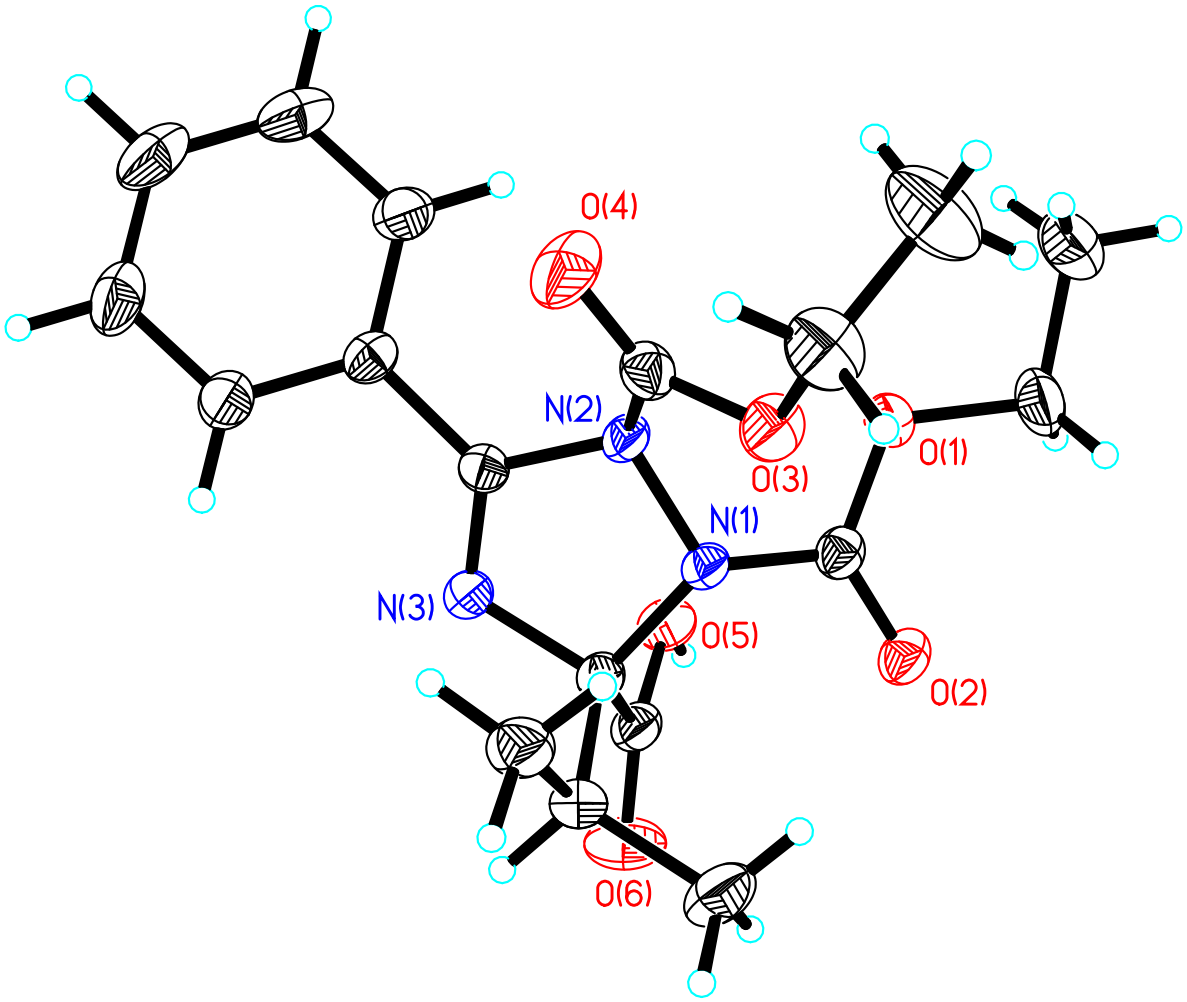

Figure 4.1. X-ray crystal structure of 124

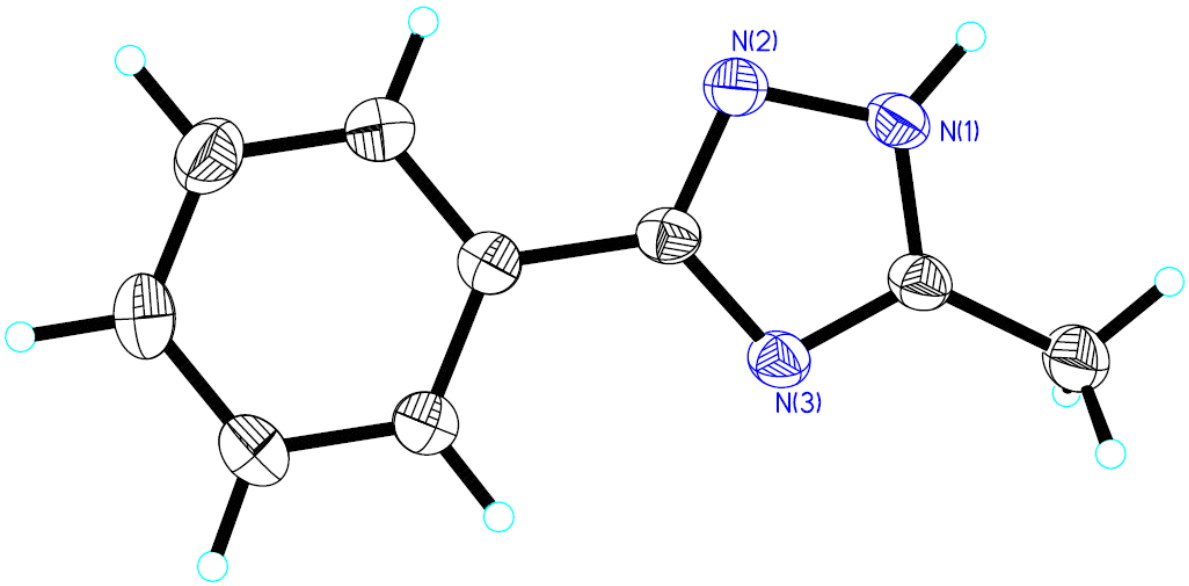

Figure 4.2. X-ray crystal structure of 132

References

4.5. References

1. (a) Schreiber, S. L., Target-oriented and diversity-oriented organic synthesis in drug discovery. *Science* **2000,** *287*, 1964-9; (b) Powers, D., Automated parallel synthesis of chalcone-based screening libraries. *Tetrahedron* **1998,** *54*, 4085-96.

2. (a) Funke, E.; Huisgen, R., Ketenoid reactivity of a mesoionic oxazol-5-one. *Chem. Ber. Recl.* **1971,** *104*, 3222-8; (b) Cremonesi, G., [2+2] Cycloaddition reactions of imines with cyclic ketenes: Synthesis of 1,3-thiazolidine derived spiro-β-lactams and their transformations. *Helv. Chim. Acta* **2005,** *88*, 1580-8.

3. (a) Huisgen, R.; Gotthard.H; Bayer, H. O.; Schaefer, F. C., 1,3-Dipolar cycloadditions .56. A convenient synthesis of N-substituted pyrroles from mesoionic oxazolones and alkynes. *Chem. Ber. Recl.* **1970,** *103*, 2611-24; (b) Hershenson, F. M.; Pavia, M. R., Synthesis of N-substituted pyrroles from azlactones via 1,3-oxazolium 5-oxides. *Synthesis* **1988**, 999-1001; (c) Okano, T.; Uekawa, T.; Morishima, N.; Eguchi, S., Synthesis of beta-(trifluoromethyl)pyrroles via the cycloaddition of munchnones to electron-deficient trifluoromethylated olefins. *J. Org. Chem.* **1991,** *56*, 5259-62; (d) Clerici, F.; Gelmi, M. L.; Trimarco, P., 5(4H)-oxazolones. Part XI. Cycloaddition reaction of oxazolones and münchnones to triphenylvinylphosphonium salts as synthetic equivalents of alkynes. *Tetrahedron* **1998,** *54*, 5763-74.

4. (a) Gotthardt, H.; Huisgen, R.; Schaefer, F. C., Δ2-pyrroline aus mesoionischen oxazolen und olefinen. *Tetrahedron Lett.* **1964,** *5*, 487-91; (b) Maryanoff, C. A.; Karash, C. B.; Turchi, I. J.; Corey, E. R.; Maryanoff, B. E., Characterization of a stable carboxylic acid intermediate from 1,3-dipolar cycloaddition of a munchnone with 1,2-dicyanocyclobutene. *J. Org. Chem.* **1989,** *54*, 3790-2; (c) Melhado, A. D.; Luparia, M.; Toste, F. D., Au(I)-catalyzed enantioselective 1,3-dipolar cycloadditions of münchnones with electron-deficient alkenes. *J. Am. Chem. Soc.* **2007,** *129*, 12638-9.

5. (a) Brunn, E.; Funke, E.; Gotthard.H; Huisgen, R., 1,3-Dipolar cycloadditions .61. Cycloadditions of N-substituted oxazolium-5-olates to nitriles, nitro, nitroso and azo compounds. *Chem. Ber. Recl.* **1971,** *104*, 1562-72; (b) Consonni, R.; Croce, P.; Ferracciolo, R.; Larosa, C., A new approach to imidazole derivatives. *J. Chem. Res., Synop .* **1991**, 188-9; (c) Bilodeau, M. T.; Cunningham, A. M., Solid-supported synthesis of imidazoles: A strategy for direct resin-attachment to the imidazole core. *J. Org. Chem.* **1998,** *63*, 2800-1.

6. (a) Peddibhotla, S.; Jayakumar, S.; Tepe, J. J., Highly diastereoselective multicomponent synthesis of unsymmetrical imidazolines. *Org. Lett.* **2002,** *4*, 3533-5; (b) Peddibhotla, S.; Tepe, J. J., Multicomponent synthesis of highly substituted imidazolines via a silicon mediated 1,3-dipolar cycloaddition. *Synthesis* **2003**, 1433-40; (c) Peddibhotla, S.; Tepe, J. J., Stereoselective synthesis of highly substituted Δ1-pyrrolines: Exo-Selective 1,3-dipolar cycloaddition reactions with azlactones. *J. Am. Chem. Soc.* **2004,** *126*, 12776-7; (d) Sharma, V.; Tepe, J. J., Diastereochemical

diversity of imidazoline scaffolds via substrate controlled TMSCl mediated cycloaddition of azlactones. *Org. Lett.* **2005,** *7*, 5091-4; (e) Keni, M.; Tepe, J. J., One-pot Friedel-Crafts/Robinson-Gabriel synthesis of oxazoles using oxazolone templates. *J. Org. Chem.* **2005,** *70*, 4211-3; (f) Fisk, J. S.; Tepe, J. J., Intermolecular ene reactions utilizing oxazolones and enol ethers. *J. Am. Chem. Soc.* **2007,** *129*, 3058-9; (g) Mosey, R. A.; Fisk, J. S.; Friebe, T. L.; Tepe, J. J., Synthesis of tert-alkyl amino hydroxy carboxylic esters via an intermolecular ene-type reaction of oxazolones and enol ethers. *Org. Lett.* **2008,** *10*, 825-8; (h) Hupp, C. D.; Tepe, J. J., Total synthesis of a marine alkaloid from the tunicate Dendrodoa grossularia. *Org. Lett.* **2008,** *10*, 3737-9; (i) Hupp, C. D.; Tepe, J. J., 1-Ethyl-3-(3-dimethylaminopropyl)carbodiimide hydrochloride-mediated oxazole rearrangement: gaining access to a unique marine alkaloid scaffold. *J. Org. Chem.* **2009,** *74*, 3406-13; (j) Mosey, R. a.; Tepe, J. J., New synthetic route to access (±) salinosporamide A via an oxazolone-mediated ene-type reaction. *Tetrahedron Lett.* **2009,** *50*, 295-7.

7. (a) Fisk, J. S.; Mosey, R. a.; Tepe, J. J., The diverse chemistry of oxazol-5-(4H)-ones. *Chem. Soc. Rev.* **2007,** *36*, 1432-40; (b) Hewlett, N.; Hupp, C.; Tepe, J., Reactivity of oxazol-5-(4H)-ones and their application toward natural product synthesis. *Synthesis* **2009,** *2009*, 2825-39.

8. Kolasa, T.; Miller, M. J., Oxidations of some [alpha]-amino acids under mitsunobu reaction conditions. *Tetrahedron Lett.* **1988,** *29*, 4661-4.

9. (a) Ibata, T.; Isogami, Y.; Tamura, H., Anomalous cycloaddition of oxazoles with PTAD. *Chem. Lett.* **1988,** *17*, 1551-4; (b) Hassner, A., Do oxazoliks undergo Diels-Alder reactions with heterodienophiles? *Tetrahedron* **1989,** *45*, 3535-46; (c) Shi, X.; Ibata, T.; Suga, H.; Matsumoto, K., Abnormal Diels-Alder reaction of 5-alkoxythiazoles with highly reactive dienophiles; 4-phenyl-3H-1, 2, 4-triazole-3, 5(4H)-dione, diethyl azodicarboxylate, and diethyl oxomalonate. *Bull. Chem. Soc. Jpn.* **1992,** *65*, 3315-21; (d) Ibata, T.; Suga, H.; Isogami, Y.; Tamura, H.; Shi, X., Abnormal diels-alder reaction of oxazoles with 4-phenyl-3H-1,2,4-triazole-3,5(4H)-dione and diethyl azodicarboxylate, and X-ray crystal structure of an adduct. *Bull. Chem. Soc. Jpn.* **1992,** *65*, 2998-3007.

10. Anderson, D. J.; Watt, W., The reaction of imidazo[1,5- a]pyridines with methyl- and phenyltriazolinediones and with diethyl azodicarboxylate. *J. Heterocycl. Chem.* **1995,** *32*, 1525-30.

11. Tsuge, O.; Hatta, T.; Tashiro, H.; Maeda, H., Cycloaddition of synthetic equivalent of non-stabilized aminonitrile ylides: A new route to amino-substituted delta(2)-imidazolines and delta(3)-1,2,4-triazolines. *Heterocycles* **2001,** *55*, 243-8.

12. (a) Todoulou, O. G.; Papadakivaliraki, A. E.; Ikeda, S.; Declercq, E., Synthesis and antiviral activity of some new 1H-1,2,4-triazole derivatives. *Eur. J. Med. Chem.* **1994,** *29*, 611-20; (b) Berikrcan, O.; Kahveci, B.; Kucuk, M., Synthesis and anticancer evaluation of some new unsymmetrical 3,5-diaryl-4H-1,2,4-triazole derivatives. *Turk. J. Chem.* **2006,** *30*, 29-40; (c) Tandon, M.; Barthwal, J. P.; Bhalla, T. N.; Bhargava, K. P.,

Synthesis and antiinflammatory activity of some new 3-(o-substituted phenyl)-4-(substituted phenyl)-5-(alkyl/alkenylthio)-1H-1,2,4-triazoles. *Ind. J. Chem.* **1981,** *20B*, 1017-18; (d) Gulerman, N.; Rollas, S.; Kiraz, M.; Ekinci, A. C.; Vidin, A., Evaluation of antimycobacterial and anticonvulsant activities of new 1-(4-fluorobenzoyl)-4-substituted-thiosemicarbazide and 5-(4-fluorophenyl)-4-substituted-2,4-dihydro-3H-1,2,4-triazole-3-thione derivatives. *Farmaco* **1997,** *52*, 691-5.

13. (a) De Clercq, E., Antiviral drugs in current clinical use. *J. Clin. Virol.* **2004,** *30*, 115-33; (b) Naito, Y.; Akahoshi, F.; Takeda, S.; Okada, T.; Kajii, M.; Nishimura, H.; Sugiura, M.; Fukaya, C.; Kagitani, Y., Synthesis and pharmacological activity of triazole derivatives inhibiting eosinophilia. *J. Med. Chem.* **1996,** *39*, 3019-29; (c) Papakonstantinou-Garoufalias, S.; Pouli, N.; Marakos, P.; Chytyroglou-Ladas, A., Synthesis antimicrobial and antifungal activity of some new 3-substituted derivatives of 4-(2,4-dichlorophenyl)-5-adamantyl-1H-1,2,4-triazole. *Farmaco* **2002,** *57*, 973-7; (d) Hester, J. B.; Rudzik, A. D.; Kamdar, B. V., 6-Phenyl-4H-S-triazolo[4,3-a][1,4]benzodiazepines which have central nervous system depressant activity. *J. Med. Chem.* **1971,** *14*, 1078-81.

14. (a) Peet, N. P.; Burkhart, J. P.; Angelastro, M. R.; Giroux, E. L.; Mehdi, S.; Bey, P.; Kolb, M.; Neises, B.; Schirlin, D., Synthesis of peptidyl fluoromethyl ketones and peptidyl alpha-keto esters as inhibitors of porcine pancreatic elastase, human neutrophil elastase, and rat and human neutrophil cathepsin G. *J. Med. Chem.* **1990,** *33*, 394-407; (b) Chen, F. M. F.; Kuroda, K.; Benoiton, N. L., A simple preparation of 5-oxo-4,5-dihydro-1,3-oxazoles (Oxazolones). *Synthesis* **1979**, 230-2; (c) Peddibhotla, S.; Tepe, J. J., Multicomponent synthesis of highly substituted imidazolines via a silicon-mediated 1,3-dipolar cycloaddition. *Synthesis* **2003,** *34*, 1433-40.

15. (a) Perez, M. A.; Dorado, C. A.; Soto, J. L., Regioselective synthesis of 1, 2, 4-triazole and 1, 2, 4-oxadiazole derivatives. *Synthesis* **1983,** *1983*, 483-6; (b) Santus, M., Studies on thioamides and their derivatives .3. Synthesis of 1,2,4-triazole 3,5-disubstituted derivatives. *Pol. J. Chem.* **1980,** *54*, 1067-72; (c) Yeung, K.-S.; Farkas, M. E.; Kadow, J. F.; Meanwell, N. a., A base-catalyzed, direct synthesis of 3,5-disubstituted 1,2,4-triazoles from nitriles and hydrazides. *Tetrahedron Lett.* **2005,** *46*, 3429-32.

CHAPTER 5

INHIBITION OF 26s PROTEASOME AND BINDING STUDIES

5.1. Introduction

One of the most common strategies in cancer treatment involves the induction of DNA damage in the cancer cells. This strategy has dramatically improved the survival rate of patients. However, as discussed in chapter 2, these strategies lead to the activation of the pathway leading to p53 mediated apoptosis. Besides, these treatments also lead to the activation of the NF-κB pathway, which is largely responsible for antiapoptotic cell signaling. Activation of the NF-κB signaling pathway induces the expression of a wide range of genes involved in cell survival responses.[1] The activation of these antiapoptotic signaling pathways limits the overall efficacy of cancer treatments. Strategy of combining present day treatments with the inhibitors of ChK2 (as discussed in chapter 2) and inhibitors of NF-κB pathway will sensitize cancerous cells and desensitize healthy cells and improve the overall efficacy of the treatment. These strategies provide potential avenues for improving the cancer therapies.

5.1.1. The NF-κB pathway

The resistance offered by cancer cells to the cytotoxic effects of chemotherapeutic agents leads to reduction in the efficiency chemotherapy. Mutation of p53 pathway[2] and activation of the NF-κB pathway contribute to this reduction. The nuclear transcription factor, NF-κB, is a multisubunit complex involved in the regulation of gene transcription

and the regulation of apoptosis.[3] Five distinct subunits of NF-κB are found in mammalian cells, which include, NF-κB1 (p105/p50), NF-κB2 (p100/p52), RelA (p65), RelB and c-Rel.[3b, 4] These subunits can compose a variety of homo/heterodimers, which control the specificity and selectivity of certain DNA control elements.[5]

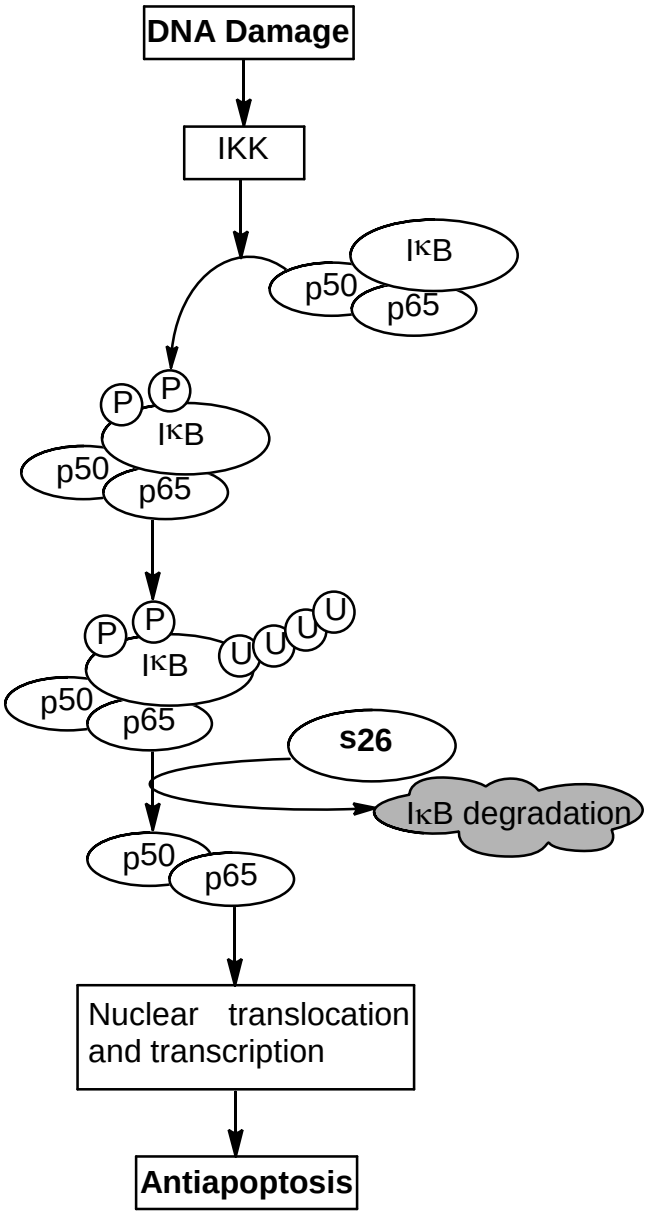

Figure 5.1 : NF-κB pathway

In most unstimulated mammalian cells, NF-κB exists mainly as a homodimer (p50/p50) or heterodimer (p50/p65) in the cytoplasm in the form of an inactive complex with the inhibitory protein IκB (Figure 5.1). Many cellular stimuli including chemotherapeutic agents[6] result in the IKK mediated phosphorylation of IκB. This is followed by ubiquitinylation and subsequent degradation of IκB by the 26s proteasome.[3a, 7] Degradation of IκB releases NF-κB.[8] Upon release, NF-κB translocates into the nucleus where the subunits bind to the DNA and regulates the transcription of a number of genes involved in antiapoptotic responses.[9] In most cells, NF-κB inhibits apoptosis via induction of these survival genes. NF-κB mediated antiapoptotic responses induced by DNA damaging agents leads to the reduction in the efficiency of the present day cancer treatments.[1c] Many clinically used chemotherapeutic agents have been shown to activate NF-κB and induce NF-κB mediated chemoresistance.[7, 10] Chemotherapeutic treatment by these agents is thus compromised by the activation of NF-κB pathway. The chemotherapeutic agents that will inhibit the activation of this pathway carry the potential of improving the cancer treatment. One strategy to inhibit the activation of this pathway is by blocking the 26s proteasome mediated degradation of the IκB.

Literature has cited a few proteasome inhibitors. Bortezomib (formally known as Velcade or PS-341)[11] is the first selective and reversible proteasome inhibitor approved for the use in USA. It acts by inhibiting the degradation of IkB.[12] MG-132 is another 26s proteasome inhibitor. Inhibition of the proteasome with MG-132 has been shown to

sensitize cells towards chemotherapeutics and TNF-α.[6d, 13] Lactacystin and the related omuralide,[14] and salinosporamide A[15] inhibit 26s proteasome by covalently binding to the N-terminal threonine in the catalytic site. However this covalent adducts also inhibit the degradation of other protease substrates, resulting in high cytotoxicity.[16]

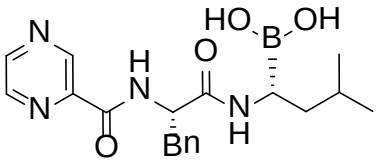

Bortezomib

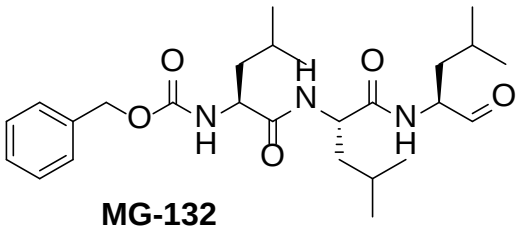

MG-132

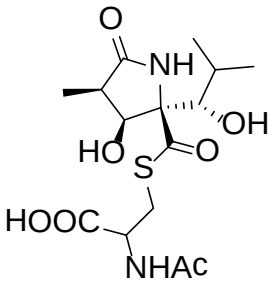

Lactacystin

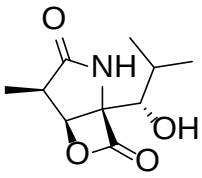

Omuralide

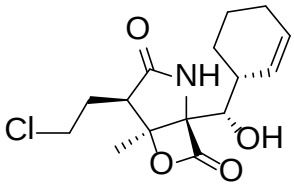

Salinosporamide A

Figure 5.2: 20s proteasome inhibitors

Our group has been interested in the diversity oriented synthesis (as introduced in the chapter 4). The group has previously reported that oxazolones undergo cycloaddition reaction with imine to give imidazoline as shown in scheme 5.1.[17] These compounds are potent inhibitor of the NF-κB pathway and act by inhibiting the 26s proteasome mediated IκB degradation.[17-18]

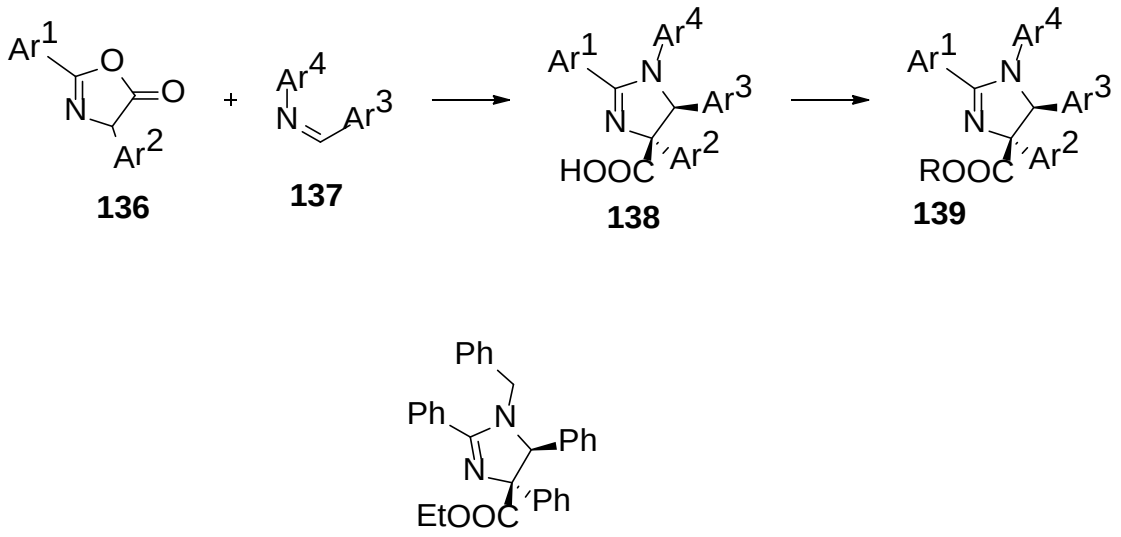

Scheme 5.1. General scheme for the synthesis of imidazolines

Unlike the previous examples of the proteasome inhibitors, these imidazoline-based compounds were found to be non-cytotoxic by themselves. However when used with other drugs, these drastically enhance the efficacy of several chemotherapeutic agents such as camptothecin and cis-platin in various cancer cell lines.[17] Unlike above mentioned drugs that target the active site in the 20S core and bind via a competitive mechanisms, these imidazolines bind at a site other than the catalytic site and act via an allosteric type mechanism. (unpublished work by Thersa Lansdell of Tepe group). We have been interested in maping the binding of these molecules on the proteasome.

In this regard, we considered under-taking the photoaffinity labeling studies of the proteasome with the imidazoline molecule. The study of structure and activity relationship has shown that the benzyl group can tolerate a wide variety of small

substituents at para-position without significantly modifying potency of these molecules.[18b] Therefore, we considered putting an azide group at this position and considered the synthesis of the compound **140** for these studies. We envisioned that compound **140** will non-covalently bind to proteasome. The azide group on the molecule will be activated by irradiation of the ultra violet light to produce active nitrene that will insert into a bond in the nearby peptide moiety of proteasome and establish covalent binding. In collaboration with Sujana Pradhan in Tepe group, our plans are to subsequently digest the proteasome and analyze the fragments. The information thus obtained will help understand the binding mode and binding site of these molecules.

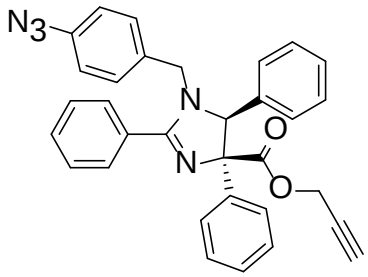

140

Figure 5.3: Proposed molecule

5.2. Synthesis of compound 140

In order to synthesize compound **140**, we generated imine **142** from benzaldehyde and p-nitrobenzyl amine and reacted it with compound **141** in the presence of TMSCl as catalyst to give the cycloadduct **143**.

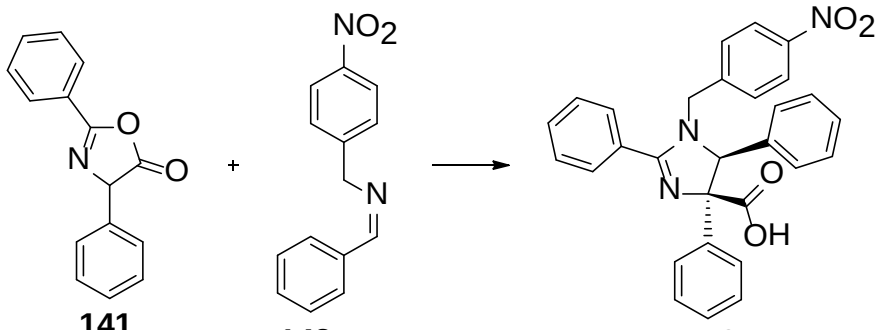

141 **142** **143**

Scheme 5.2. Synthesis of compound 143

Reactions and conditions: TMSCl, DCM, 60^{o}C, 12h, 54%

In the next step the carboxylic acid on the compound **143** was treated with propargyl alcohol to prepare the propargyl ester. This was achieved by converting the carboxylic acid into acid chloride using oxalyl chloride and then reacting the acid chloride with propargyl alcohol giving compound **144**.

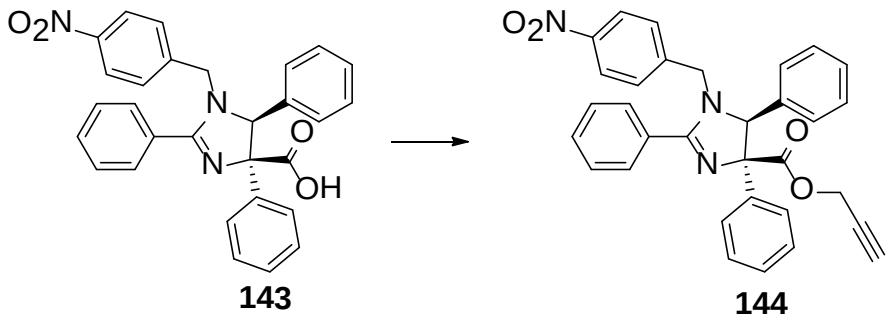

143 **144**

Scheme 5.3. Synthesis of compound 144

Reactions and conditions: (i) $(COCl)_2$, DMF, DCM, rt, 12h (ii) propargyl alcohol, rt, 3h, 82%

In the last step the functional group transformation was carried out and the nitro-group on compound **144** was converted into the azide group. The conversion was afforded by reducing nitro-group on compound **144** using zinc dust, which followed the diazotization and displacement of the diazonium with azide giving compound **140**.

5.3. Evaluation of compound 140

Compound **140** was evaluation for its ability to inhibit the proteasome by Theresa A. Lansdell using CT-L inhibition of the human 20s proteasome assay. The IC_{50} for compound **140** for inhibition of 20s proteasome was 592nM. This result is encouraging as it shows that this molecule is active in inhibiting the proteasome. The photoaffinity labeling studies are in progress in Tepe group.

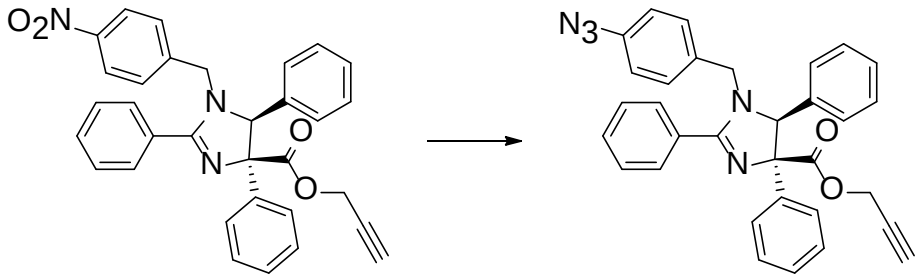

Scheme 5.4. Synthesis of compound 140

Reactions and conditions: (i) Zn, AcOH, rt, 20min (ii) $NaNO_2$, H_2SO_4, AcOH, H_2O, 0^oC, 10min (iii) NaN_3, H_2O, 0^oC, 30min, 70%

5.4. Evaluation of HMD derivatives

The HMD derivative **60** and **64-71** were also tested for their ability to inhibit the 20s proteasome by Theresa A. Lansdell. The results are tabulated below (Table 5.1). The results are exciting and show a very good structure activity relationship. In the CT-L inhibition of the human 20s proteasome assay, the compounds with either the phenyl ring (compound **64** and **65**), or the compound with bulky aliphatic cyclohexyl-group (compound **66**) showed single digit micro-molar inhibition of the proteasome. Compound **67**, with ethoxycarbonylethyl group had the IC_{50} of 18.2μM, whereas the compounds with no substituent on nitrogen-atom but different aromatic groups on pyrrole ring (compound **60**, **70** and **71**), shared the similar range of IC_{50} (25-31μM).

Table 5.1. Inhibition of 20s proteasome compounds 60, 64-71

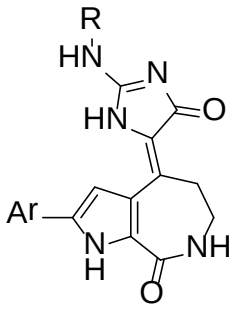

Compound			20S
Number	Ar	R	$IC_{50}(\mu M)$
60	Ph	H	30.7
64	Ph	Bn	5.0
65	Ph	$4\text{-}MeOC_6H_4CH_2$	4.3
66	Ph	Cy	4.2
67	Ph	$EtOOCCH_2CH_2$	18.2
68	Ph	$CH_3CH_2CH_2$	437.4
69	Ph	CH_3	45.4
70	3,4-dimethoxyphenyl	H	31.7
71	4-methoxyphenyl	H	25.5

On the other hand presence of small straight chain aliphatic groups like methyl and n-propyl lead to erosion of the inhibition.

These results are very interesting as these analogs provide structure-based tuning for inhibiting ChK2, ChK1 or 20s proteasome. The data shows that the presence of the aliphatic substituent (methyl, n-propyl) makes the molecules more potent and selective for ChK2, while these molecules have very poor or no inhibition of 20s proteasome. On the other hand, compound **64** with benzyl group inhibits ChK2 as well as the proteasome. Compound **65** with 4-methoxyphenyl and compound **66** were good inhibitors of 20s proteasome, while exhibited poor inhibition of ChK2, compound **66** showed reversal of the selectivity for ChK2 over ChK1. These results are intriguing and should act as the light-house for the future voyages into the synthesis of new derivatives to enhance the understanding of the SAR relationship and develop next generation of HMD-based inhibitors. In the meanwhile compound **69** and **71** are good candidates to undergo extensive kinase profiles, to access their ability to inhibit other kinases and their selectivity for ChK2. On the other hand compound **66** seems as be a good lead to develop new class of 20s proteasome inhibitors.

5.5. Experimental section

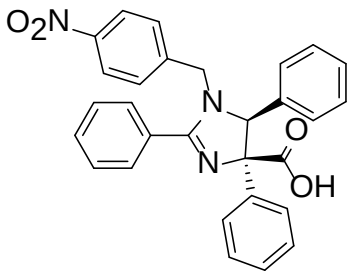

1-(4-nitrobenzyl)-2,4,5-triphenyl-4,5-dihydro-1H-imidazole-4-carboxylic acid (143):

Benzaldehyde (2mL, 20.4mmol) was dissolved in DCM (100mL) in a 250mL round bottom flask. Triethyl amine (2.84mL, 20.4mmol) and p-nitrobenzyl amine (3.5g, 18.55mmol) were added to the reaction mixture and the reaction mixture was refluxed for 12 hours. At this stage the solvent was removed and the residue was dried under vacuum for 4 hours. Then the residue was dissolved in DCM (100mL) and **141** (4.35g, 18.16mmol) and TMSCl (2.99mL, 23.53mmol) were added to the reaction mixture. The reaction mixture was refluxed at 60^{o}C for 12 hours. Then the solvent was removed and the crude product was purified by column chromatography (silica, DCM/MeOH 9:1) to afford the compound **143** (4.7g, 54%). ^{1}H NMR (600MHz, $CDCl_3$) δ 7.90 (2H, d, J=8.55 Hz), 7.83 (2H, m), 7.61 (2H, d, J=7.08 Hz), 7.54 (1H, t, J=7.32 Hz), 7.47 (2H, t, J=7.32 Hz), 7.34 (8H, m), 6.78 (2H, d, J=8.55 Hz), 4.84 (3H, s), 4.69 (1H, d, J=16.36 Hz), 3.95 (1H, d, J=16.60 Hz); ^{13}C NMR (150MHz, $CDCl_3$) δ 168.1, 165.2, 147.6, 142.8, 141.4, 135.5, 133.0(s), 129.4(s), 129.2(s), 129.1(s), 128.8(s), 128.4(s), 127.8(s), 127.4(s), 127.4(s), 125.6(s), 124.0(s), 123.0, 79.4, 76.0 (s), 47.7 (d); IR (film): 3433, 2525, 1635,

1522, 1344cm$^{-1;}$ MS (ES) m/z: 478.2 $[M+H]^+$; m.p. 110-112^{o}C; HRMS (ES+) calcd for $C_{29}H_{24}N_3O_4$ $[M+H]^+$ 478.1767, found 478.1775

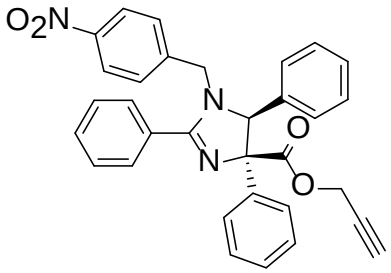

Prop-2-yn-1-yl 1-(4-nitrobenzyl)-2,4,5-triphenyl-4,5-dihydro-1H-imidazole-4-carboxylate (144):

Compound **143** (4.7g, 9.84mmol) was dissolved in DCM (70mL) in a 250mL round bottom flask. The reaction mixture was cooled to 0^{o}C and oxalyl chloride (2.5mL, 29.53mmole) was added to the reaction mixture. Then DMF (0.8mL) was added to reaction mixture in drop-wise manner. The reaction mixture was stirred for 3 hours. The solvent was removed and the residue was dried over vacuum for 30 minutes. Then propagyl alcohol (6mL) was added to the reaction mixture and mixture was stirred at room temperature for 3 hours. At this stage the excess of alcohol was removed by rotary evaporator and the crude product was purified by column chromatography (silica, EtOAc/Hex 1:1) affording compound **144** (4.1g, 82%).

^{1}H NMR (600MHz, $CDCl_3$) δ 7.88 (2H, d, J=8.55 Hz); 7.79 (2H, d, J=7.32 Hz), 7.74 (2H, dd, J=7.32, 1.71 Hz), 7.35 (8H, m), 7.48 (3H, m), 6.87 (2H, d, J=8.55 Hz), 4.83 (1H, s),

4.64 (1H, d, J=16.60 Hz), 4.25 (1H, dd, J=15.63, 2.44 Hz), 4.06 (1H, dd, J=15.50, 2.56 Hz), 3.97 (1H, d, J=16.60 Hz), 2.20 (1H, t, J=2.44 Hz); ^{13}C NMR (125MHz, $CDCl_3$) δ 169.7, 165.6, 147.2, 144.3, 143.4, 137.0, 130.8, 130.0 (s), 128.9 (s), 128.8 (s), 128.7 (s), 128.7 (s), 128.4 (s), 128.3 (s), 128.0 (s), 127.8 (s), 126.7 (s), 123.7 (s), 83.0, 77.0, 74.9 (s), 74.7, 52.5 (d), 48.4 (d); IR (film): 3408, 2117, 1740, 1595, 1510, 1217cm^{-1}; MS (ES) m/z: 516.2 $[M+H]^+$; m.p. 48-50^{o}C; HRMS (ES+) calcd for $C_{32}H_{26}N_3O_4$ $[M+H]^+$ 516.1923, found 516.1927.

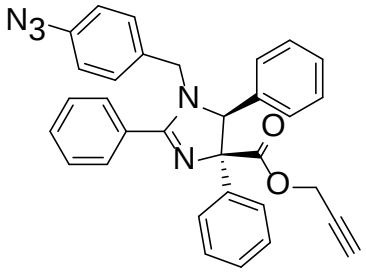

Prop-2-yn-1-yl 1-(4-azidobenzyl)-2,4,5-triphenyl-4,5-dihydro-1H-imidazole-4-carboxylate (140):

Compound **144** (2g, 3.88mmol) was dissolved in acetic acid (30mL) at room temperature in a 100mL flask. Zn dust (7.6g, 116.37mmol) was added to the reaction mixture. The mixture was stirred for 20 minutes and then filtered to remove the suspended particles. The filterate was collected into a 100mL flask and cooled to 0^{o}C. Sulfuric acid (1mL) was added to the reaction mixture. Sodium nitrite (400mgs, 5.82mmol) was dissolved in water (1mL) and this aqueous solution was added to the reaction mixture in dropwise. The reaction mixture was stirred for 10 minutes. Sodium azide (278mgs, 4.27mmol) was dissolved in water (1mL) and this aqueous solution was

added to the reaction mixture in dropwise manner. The mixture was stirred at 0^{o}C for 30 minutes. At this stage the contents of the reaction flask were transferred to a separating funnel (250mL) and diluted with ethyl acetate (125mL) and water (75mL). The aqueous layer was removed and the organic layer was washed with brine (100mL). Then the organic layer was collected and dried over magnesium sulfate. The solvent was removed and the product was purified by column chromatography (silica, EtOAc/Hex 1:1) to afford compound **140** (1.4g, 70%). ^{1}H NMR (600MHz, $CDCl_3$) δ 7.75 (4H, m), 7.48 (3H, m), 7.38 (4H, d, J=7.30 Hz), 7.34 (3H, t, J=7.32 Hz), 7.29 (1H, t, J=7.32 Hz), 6.69 (4H, s), 4.85 (1H, s), 4.56 (1H, d, J=15.87 Hz), 4.24 (1H, dd, J=15.63, 2.44 Hz), 4.03 (1H, dd, J=15.50, 2.56 Hz), 3.80 (1H, d, J=15.87 Hz), 2.21 (1H, t, J=2.44Hz); ^{13}C NMR (150MHz, $CDCl_3$) δ 170.0, 165.7, 143.5, 139.2, 137.3, 133.2, 130.5 (s), 130.3(s), 128.8 (s), 128.7(s), 128.6 (s), 128.5(s), 128.4 (s), 128.1 (s), 128.0, 127.6 (s), 126.8 (s), 119.0 (s), 83.0, 77.1, 74.6, 74.1 (s), 52.8 (d), 48.3 (d); IR (film): 3292, 2112, 1738, 1595, 1506, 1217 cm^{-1}; MS (ES) m/z: 512.2 $[M+H]^{+}$; m.p. 56-58^{o}C; HRMS (ES+) calcd for $C_{32}H_{26}N_5O_2$ $[M+H]^{+}$ 512.2087, found 512.2089.

References

5.7. References

1. (a) Beg, A. A.; Baltimore, D., An essential role for NF-Kappa B in preventing TNF-alpha-induced cell death. *Science* **1996,** *274*, 782-4; (b) Karin, M.; Lin, A., NF-kappa B at the crossroads of life and death. *Nat. Immunol.* **2002,** *3*, 221-7; (c) Boland, M. P., DNA damage signalling and NF-kappa B: implications for survival and death in mammalian cells. *Biochem. Soc. Trans.* **2001,** *29*, 674-8.

2. (a) Levine, A. J.; Momand, J.; Finlay, C. A., The p53 tumour suppressor gene. *Nature* **1991,** *351*, 453-6; (b) Hollstein, M.; Sidransky, D.; Vogelstein, B.; Harris, C. C., p53 mutations in human cancers. *Science* **1991,** *253*, 49-53; (c) LEVINE, A., p53, the cellular gatekeeper for growth and division. *Cell* **1997,** *88*, 323-31; (d) Hollstein, M.; Rice, K.; Greenblatt, M. S.; Soussi, T.; Fuchs, R.; Sorlie, T.; Hovig, E.; Smith-Sorensen, B.; Montesano, R.; Harris, C. C., Database of p53 gene somatic mutations in human tumors and cell lines. *Nucleic Acids Res.* **1994,** *22*, 3551-5.

3. (a) Baeuerle, P. A.; Henkel, T., Function and activation of NF-kappaB in the immune system. *Annu. Rev. Immunol.* **1994,** *12*, 141-79; (b) Baldwin, A. S., The NF-κB and IκB proteins: New discoveries and insights. *Annu. Rev. Immunol.* **1996,** *14*, 649-81.

4. Hoffmann, A.; Baltimore, D., Circuitry of nuclear factor kappaB signaling. *Immunol. Rev.* **2006,** *210*, 171-86.

5. (a) Webster, G. A.; Perkins, N. D., Transcriptional cross talk between NF-kappa B and p53. *Mol. Cell. Biol.* **1999,** *19*, 3485-95; (b) Perkins, N. D., Achieving transcriptional specificity with NF-kappa B. *Int. J. Biochem. Cell Biol.* **1997,** *29*, 1433-48.

6. (a) Bottero, V.; Busuttil, V.; Loubat, A.; Magne, N.; Fischel, J. L.; Milano, G.; Peyron, J. F., Activation of nuclear factor kappa B through the IKK complex by the topoisomerase poisons SN38 and doxorubicin: A brake to apoptosis in HeLa human carcinoma cells. *Cancer Res.* **2001,** *61*, 7785-91; (b) Weldon, C. B.; Burow, M. E.; Rolfe, K. W.; Clayton, J. L.; Jaffe, B. M.; Beckman, B. S., NF-κB–mediated chemoresistance in breast cancer cells. *Surgery* **2001,** *130*, 143-50; (c) Baldwin, A. S., Control of oncogenesis and cancer therapy resistance by the transcription factor NF-kappaB. *J. Clin. Invest.* **2001,** *107*, 241-6; (d) Arlt, A.; Vorndamm, J.; Breitenbroich, M.; Folsch, U. R.; Kalthoff, H.; Schmidt, W. E.; Schafer, H., Inhibition of NF-kappaB sensitizes human pancreatic carcinoma cells to apoptosis induced by etoposide (VP16) or doxorubicin. *Oncogene* **2001,** *20*, 859-68; (e) Khanna, K. K.; Jackson, S. P., DNA double-strand breaks: signaling, repair and the cancer connection. *Nat. Genet.* **2001,** *27*, 247-54; (f) Kim, J. Y.; Lee, S.; Hwangbo, B.; Lee, C. T.; Kim, Y. W.; Han, S. K.; Shim, Y. S.; Yoo, C. G., NF-kappaB activation is related to the resistance of lung cancer cells to TNF-alpha-induced apoptosis. *Biochem. Biophys. Res. Commun.* **2000,** *273*, 140-6.

7. Castedo, M.; Perfettini, J. L.; Roumier, T.; Valent, A.; Raslova, H.; Yakushijin, K.; Horne, D.; Feunteun, J.; Lenoir, G.; Medema, R.; Vainchenker, W.; Kroemer, G., Mitotic catastrophe constitutes a special case of apoptosis whose suppression entails aneuploidy. *Oncogene* **2004,** *23*, 4362-70.

8. Lin, Y. C.; Brown, K.; Siebenlist, U., Activation of NF-Kappa-B requires proteolysis of the inhibitor I-Kappa-Alpha - signal-induced phosphorylation of I-Kappa-B-Alpha alone does not release active NF-Kappa-B. *P. Natl. Acad. Sci. USA* **1995,** *92*, 552-6.

9. (a) Siebenlist, U.; Franzoso, G.; Brown, K., Structure, regulation and function of NF-Kappa-B. *Annu. Rev. Cell Biol.* **1994,** *10*, 405-55; (b) Baeuerle, P. A.; Baichwal, V. R., NF-kappa B as a frequent target for immunosuppressive and anti-inflammatory molecules. *Adv. Immunol.* **1997,** *65*, 111-37.

10. Sodhi, A.; Singh, R. A. K., Mechanism of NF-kappa B translocation in macrophages treated in vitro with cisplatin. *Immunol. Lett.* **1998,** *63*, 9-17.

11. (a) Adams, J.; Elliott, P. J., New agents in cancer clinical trials. *Oncogene* **2000,** *19*, 6687-92; (b) Adams, J., Proteasome inhibition in cancer: Development of PS-341. *Semin. Oncol.* **2001,** *28*, 613-9; (c) Adams, J., Development of the proteasome inhibitor PS-341. *Oncologist* **2002,** *7*, 9-16.

12. Richardson, P. G.; Mitsiades, C.; Hideshima, T.; Anderson, K. C., Proteasome inhibition in the treatment of cancer. *Cell cycle* **2005,** *4*, 290-6.

13. Shirley, R. B.; Kaddour-Djebbar, I.; Patel, D. M.; Lakshmikanthan, V.; Lewis, R. W.; Kumar, M. V., Combination of proteasomal inhibitors lactacystin and MG132 induced synergistic apoptosis in prostate cancer cells. *Neoplasia* **2005,** *7*, 1104-11.

14. (a) Fenteany, G.; Schreiber, S. L., Lactacystin, proteasome function, and cell fate. *J. Biol. Chem.* **1998,** *273*, 8545-8; (b) Corey, E. J.; Li, W. D. Z., Total synthesis and biological activity of lactacystin, omuralide and analogs. *Chem. Pharm. Bull.* **1999,** *47*, 1-10.

15. Feling, R. H.; Buchanan, G. O.; Mincer, T. J.; Kauffman, C. A.; Jensen, P. R.; Fenical, W., Salinosporamide A: A highly cytotoxic proteasome inhibitor from a novel microbial source, a marine bacterium of the new genus Salinospora. *Angew. Chem. Int. Ed.* **2003,** *42*, 355-7.

16. Groll, M.; Huber, R., Inhibitors of the eukaryotic 20S proteasome core particle: A structural approach. *BBA-Mol. Cell Res.* **2004,** *1695*, 33-44.

17. Sharma, V.; Peddibhotla, S.; Tepe, J. J., Sensitization of cancer cells to DNA damaging agents by imidazolines. *J. Am. Chem. Soc.* **2006,** *128*, 9137-43.

18. (a) Kahlon, D. K.; Lansdell, T. A.; Fisk, J. S.; Hupp, C. D.; Friebe, T. L.; Hovde, S.; Jones, A. D.; Dyer, R. D.; Henry, R. W.; Tepe, J. J., Nuclear factor-kappaB mediated inhibition of cytokine production by imidazoline scaffolds. *J. Med. Chem.* **2009,** *52*, 1302-9; (b) Kahlon, D. K.; Lansdell, T. a.; Fisk, J. S.; Tepe, J. J., Structural-activity relationship study of highly-functionalized imidazolines as potent inhibitors of nuclear transcription factor-kappaB mediated IL-6 production. *Biorg. Med. Chem.* **2009,** *17*, 3093-103.